Agenzia nazionale per le nuove tecnologie, l'energia
e lo sviluppo economico sostenibile

Ministero dello Sviluppo Economico

RICERCA DI SISTEMA ELETTRICO

Deterministic safety analysis of Station Blackout postulater accident on the basis of the SMR simulator MASLWR

A. Del Nevo

Report RdS/2012/014

DETERMINISTIC SAFETY ANALYSIS OF STATION BLACKOUT POSTULATED ACCIDENT ON THE BASIS OF THE SMR SIMULATOR MASLWR

A. Del Nevo, ENEA

Settembre 2012

Report Ricerca di Sistema Elettrico
Accordo di Programma Ministero dello Sviluppo Economico - ENEA
Area: Governo, gestione e sviluppo del sistema elettrico nazionale
Progetto: Nuovo nucleare da fissione: collaborazioni internazionali e sviluppo competenze in materia nucleare
Responsabile del Progetto: Paride Meloni, ENEA

ENEA Ricerca Sistema Elettrico	Sigla di identificazione NNFISS-LP2-085	Distrib. L	Pag. 1 di 82

Titolo

Deterministic safety analysis of Station Blackout postulated accident on the basis of the SMR simulator MASLWR

Descrittori

Tipologia del documento: Rapporto tecnico

Collocazione contrattuale: Accordo di programma ENEA-MSE: tema di ricerca "Nuovo nucleare da fissione"

Argomenti trattati: Sistemi nucleari innovati
Simulazione numerica con codice di sistema RELAP5
Analisi di sicurezza

Sommario

L'attività riguarda la simulazione di un progetto di reattore modulare integrale di piccola taglia moderato e refrigerato ad acqua leggera. Due sono i principali obbiettivi perseguiti: 1) la qualifica del modello RELAP5/Mod3.3 utilizzato per le simulazioni e 2) alcuni studi preliminari riguardanti la risposta del progetto di impianto ad un ipotetico scenario di station blackout.
Il documento si articola in sette capitoli di cui il primo, introduttivo, riporta l'ambito nel quale l'attività va inquadrata, gli obiettivi e la struttura del presente report. L'ultimo capitolo riguarda le osservazioni conclusive dell'attività svolta. Il secondo ed il terzo capitolo si focalizzano sul progetto del reattore modulare integrale di piccolo taglia preso a riferimento (MASLWR) e sull'apparecchiatura sperimentale progettata, costruita ed esercita ad *Oregon State Univeristy* (OSU), che ne rappresenta il modello scalato (1:254 in volume). Il quarto capitolo descrive il modello messo a punto con il codice RELAP5/Mod3.3 per la simulazione dell'apparecchiatura sperimentale. I risultati della simulazione di due transitori (circolazione naturale e *loss of feed water flow*) sono stati ottenuti sulla base delle specifiche dei due test e, successivamente, confrontati con i dati disponibili messi a disposizione da OSU. L'analisi dei risultati (riportata nel capitolo quinto) ha consentito di dimostrare che il codice ha la capacità di predire i fenomeni termoidraulici rilevanti e di concludere sulla sua affidabilità delle simulazioni relative ad un ipotetico transitorio di station blackout. Pertanto il modello RELAP5 è stato impiegato per effettuare alcune investigazioni deterministiche di sicurezza relative alla riposta del sistema OSU-MASLWR a fronte di uno station blackout completo. I risultati preliminari consentono di dimostrare la potenzialità di tale progetto a resistere per oltre 7 giorni in completa assenza di potenza "*onsite*" ed "*offsite*", grazie alla relativa bassa densità di potenza e grande riserva d'acqua.

Note

Copia n. In carico a:

1			NOME			
			FIRMA			
0	EMISSIONE	14/09/2012	NOME	A. Del Nevo	P. Agostini	P. Meloni
			FIRMA	[signature]	[signature]	[signature]
REV.	DESCRIZIONE	DATA		REDAZIONE	CONVALIDA	APPROVAZIONE

(Pagina lasciata intenzionalmente bianca)

EXECUTIVE SUMMARY

The aim of the activity is related to the simulation of a small modular reactor (SMR) design, cooled and moderated with light water and having an integral primary system layout. Two main objectives have been pursued: 1) the qualification of a RELAP5/Mod3.3 nodalization used for the numerical simulation of the system and 2) deterministic investigations related to the capability of this small modular reactor design to cope with a station blackout postulated accident scenario.

The report is divided into seven sections. Among these, the first provides the framework of the activity, the objectives and the structure of the report and the last describes the main conclusions. The second and the third sections are focused on the brief description of the reference reactor design (i.e. MASLWR) and on its scaled down (1:254 in volume) experimental facility, designed, constructed and operated at Oregon State University (OSU). The forth section reports the main features of the nodalization set up for RELAP5/Mod3.3 code. The main results of two blind simulations (natural circulation and loss of feed water tests) are reported in section fifth. The analysis, based on the comparisons with the experimental data provided by OSU, demonstrates that the code is able to predict the main thermal-hydraulic phenomena and provides reliable prediction of the main parameter trends. Finally the OSU-MASLWR nodalization has been employed to carry out deterministic investigations of station blackout scenarios (section six). The preliminary results highlight the potential capability of this design to cope with a station blackout without any external intervention for at least 72 hours, thanks to the low power density and the large water inventory.

LIST OF CONTENTS

LIST OF FIGURES

LIST OF TABLES

1 INTRODUCTORY REMARKS

1.1 Framework

The activity is carried out in the framework of the "*Linea Progettuale*" 2 (LP2) of the "*Piano Annuale di Realizzazione dell'Accordo di Programma*" (AdP) between ENEA and MSE. The task deals with the evaluation of the safety by design features of small modular reactor design, characterized by integral primary system layout.

Generally, small modular reactor designs are featured with high level of passive safety systems or they are inherently safe. Moreover they are characterized by a tight coupling of primary system and containment in case of the occurrence of postulated accident. In particular , the enhanced safety features of the SMR are connected with the reduced source term; the lower decay heat generated in the reactor core; the more efficient passive decay heat removal from reactor vessel and, finally, the elimination of some postulated accident. Therefore, thanks the safety features and their attractiveness for small and medium electric grids, the interest in developing these reactor design is increasing.

In this connection, ENEA is also participating in the Coordinated Research Program (CRP) on Natural Circulation Phenomena, Modeling, and Reliability of Passive Systems that Utilize Natural Circulation. This activity is a collaborative project with 18 participating organizations, based on OSU-MASLWR experimental facility experiments, which will be completed at the beginning of the 2013.

1.2 Objectives

The aim of the activity is related to the simulation of a small modular reactor design, cooled and moderated with light water and having an integral primary system layout. Two main general objectives have been pursued: 1) the qualification of a RELAP5/Mod3.3 nodalization used for the numerical simulation of the system and 2) deterministic investigations related to the capability of this small modular reactor design to cope a station blackout postulated accident scenario.

In view of these, the following specific objectives are identified and connected with the overall activity:

1. to improve the understanding of thermal-hydraulic phenomena expected to occur in normal operation and transients of SMR design;
2. to develop a numerical model by RELAP5/Mod3.3suitable for simulating a SMR design;
3. to evaluate the capability of computer codes (i.e. RELAP5/Mod3.3) to adequately predict the occurrence of important phenomena, and the corresponding behavior of nuclear systems during operating, upset and accident conditions, which are represented in experiments;

4. to identify and to select, through the code assessment (post tests) activities, those phenomena and models of interest which requires an up-date or an improvement of the capabilities of RELAP5 code;
5. to participate in the Coordinated Research Program (CRP) on Natural Circulation Phenomena, Modeling, and Reliability of Passive Systems that Utilize Natural Circulation
6. to perform preliminary detterministic investigations of a station blackout scenario to demostrate the features and the safety margins of this SMR design.

1.3 Structure of the report

The present report is divided into seven sections.
Besides the present section (one) and the conclusions (section seven), the second section is focused on a the description of the MASLWR reactor design. The reactor layout is described togheter with the main operating conditions and the engineering safety features.

The third section describes the experimental facility OSU-MASLWR, which is scaled down model of the MASLWR design. The features of the experimental facility are outline in order to better understand its RELAP5/Mod3.3 model, reported in section four. The main features, code options and user choices are provided in the nodalization description, together with the nodalization scheme.

The main results of two blind simulations (natural circulation and loss of feed water tests) are reported in chapter fifth. The code calculations were performed on the basis of the experimental specifications, therefore without the availability of the experimental data. The analysis, based on the comparisons with the experimental data distributed by OSU, demonstrates that the code is able to predict the main thermal-hydraulic phenomena and provides reliable prediction of the main parameter trends.
Finally the OSU-MASLWR nodalization has been employed to carry out deterministic investigations of station blackout scenarios. The preliminary results highlight the capability of this design to cope with a station blackout without any external intervention for at least 72 hours, thanks to the low power density and the large water inventory.

2 DESCRIPTION OF MASLWR

2.1 Introductory remarks on SMR

Nowadays, there is revival of interest in small and simpler units for generating electricity from nuclear power and for process heat. This interest in small nuclear power reactors is driven both by a desire to reduce capital costs and to provide power for small and medium electric grid systems. The technologies involved are very diverse (see Tab. 2.1) and Ref. [1].

The International Atomic Energy Agency (IAEA) defines 'small' reactors, those having a electrical output under 300 MWe and 'medium' up to 700 MWe.

Tab. 2.1 – Sample list of SMR designs

Name	Capacity	Type	Developer
KLT-40S	35 MWe	PWR	OKBM, Russia
VK-300	300 MWe	PWR	Atomenergoproekt, Russia
CAREM	27 MWe	PWR	CNEA & INVAP, Argentina
IRIS	100-335 MWe	PWR	Westinghouse
mPower	125 MWe	PWR	Babcock & Wilcox, USA
SMART	100 MWe	PWR	KAERI, South Korea
NuScale	45 MWe	PWR	NuScale Power, USA
HTR-PM	2×105 MWe	HTR	INET & Huaneng, China
PBMR	80 MWe	HTR	Eskom, South Africa
GT-MHR	285 MWe	HTR	General Atomics, USA – Rosatom, Russia
BREST	300 MWe	LMR	RDIPE, Russia
SVBR-100	100 MWe	LMR	Rosatom/En+, Russia
FUJI	100 MWe	MSR	ITHMSO, Japan-Russia-USA

If compared with the current NPP in operation, the general features of the SMR would be: greater simplicity of design; enhanced robustness (safety margins); economy of mass production; reduced siting costs; high level of passive or inherent safety in the event of malfunction. In general, the designs belong to the Gen. III+ and Gen. IV types.

The main reasons for developing and constructing a SMR are connected with the smaller capital cost needed. These may be built independently or as modules in a larger complex, with capacity added incrementally as required (see section below on Modular construction using small reactor units). Economies of scale are provided by the numbers produced. These have the possibility to be better integrated in small electricity grids (< 4 Gwe), typical of new developing countries or for remote sites.

Generally, modern small reactors for power generation are expected to have greater simplicity of design, economy of mass production, and reduced siting costs. Most are also designed for a high level of passive or inherent safety in the event of malfunction.
In particular, the enhanced safety features of the SMR are connected with the reduced source term; the lower decay heat generated in the reactor core; the more efficient passive decay heat removal from reactor vessel and, finally, the elimination of some postulated accident.

2.2 Main features of the MASLWR design

The Multi-Application Small Light Water Reactor (MASLWR) [2] concept is a small, safe and economic natural circulation pressurized light water reactor, which has been developed by the Idaho National Laboratory (INL), Nexant Inc. and the Oregon State University (OSU). Besides, the electric power, it can be used for process heat applications such as water desalination or district heating, with deployment in a variety of locations.

The reactor concept is flexible enough for early deployment using LWR oxide fuels, in a later phase using Uranium-Thorium fuels and eventually new advanced fuels, such as metal fuels, that promise additional safety features, increased e efficiency, and more economic fuel cycle. This approach to gradual development of a nuclear power system, not practical for large high power systems, is possible only for small size modular reactors such as the MASLWR, because of simplicity of the reactor design, low cost of the module, and simplified licensing procedures based on prototype testing [2].

The power of MASLWR[3] is 150 MWth. It is designed to rely exclusively on the natural circulation and, thus has no pump on its primary side. The reactor vessel houses the core and support structures, core barrel, upper internals, shielding, control rod guides and the control and safety instrumentation, steam generator, pressurizer, heaters. Such an arrangement eliminates separate loops with steam generators, pressurizer, connecting pipes and supports.

The unit consists of three basic modules[4]: the reactor module, which includes the primary vessel with the reactor and the steam generator, and the containment vessel, the turbine generator module and the main condenser module. The entire reactor module is 4.3 m (14 ft) diameter, 18.3 m (60 ft) long. This is within the state of the art fabrication capabilities[4]. It allows it to be entirely shop fabricated and transported to site on most railways or roads.

Its primary flow is quite simple[5], as reported in Fig. 2.1. The long vertical tube in the center of the vertical vessel is called the riser and functions like a chimney to enhance the driving (gravity) head of the natural circulation flow. Starting from the bottom of the riser, fluid enters the core which is located in a shroud connected to the riser entrance. Flowing through the core. Here, the fluid is heated and thus ascend through the riser due to its buoyancy. Once the top of the riser is reached, the fluid is turned below the pressurizer plate and begins to descend through the outer annulus formed by the outer wall of the riser and the inner wall of the reactor vessel. Heat is removed from the primary to the secondary fluid by means of a helical coil tubes steam generator, wrapped around the riser. Thus, steam generation occurs within the reactor vessel itself with the primary fluid constituting the shell side and the secondary fluid constituting the tube side of the steam generation process. The primary fluid is cooled by contact with the coils and thus becomes negatively buoyant. As result, it descends through the outer annulus to the bottom of the vessel where it is turned upward into the riser, thereby completing its loop.

The steady state operating conditions are reported in Tab. 2.2. The design provides primary coolant temperature alsways below the saturated conditions. In addition, MASLWR is designed to provide superheated steam at the helical coil outlet to eliminate the need for separators and driers. The secondary side pressure was selected so that off-shelf low pressure steam turbine could be implemented.

Because MASLWR system has an integrated layout[4], some typycal PWR postulated accident are not plausible. The elimination of the large LOCAs, since no large primary penetrations of the reactor vessel or large loop piping exist, is only the most easily visible of the safety potential characteristics of integral reactors. Many others are possible, but they must be carefully exploited through an appropriate design that is kept focused on selecting design characteristics that are most amenable to eliminate accident initiating events.

MASLWR system relies on the following Engineered Safety Features:

- High Pressure Containment Vessel;
- Passive Safety Systems;
- Decay Heat Removal System (DHRS);
- Containment Heat Removal System (CHRS);
- Severe Accident Mitigation and Prevention Design Features.

The containment (Fig. 2.3a) is designed in order to have an equilibrium pressure between reactor and containment following any LOCA always below maximum pressure. The Passive Safety Systems consist of the following componenets:

- Two independent, small diameter, Steam Vent Valves;
- Two independent, small diameter steam, Automatic Depressurization System valves;
- Two independent, small diameter steam, Sump Recirculation Valves

The Decay Heat Removal System (DHRS) consist of the following features (Fig. 2.3b):
Two independent trains of emergency FW.

- Water is drawn from the containment cooling pool through a sump screen.
- Steam is vented through spargers and condensed in the containment pool.
- FW accumulators provide initial feed flow while DHRS transitions to natural circulation flow.
- Pool provides a 3 day cooling supply for decay heat removal

The Decay Heat Removal Using Containment (CHRS) has the following functions (Fig. 2.3c):

- provides a means of removing core decay heat and limits containment pressure by: steam condensation, convective heat transfer, heat conduction and sump recirculation;
- vents the RPV steam through the reactor vent valves (flow limiter);
- condenses the steam in containment;
- collects the condensate in lower containment region (sump);
- operates the sump valves to provide recirculation path through the core.

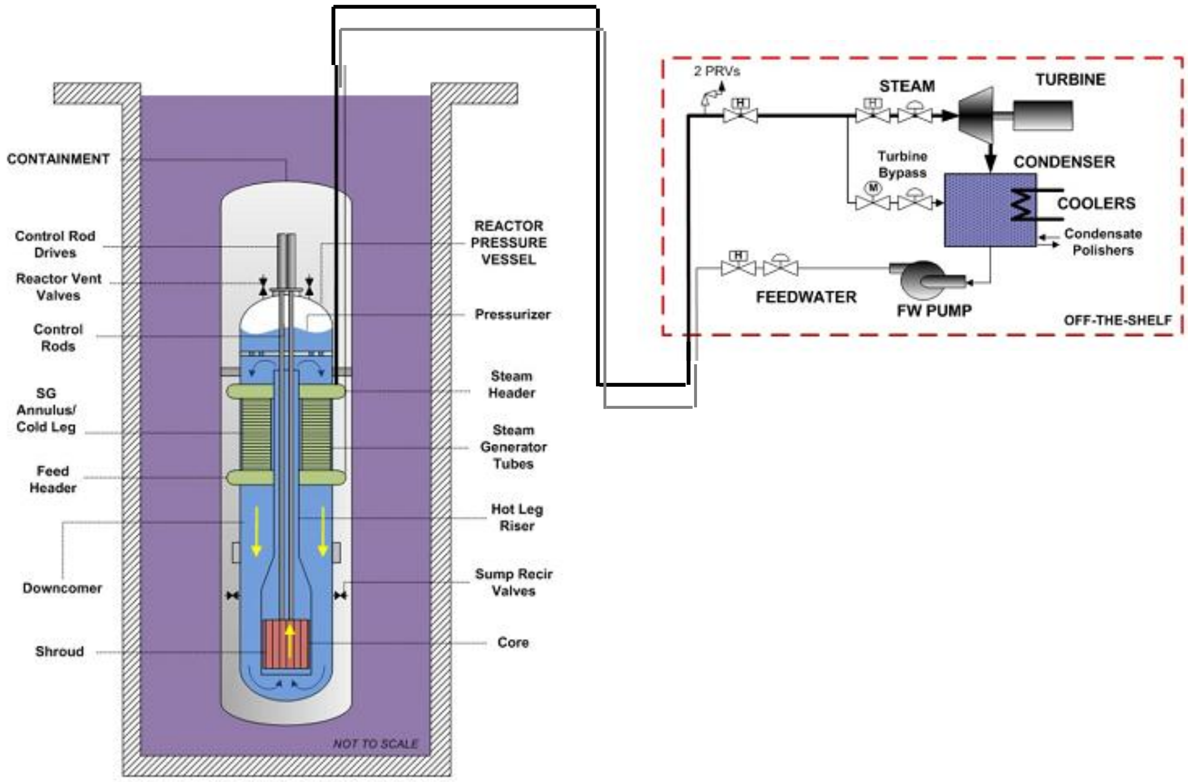

Fig. 2.1 – MASLWR layout

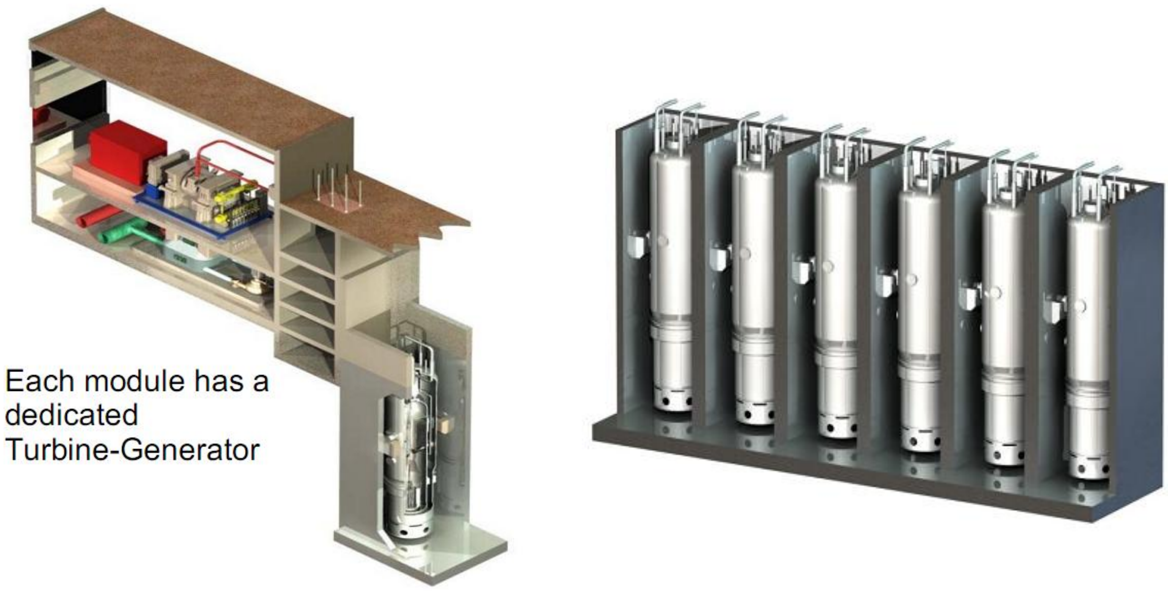

(a) Schematic of the MASLWR exterior cooling pool and turbine generator set

(b) Sample of multiple installation

Fig. 2.2 – THE SMR MASLWR

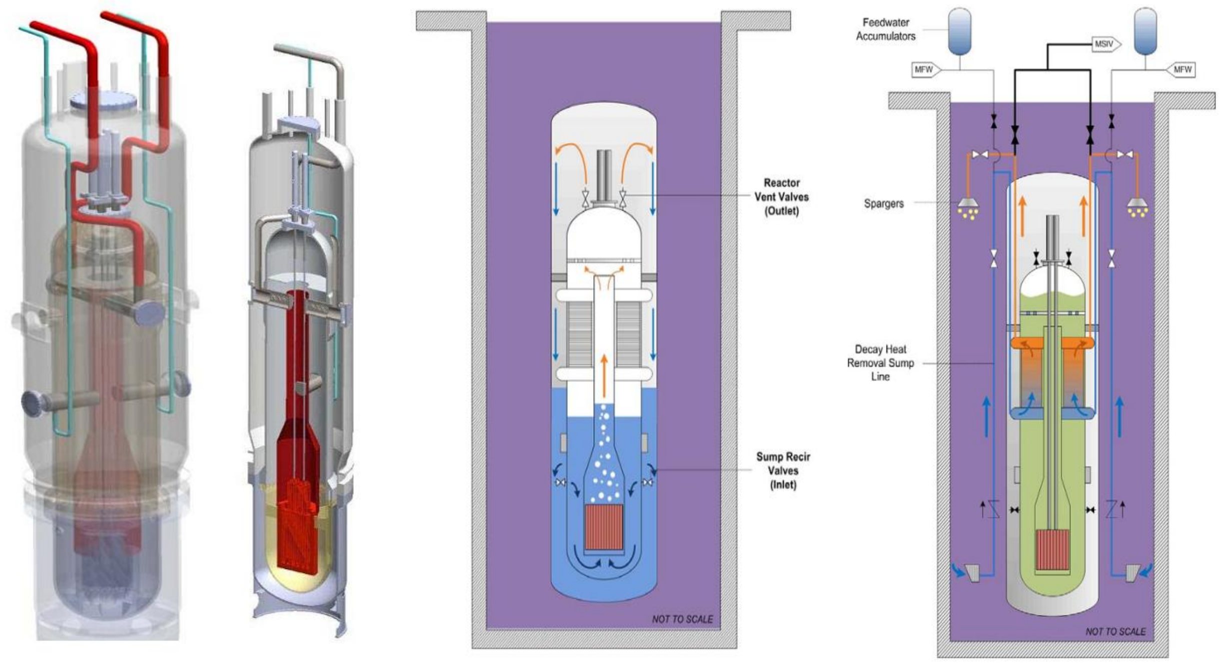

(a) High Pressure Containment Vessel and Reactor Pressure Vessel

(b) Decay Heat Removal SGs (DHRS)

(c) Decay Heat Removal Using Containment (CHRS)

Fig. 2.3 – Overview of the MASLWR Engineered Safety Features

Tab. 2.2 – Steady state design operating conditions

System	Parameter	Unit	Value
Primary system	*Reactor power*	MWth	150
	Primary pressure	MPa	7.60
	Primary mass flow rate	kg/s	597
	Reactor inlet temperature	K	491
	Reactor outlet temperature	K	544
	Saturation temperature	K	565
	Reactor outlet void fraction	--	0.0
Secondary system	*Steam pressure*	MPa	1.50
	Steam outlet quality	--	1.0
	Steam temperature	K	481
	Stauration temperature	K	471
	Feedwater temperature	K	310
	Feedwater flowrate	kg/s	56.1

3 OSU-MASLWR INTEGRAL TEST FACILITY

OSU-MASLWR integral test facility [6] is designed on the basis of the results of the scaling analysis in order to properly model steady state and transient behavior of the prototype reactor. The following specific objectives have been met for each mode of operation:

- the similarity groups which should be preserved between the test facility and the full scale prototype were obtained;
- the priorities for preserving the similarity groups were established;
- the important processes were identified and addressed;
- the specifications for the facility design were provided; and
- the biases due to scaling distortions were identified.

OSU-MASLWR test facility (Fig. 3.1) models the MASLWR conceptual design including reactor pressure vessel cavity and containment structure[5]. It is scaled at 1:3 length scale, 1:254 volume scale and 1:1 time scale. It is constructed entirely of stainless steel, and is designed for full pressure (11.4 MPa) and full temperature (590 K) prototype operation of the original design in Ref. [3].

The test facility includes three major component packages[6]. The first is the **primary circuit**, which includes the reactor pressure vessel with its internal components (core, hot leg riser, steam generator, pressurizer) and ADS blowdown lines, vent lines and sump recirculation lines. Then, there is the **secondary circuit**, which includes the steam generator (internal to vessel), feed water pumps, and associated feed water and steam valves. The third is the **containment structure**. OSU-MASLWR test facility models the containment structure, in which the reactor pressure vessel sits, and the cavity within which the containment structure is located.

In addition to the physical structures that comprise the test facility, there is an instrumentation and control systems. The data generated by the testing program is being used to validate computer code calculations and to provide a better understanding of the core natural circulation thermal-hydraulic phenomena. Indeed, it has being used to aid in the design of the MASLWR and it is involved in a IAEA ICSP on MASLWR – Experiments and TH Code Benchmarks.

The primary circuit[6] of the test facility models the self-contained integrated reactor core and steam generator system. The core is simulated with electric heaters. The steam generator is comprised of helical coils that are located in the primary pressure vessel, above the core and outside of the hot leg chimney. The relative thermal barycentre hights of core and steam generator is designed to provide a sufficient natural circulation flow under normal steady state and transient operating conditions.

The primary circuit of the test facility has been designed with limits for operation at a primary side pressure of 11.4 MPa and a primary side temperature of 590 K. Primary coolant flow is upwards through the core and hot leg riser. This hot fluid is cooled by the steam generator in the upper portion of the vessel. The cooler fluid flows downward around the outside of the hot leg riser into the lower plenum. From the lower plenum the fluid is drawn back into the core and heated once more. Fig. 3.2 shows the scheme of the test facility primary circuit components. The test facility core consists of 56 electric heaters distributed in a square array with a maximum core power of 700 kW (reduced to 398 kW after the installation of the new fuel core bundle) [7]. The core geometry and thermal characteristics (flow areas, hydraulic diameters and local heat flux) have been preserved on a scaled basis.

The steam generator[6] (SG) is a helical coil, once through heat exchanger located within the pressure vessel in the annular space between the hot leg riser and the inside surface of the pressure vessel shell. Feed water is pumped into the SG tubes from a feedwater storage tank. This pump uses a variable speed controller to allow for precise control of the feed water mass flow rate. The steam produced is vented to atmosphere. The SG consists of three separate parallel helical coil tube sections. The outer and middle coils consist of five tubes each while the inner coil consists of four tubes. Each coil is separate from the others but the tubes within a coil are joined at a common inlet header to ensure pressure equilibrium. Cold feedwater enters at the bottom of the SG and boils off after traveling a certain length in the SG tubes. This boil off length is a function of both core power and feed water flow rate. Nominally, this boil off length is approximately 40% shorter than the actual length of the steam generator tubes so the steam will leave the SG superheated. Each SG coil exhausts the superheated steam into a common steam drum from where it is subsequently exhausted to atmosphere.

The MASLWR containment vessel[6] and the surrounding containment pool are modeled in the OSU MASLWR test facility as two separate vessels. One vessel models the suppression pool volume, vapor bubble volume and the condensation surface inside of the containment vessel. The second vessel models the heat capacity of the water pool within which the containment vessel is held. The two vessels are separated by a stainless steel plate. This plate models the scaled heat transfer surface between the containment vessel and the surrounding vessel pool. Fig. 3.1 and Fig. 3.3 show these two vessels. The containment vessel is connected to the reactor pressure vessel (RPV) by six independent automatic depressurization system (ADS) lines. There are two blowdown lines, two vent lines and two sump recirculation (core makeup) lines. Flow through each of these lines is via an independent automatically operated valve controlled through the test facility control system. The containment vessel is capable of prolonged operation at 2.07 MPa and 477.6 K.

The test facility is instrumented[6] to capture the behavior of the facility during steady-state and transient operation. The following information can be obtained by the test facility data acquisition system:

- Feed water—mass flow rate and temperature,
- Feed water through each SG coil—mass flow rate, temperature and pressure,
- Main steam—volumetric flow rate and pressure,
- Differential pressure—across core, hot leg chimney, SG, and annulus below SG,
- Pressurizer—coolant level, pressure and temperature, and
- Temperatures—core inlet, core exit, primary loop at SG.

The test facility control system accomplishes two tasks. The first is to process input signals from the various facility instrumentation (thermocouples, pressure meters, flow meters, valve and relay positions). The second is to generate control signals determined by the system logic (valve and relay control signals, heater and pump control signals). The following systems can be regulated by the test facility control system:

- Core heaters (including decay power modeling),
- Main feed water pump,
- Pressurizer heaters,
- Feedwater storage tank level,
- Pressurizer water level (draining during system heatup only), and
- Containment heaters (used to maintain an adiabatic boundary condition on all walls of containment except for the prescribed condensation wall ensuring that heat transfer only takes place between the containment pool vessel and the high pressure containment vessel).

Fig. 3.1 – Photo of OSU MASLWR Test Facility

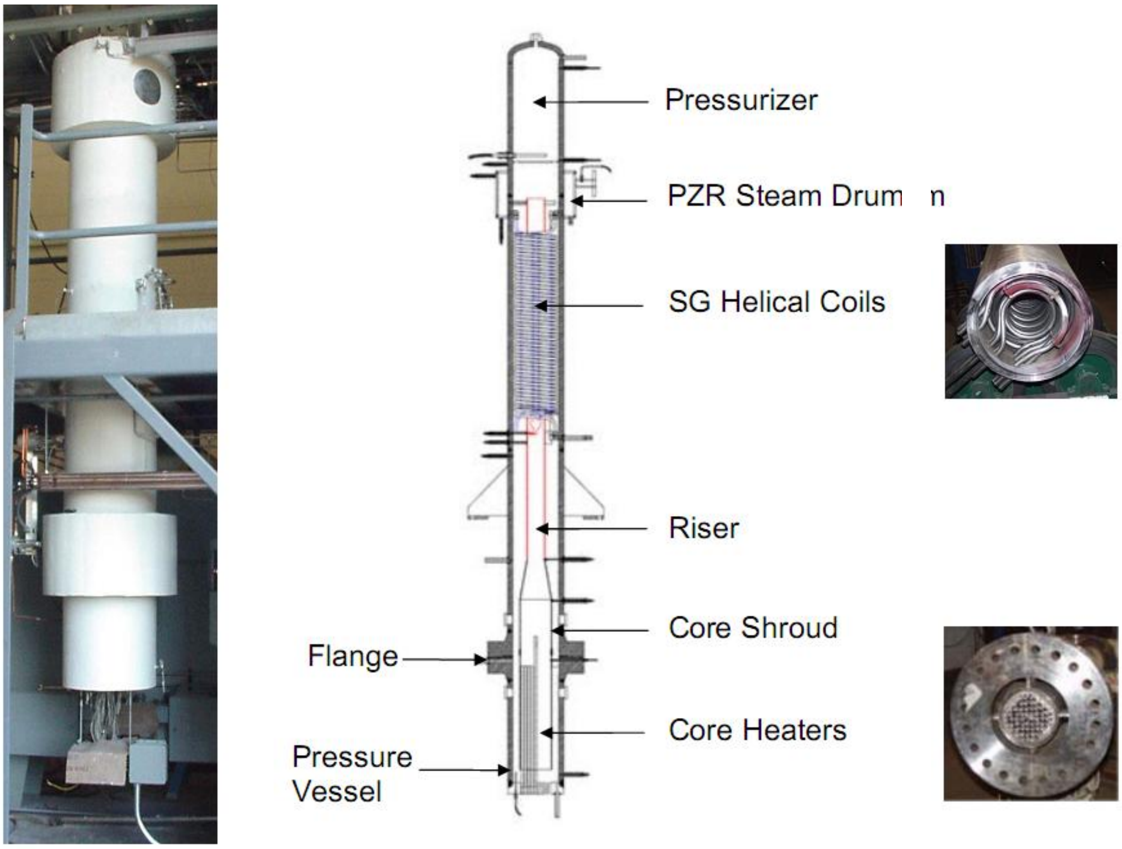

(a) Photo *(b) Schematization* *(c) Deatils*

Fig. 3.2 – OSU MASLWR Test Facility: reactor pressure vessel

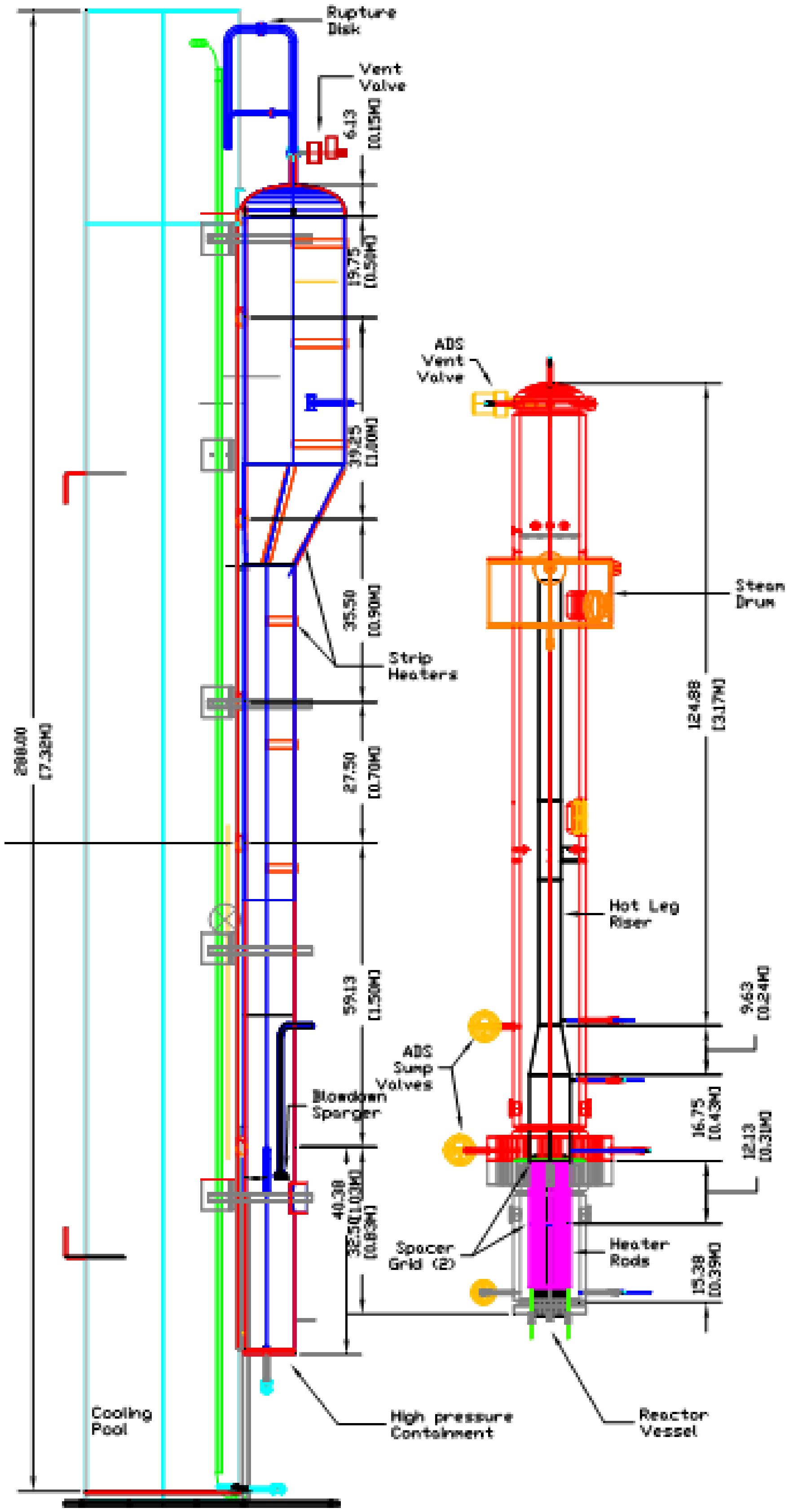

Fig. 3.3 – OSU MASLWR Test Facility: overall schematization

4 RELAP5 NODALIZATION OF OSU-MASLWR ITF

4.1 RELAP5/Mod3.3 code

RELAP5 code is a widely diffused code and constitutes the object of continuous assessment in various international institutions. Wide qualification projects and sensitivity and uncertainty analyses of physical models have been performed all over the world, Refs. [8], [9] and [10]. The RELAP5 is well known and a wide literature exists about the code description, capability and application.

The light water reactor transient analysis code, RELAP5, was developed at Idaho National Engineering Laboratory (INEL) for the U.S. Nuclear Regulatory Commission (NRC). The RELAP5 code has been developed for the best estimate simulation of LWR coolant system transients during normal and off normal conditions. The code models the coupled behavior of the reactor coolant system and the core (point kinetic) for simulating accidents in LWR: such as loss of coolant, Anticipated Transients Without Scram (ATWS) and operational transients, such as loss of feed-water, loss of offsite power and turbine trip. A generic modeling approach is used that permits simulating a variety of thermal hydraulic systems such as turbines, condensers and secondary feed-water systems. The component models include also pumps, valves, pipes, heat releasing or absorbing structures, reactor point kinetics, electric heaters, jet pumps, etc.

This code is highly generic and can be used for simulation of a wide variety of hydraulic and thermal transients in both nuclear and non-nuclear systems involving mixtures of steam, water, non-condensable and solute. The developers of the RELAP5/Mod3 wanted to create a code version suitable for the analysis of all transient and postulated accidents in LWR systems, including small and large break Loss Of Coolant Accidents (LOCA).

Based on one-dimensional, transient, and non-homogeneous and non-equilibrium hydrodynamic model for the steam and liquid phases, RELAP5/Mod3 code uses a set of six partial derivative balance equations and can treat a non-condensable component in the steam phase and a non-volatile component (boron) in the liquid phase.

A semi-implicit numeric scheme is used to solve the equations inside control volumes connected by junctions. The fluid scalar properties (pressure, energy, density and void fraction) are the average fluid condition in the volume and are viewed located at the control volume center. The fluid vector properties, i.e. velocities, are located at the junctions and are associated with mass and energy flows between control volumes that are connected in series, using junctions to represents flow paths. The direction associated to the control volume is positive from the inlet to the outlet.

Heat flow paths are also modeled in a one-dimensional sense, using a staggered mesh to calculate temperatures and heat flux vectors. Heat structures and hydrodynamic control volumes are connected through heat flux, calculated using a boiling heat transfer formulation.

These structures are used to simulate pipe walls, heater elements, nuclear fuel pins and heat exchanger surfaces.

4.2 Computer hardware and software tools

All calculations described hereafter have been carried out using the following tools:

- Workstation HP
  - Operative system WINDOWS 7 Professional (64bit)
  - Intel® XEON @ 3.2GHz
  - RAM 16 GB
- Software
  - EC Wingraf and MS EXCEL 2010 for the post processing phase

4.3 OSU-MASLWR nodalization description

The nodalization derives from the preliminary 3D model set up for RELAP5-3D© representing OSU-MASLWR facility (Ref. [11]) by means of merging the azimuthal subdivisions of the models. It has been tested against two experimental tests consisting in a natural circulation test and a loss of normal feedwater [12], [13]. The code results were calculated as blind exercise, as discussed in section 5.

Modeling
The OSU-MASLWR facility is represented by the RELAP5 nodalization, as following:

RPV

- The bottom region, connecting the downcomer part and the core zone, is represented with a BRANCH component.
- The core and the riser are modeled with a single pipe having 33 sub-volumes. The core region consists of 6 out of 33 sub-volumes.
- The region below the top plate of the primary system, which separates the PRZ zone and the ascending and descending sides concentric regions, has been modeled with a single BRANCH.
- The cold side and the downcomer regions are modeled with a single pipe having 33 sub-volumes. 8 out of 33 sub-volumes are linked to the secondary system by means of thermal structures.
- The pipe on the top represents the PRZ region

Secondary system

- It is represented with a single equivalent channel plus a PIPE representing the plugged tube.
- The helical coil SG is represented with a single pipe having 42 sub-volumes. The heat exchange with the primary system is modeled with a thermal structure connected to 38 out of 42 sub-volumes.
- The FW temperature is imposed with a TIME DEPENDENT VOLUME component.
- The mass flow rate can regulated with a PI controller connected with a TMDPJUN component.
- The system pressure is imposed with a TIME DEPENDENT VOLUME component at the steam line outlet.

The **CPV** and the **HPC** are modeled with two parallel stack of PIPE and BRANCH components. The model approach is based on Ref. [17].

The following modeling features apply[12]:

- the elevations of the different parts of the facility are maintained in the nodalization;
- the SG secondary side tubes are modeled using the “average” inclination angle of the real geometry, thus horizontal flow regime is applied in the equivalent tube;
- the node to node ratio is kept uniform with a maximum ratio of 1.2 between adjacent sub-volumes;
- the sliced approach is applied at all systems (i.e. primary, secondary, HPC, CPV and interfacing systems).
- the chocked flow is calculated using the Henry Fauske model.

Nodalization diagram
The nodalization used for all analyses described in the present report is depicted in Fig. 4.1.

Geometric data used in code and the list of parameters
The main hydraulic geometrical features and the adopted code resources are reported respectively in Tab. 4.1 and Tab. 4.2 reports the number of each RELAP5 component, the corresponding zone in OSU-MASLWR facility, the component type, the geometrical description (area and length), and the inclination. The energy loss coefficients used in the junctions are evaluated or estimated on the basis of the geometry. The roughness is set 5.0E-5 m with the exception of the core region and the SG tubes (5.0E-6 m).

Heat structure data
The main heat structures modeling features are reported in Ref. [12], where the different part of the OSU-MASLWR are connected with the nodalization components and described in terms of options and geometrical characteristics. The material proprieties are taken by the IAEA ICSP documentation [13], when available.

Control logic
The nodalization is set up considering the facility configuration as reported in Tab. 4.3.

Tab. 4.1 – OSU-MASLWR test facility nodalization: main hydraulic geometrical features

RELAP Component	RELAP Component Type	MASLWR Region	Length (m)	Area (m^2)	Vertical Angle (°)	Note
PRIMARY SYSTEM						
110	Branch	Lower plenum	0.07470	--	90	
115-01	Pipe	Core region	0.1046	8.413E-03	90	
115-02			0.1046	8.413E-03	90	
115-03			0.1046	8.317E-03	90	
115-04			0.1012	8.399E-03	90	
115-05			0.1012	8.399E-03	90	
115-06			0.1012	9.783E-03	90	
115-07		Hot leg region lower	0.1080	3.046E-02	90	
115-08			0.1058	3.052E-02	90	
115-09			0.1058	3.052E-02	90	
115-10			0.1058	3.052E-02	90	
115-11		Hot leg region conical	9.4050E-02	2.679E-02	90	
115-12			9.4050E-02	1.797E-02	90	
115-13			0.1000	8.500E-03	90	
115-14		Hot leg region upper	0.1021	8.227E-03	90	
115-15			0.1021	8.227E-03	90	
115-16			0.1021	8.227E-03	90	
115-17			0.1021	8.227E-03	90	
115-18			0.1021	8.227E-03	90	
115-19			0.1021	8.227E-03	90	
115-20			0.1021	8.227E-03	90	
115-21			0.1021	8.227E-03	90	
115-22			0.1040	6.540E-03	90	
115-23			0.1040	8.175E-03	90	
115-24			0.1117	8.235E-03	90	
115-25			0.1117	8.235E-03	90	
115-26			0.1117	8.235E-03	90	
115-27			0.1117	8.235E-03	90	
115-28			0.1117	8.235E-03	90	
115-29			0.1117	8.235E-03	90	
115-30			0.1117	8.235E-03	90	
115-31			0.1117	8.235E-03	90	
115-32			0.1191	8.232E-03	90	
115-33			0.1191	8.232E-03	90	
120	Branch	UpperSteamDrum	0.2254	--	90	
125-01	Pipe	Downcomer	0.1046	3.260E-02	90	
125-02			0.1046	3.461E-02	90	
125-03			0.1046	3.461E-02	90	
125-04			0.1012	3.459E-02	90	

RELAP Component	RELAP Component Type	MASLWR Region	Length (m)	Area (m^2)	Vertical Angle (°)	Note
125-05			0.1012	3.419E-02	90	
125-06			0.1012	3.241E-02	90	
125-07		Cold leg	0.1080	3.454E-02	90	
125-08			0.1058	3.458E-02	90	
125-09			0.1058	3.458E-02	90	
125-10			0.1058	3.458E-02	90	
125-11			9.4050E-02	3.690E-02	90	
125-12			9.4050E-02	4.157E-02	90	
125-13			0.1000	5.130E-02	90	
125-14			0.1021	5.671E-02	90	
125-15			0.1021	5.671E-02	90	
125-16			0.1021	5.671E-02	90	
125-17			0.1021	5.671E-02	90	
125-18			0.1021	5.671E-02	90	
125-19			0.1021	5.671E-02	90	
125-20			0.1021	5.671E-02	90	
125-21			0.1021	5.495E-02	90	
125-22			0.1040	4.847E-02	90	
125-23		SG primary side outlet	0.1040	4.116E-02	90	
125-24		SG primary tube region	0.1117	4.117E-02	90	
125-25			0.1117	4.117E-02	90	
125-26			0.1117	4.117E-02	90	
125-27			0.1117	4.117E-02	90	
125-28			0.1117	4.117E-02	90	
125-29			0.1117	4.117E-02	90	
125-30			0.1117	4.117E-02	90	
125-31			0.1117	4.180E-02	90	
125-32		SG primary side inlet	0.1191	5.216E-02	90	
125-33		--	0.1191	5.678E-02	90	
130-01	Pipe	PRZ	0.1153	6.411E-02	90	
130-02			0.1153	5.075E-02	90	
130-03			0.1153	6.567E-02	90	
130-04			0.1153	6.567E-02	90	
130-05			0.1153	6.567E-02	90	
130-06			8.2000E-02	4.878E-02	90	
SECONDARY SYSTEM						
200	Tmdpvol	FW Tank	--	--	--	
201	Tmdpjun	FW Pump	--	--	--	
202-01	Pipe	FW pipeline (fictitious)	0.2000	5.950E-02	0	
202-02			0.2000	5.950E-02	0	
202-03			0.2000	5.950E-02	0	

RELAP Component	RELAP Component Type	MASLWR Region	Length (m)	Area (m^2)	Vertical Angle (°)	Note
202-04			0.2000	5.950E-02	0	
202-05			0.2000	5.950E-02	0	
203	Valve	Inlet valve	--	--	--	
204	Branch	SG tube distributor	0.20	0.02780	0	
220-01	Pipe	SG tubes (equivalent)	0.2000	1.62E-03	0	
220-02			0.2000	1.62E-03	0	
220-03			0.2000	1.62E-03	0	
220-04			0.2000	1.62E-03	0	
220-05			0.2000	1.62E-03	0	
220-06			0.1922	1.62E-03	90	
220-07			0.1922	1.62E-03	90	
220-08			0.1922	1.62E-03	90	
220-09			0.1922	1.62E-03	90	
220-10			0.1922	1.62E-03	90	
220-11			0.1922	1.62E-03	90	
220-12			0.1922	1.62E-03	90	
220-13			0.1922	1.62E-03	90	
220-14			0.1922	1.62E-03	90	
220-15			0.1922	1.62E-03	90	
220-16			0.1922	1.62E-03	90	
220-17			0.1922	1.62E-03	90	
220-18			0.1922	1.62E-03	90	
220-19			0.1922	1.62E-03	90	
220-20			0.1922	1.62E-03	90	
220-21			0.1922	1.62E-03	90	
220-22			0.1922	1.62E-03	90	
220-23			0.1922	1.62E-03	90	
220-24			0.1922	1.62E-03	90	
220-25			0.1922	1.62E-03	90	
220-26			0.1922	1.62E-03	90	
220-27			0.1922	1.62E-03	90	
220-28			0.1922	1.62E-03	90	
220-29			0.1922	1.62E-03	90	
220-30			0.1922	1.62E-03	90	
220-31			0.1922	1.62E-03	90	
220-32			0.1922	1.62E-03	90	
220-33			0.1922	1.62E-03	90	
220-34			0.1922	1.62E-03	90	
220-35			0.1922	1.62E-03	90	
220-36			0.1922	1.62E-03	90	
220-37			0.1922	1.62E-03	90	
220-38			0.2000	1.62E-03	0	
220-39			0.2000	1.62E-03	0	

RELAP Component	RELAP Component Type	MASLWR Region	Length (m)	Area (m^2)	Vertical Angle (°)	Note
220-40			0.2000	1.62E-03	0	
220-41			0.2000	1.62E-03	0	
220-42			0.2000	1.62E-03	0	
221-01	Pipe	SG tubes (plugged)	0.2000	1.24E-04	0	
221-02			0.2000	1.24E-04	0	
221-03			0.2000	1.24E-04	0	
221-04			0.2000	1.24E-04	0	
221-05			0.2000	1.24E-04	0	
221-06			0.1922	1.24E-04	90	
221-07			0.1922	1.24E-04	90	
221-08			0.1922	1.24E-04	90	
221-09			0.1922	1.24E-04	90	
221-10			0.1922	1.24E-04	90	
221-11			0.1922	1.24E-04	90	
221-12			0.1922	1.24E-04	90	
221-13			0.1922	1.24E-04	90	
221-14			0.1922	1.24E-04	90	
221-15			0.1922	1.24E-04	90	
221-16			0.1922	1.24E-04	90	
221-17			0.1922	1.24E-04	90	
221-18			0.1922	1.24E-04	90	
221-19			0.1922	1.24E-04	90	
221-20			0.1922	1.24E-04	90	
221-21			0.1922	1.24E-04	90	
221-22			0.1922	1.24E-04	90	
221-23			0.1922	1.24E-04	90	
221-24			0.1922	1.24E-04	90	
221-25			0.1922	1.24E-04	90	
221-26			0.1922	1.24E-04	90	
221-27			0.1922	1.24E-04	90	
221-28			0.1922	1.24E-04	90	
221-29			0.1922	1.24E-04	90	
221-30			0.1922	1.24E-04	90	
221-31			0.1922	1.24E-04	90	
221-32			0.1922	1.24E-04	90	
221-33			0.1922	1.24E-04	90	
221-34			0.1922	1.24E-04	90	
221-35			0.1922	1.24E-04	90	
221-36			0.1922	1.24E-04	90	
221-37			0.1922	1.24E-04	90	
221-38			0.2000	1.24E-04	0	
221-39			0.2000	1.24E-04	0	
221-40			0.2000	1.24E-04	0	

RELAP Component	RELAP Component Type	MASLWR Region	Length (m)	Area (m^2)	Vertical Angle (°)	Note
221-41			0.2000	1.24E-04	0	
221-42			0.2000	1.24E-04	0	
240	Branch	SG collector (fictitious)	0.20	0.16980	0	
241	Valve	Regulation valve	--	--	--	
242	Tmdpvol	--	--	--	--	
HIGH PRESSURE CONTAINMENT SYSTEM						
400-01	Pipe	Lower cylindrical vessel outer part 1	0.2000	1.6130E-02	90	
400-02			0.1793	1.6130E-02	90	
400-03			0.2092	1.6130E-02	90	
400-04			0.2024	1.6130E-02	90	
401-01	Pipe	Lower cylindrical vessel inner part 1	0.2000	3.7630E-02	90	
401-02			0.1793	3.7630E-02	90	
401-03			0.2092	3.7630E-02	90	
401-04			0.2024	3.7630E-02	90	
402	Multiple Junction	Connections inner-outer	--	--	--	
405	Branch	Lower cylindrical vessel outer part 2	0.20920	0.01613	90	
406	Branch	Lower cylindrical vessel inner part 2	0.20920	0.03763	90	
410-01	Pipe	Lower cylindrical vessel outer part 3	0.2117	1.6130E-02	90	
410-02			0.1999	1.6130E-02	90	
411-01	Pipe	Lower cylindrical vessel inner part 3	0.2117	3.7630E-02	90	
411-02			0.1999	3.7630E-02	90	
412	Multiple Junction	Connections inner-outer	--	--	--	
415	Branch	Lower cylindrical vessel outer part 4	0.19405	0.01613	90	
416	Branch	Lower cylindrical vessel inner part 4	0.19405	0.03763	90	
420-01	Pipe	Lower cylindrical vessel outer and eccentric parts	0.2042	1.6130E-02	90	
420-02			0.2042	1.6130E-02	90	
420-03			0.2042	1.6130E-02	90	
420-04			0.2042	1.6130E-02	90	
420-05			0.2080	1.6130E-02	90	
420-06			0.2234	1.6130E-02	90	
420-07			0.2234	1.6130E-02	90	
420-08			0.2234	1.6130E-02	90	
420-09			0.2234	1.6130E-02	90	
420-10			0.2381	1.6130E-02	90	
420-11			0.3407	3.6140E-02	90	
420-12			0.2306	3.6140E-02	90	

RELAP Component	RELAP Component Type	MASLWR Region	Length (m)	Area (m^2)	Vertical Angle (°)	Note
421-01	Pipe	Lower cylindrical vessel inner and eccentric parts	0.2042	3.7630E-02	90	
421-02			0.2042	3.7630E-02	90	
421-03			0.2042	3.7630E-02	90	
421-04			0.2042	3.7630E-02	90	
421-05			0.2080	3.7630E-02	90	
421-06			0.2234	3.7630E-02	90	
421-07			0.2234	3.7630E-02	90	
421-08			0.2234	3.7630E-02	90	
421-09			0.2234	3.7630E-02	90	
421-10			0.2381	3.7630E-02	90	
421-11			0.3407	8.4320E-02	90	
421-12			0.2306	8.4320E-02	90	
422	Multiple Junction	Connections inner-outer	--	--	--	
425	Branch	Upper cylindrical vessel outer part 1	0.23056	0.05855	90	
426	Branch	Upper cylindrical vessel inner part 1	0.23056	0.13661	90	
430-01	Pipe	Upper cylindrical vessel outer part 2	0.2099	5.8550E-02	90	
430-02			0.2500	5.8550E-02	90	
430-03			0.3000	5.8550E-02	90	
430-04			0.2759	5.8550E-02	90	
431-01	Pipe	Upper cylindrical vessel inner part 2	0.2099	0.1366	90	
431-02			0.2500	0.1366	90	
431-03			0.3000	0.1366	90	
431-04			0.2759	0.1366	90	
432	Multiple Junction	Connections inner-outer	--	--	--	
435	Branch	Top cylindrical vessel outer part 1	0.17000	0.040985	90	
436	Branch	Top cylindrical vessel inner part 1	0.17000	0.095627	90	
440-01	Pipe	Vent line top (estimation based on drawings)	0.2500	3.1416E-04	90	
440-02			0.2500	3.1416E-04	90	
440-03			0.2500	3.1416E-04	0	
440-04			0.2500	3.1416E-04	-90	
440-05			0.2500	3.1416E-04	-90	
441	Valve	Relief valve	--	--	--	
442	Tmdpvol		--	--	--	
CONTAINMENT COOLING POOL						
500-01	Pipe	CPV inner part	0.3000	0.3087	90	
500-02			0.3000	0.3087	90	
500-03			0.2000	0.3087	90	

RELAP Component	RELAP Component Type	MASLWR Region	Length (m)	Area (m^2)	Vertical Angle (°)	Note
500-04			0.1793	0.3087	90	
500-05			0.2092	0.3087	90	
500-06			0.2024	0.3087	90	
500-07			0.2092	0.3087	90	
500-08			0.2117	0.3087	90	
500-09			0.1999	0.3087	90	
500-10			0.1941	0.3087	90	
500-11			0.2042	0.3087	90	
500-12			0.2042	0.3087	90	
500-13			0.2042	0.3087	90	
500-14			0.2042	0.3087	90	
500-15			0.2080	0.3087	90	
500-16			0.2234	0.3087	90	
500-17			0.2234	0.3087	90	
500-18			0.2234	0.3087	90	
500-19			0.2234	0.3087	90	
500-20			0.2381	0.3087	90	
500-21			0.3407	0.3087	90	
500-22			0.2306	0.3087	90	
500-23			0.2306	0.3087	90	
500-24			0.2099	0.3087	90	
500-25			0.2500	0.3087	90	
500-26			0.3000	0.3087	90	
500-27			0.2759	0.3087	90	
500-28			0.1700	0.3087	90	
500-29			0.1700	0.3087	90	
500-30			0.1700	0.3087	90	
500-31			0.1700	0.3087	90	
500-32			0.2350	0.3087	90	
501-01	Pipe	CPV outer part	0.3000	0.1323	90	
501-02			0.3000	0.1323	90	
501-03			0.2000	0.1323	90	
501-04			0.1793	0.1323	90	
501-05			0.2092	0.1323	90	
501-06			0.2024	0.1323	90	
501-07			0.2092	0.1323	90	
501-08			0.2117	0.1323	90	
501-09			0.1999	0.1323	90	
501-10			0.1941	0.1323	90	
501-11			0.2042	0.1323	90	
501-12			0.2042	0.1323	90	
501-13			0.2042	0.1323	90	
501-14			0.2042	0.1323	90	

RELAP Component	RELAP Component Type	MASLWR Region	Length (m)	Area (m^2)	Vertical Angle (°)	Note
501-15			0.2080	0.1323	90	
501-16			0.2234	0.1323	90	
501-17			0.2234	0.1323	90	
501-18			0.2234	0.1323	90	
501-19			0.2234	0.1323	90	
501-20			0.2381	0.1323	90	
501-21			0.3407	0.1323	90	
501-22			0.2306	0.1323	90	
501-23			0.2306	0.1323	90	
501-24			0.2099	0.1323	90	
501-25			0.2500	0.1323	90	
501-26			0.3000	0.1323	90	
501-27			0.2759	0.1323	90	
501-28			0.1700	0.1323	90	
501-29			0.1700	0.1323	90	
501-30			0.1700	0.1323	90	
501-31			0.1700	0.1323	90	
501-32			0.2350	0.1323	90	
502	Multiple Junction	Connections inner-outer	--	--	--	
AUTOMATIC DEPRESSURIZATION SYSTEMS						
300	Branch	SUMP line 1 inlet	0.18	6.95E-05	0	
301	Valve	SUMP valve 1	--	6.91 E-05	--	
302-01	Pipe	SUMP line 1	0.25000	0.000193	0	
302-02			0.25000	0.000193	0	
302-03			0.25000	0.000193	0	
302-04			0.25000	0.000193	0	
302-05			0.25000	0.000193	0	
302-06			0.25000	0.000193	0	
302-07			0.33000	0.000193	0	
302-08			0.33000	0.000193	0	
302-09			0.33000	0.000193	0	
302-10			0.33000	0.000193	0	
302-11			0.2092	0.000279	-90	
302-12			0.2024	0.000279	-90	
303	Sngljun	SUMP line 1 outlet	--	--	--	
320	Branch	SUMP line 2 inlet	0.18	6.95E-05	0	
321	Valve	SUMP valve 2	--	6.91 E-05	--	
322-01	Pipe	SUMP line 2	0.25000	0.000193	0	
322-02			0.25000	0.000193	0	
322-03			0.25000	0.000193	0	
322-04			0.25000	0.000193	0	
322-05			0.25000	0.000193	0	

RELAP Component	RELAP Component Type	MASLWR Region	Length (m)	Area (m^2)	Vertical Angle (°)	Note
322-06			0.25000	0.000193	0	
322-07			0.33000	0.000193	0	
322-08			0.33000	0.000193	0	
322-09			0.33000	0.000193	0	
322-10			0.33000	0.000193	0	
322-11			0.2092	0.000279	-90	
322-12			0.2024	0.000279	-90	
323	Sngljun	SUMP line 2 outlet	--	--	--	
310	Branch	ADS vent line 1 inlet	0.2600	6.95E-05	0	
311	Valve	ADS vent valve 1	--	3.17690E-5	--	
312-01	Pipe	ADS vent line 1	0.2300	0.000193	0	
312-02			0.2450	0.000193	0	
312-03			0.2450	0.000193	0	
312-04			0.2450	0.000193	0	
312-05			0.2450	0.000193	0	
312-06			0.2500	0.000193	0	
312-07			0.2600	0.000193	0	
312-08			0.2200	0.000279	0	
313	Sngljun	ADS vent line 1 outlet	--	--	--	
330	Branch	ADS vent line 2 inlet	0.2600	6.95E-05	0	
331	Valve	ADS vent valve 2	--	3.17690E-5	--	
332-01	Pipe	ADS vent line 2	0.2300	0.000193	0	
332-02			0.2450	0.000193	0	
332-03			0.2450	0.000193	0	
332-04			0.2450	0.000193	0	
332-05			0.2450	0.000193	0	
332-06			0.2500	0.000193	0	
332-07			0.2600	0.000193	0	
332-08			0.2200	0.000279	0	
333	Sngljun	ADS vent line 2 oulet	--	--	--	

Tab. 4.2 – OSU-MASLWR test facility nodalization: adopted code resources

#	QUANTITY	Unit	Value
1	Tot. No. of HYDR volumes	--	319
2	Tot. No. of HYDR junctions	--	378
3	Tot. No. of HYDR sub-volumes in the core	--	6
4	Tot. No. of heat structures	--	314
5	Tot. No. of mesh points in the heat structures	--	3310
6	Tot. No.of core active structures (radial x axial meshes)		17 x 6

Tab. 4.3 – OSU-MASLWR test facility configuration

#	SYSTEM	CHARACTERISTICS	STATUS (1)	REMARKS
1	ADS vent valve 1	Orifice flow area 3.177e-5m2	Active	Chocked flow model Henry Fauske
2	ADS vent valve 2	Orifice flow area 3.177e-5m2	Active	--
3	ADS valve 1	Orifice flow area 6.95E-5m2	Not operated	--
4	ADS valve 2	Orifice flow area 6.95E-5m2	Not operated	--
5	SUMP valve 1	Orifice flow area 6.90E-5m2	Active	--
6	SUMP valve 2	Orifice flow area 6.90E-5m2	Active	--
7	PRZ heaters	Power: 0 – 12kW Regulated with PI control based on primary pressure signal	Active	Dummy geometry
8	Core power	Power imposed in general table data	Active	--
9	HPC relief valve	Orifice flow area 0.0003m2 HPC pressure >1.99MPa: valve opened HPC pressure <1.82MPa: valve closed	Active	Dummy flow area Operated to avoid HPC overpressure
10	HPC heaters	--	Not operated	--
11	CPV relief valve	Orifice flow area 0.0003m2	Not operated	Dummy flow area Always open
12	FW	Imposed mass flow rate according with the specifications	Active	
13	FW valve	--	Not operated	The FW is imposed using a time dependent junction Always open
14	SL valve	--	Not operated	Always open

(1) consistent also with the experiments ISCP SP2 and SP3.

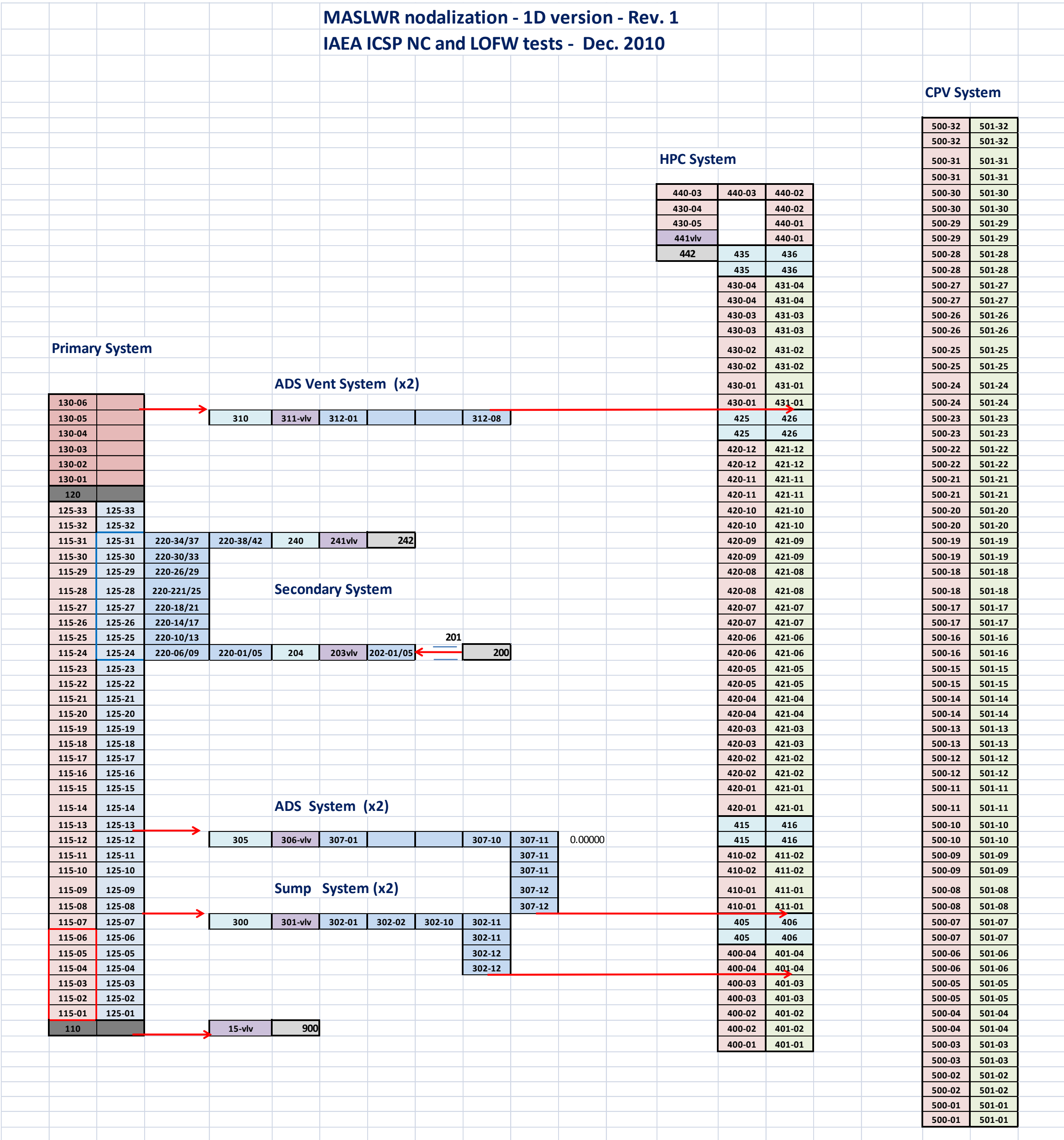

Fig. 4.1 – ENEA nodalization: overall sketch

5 QUALIFICATION OF THE NODALIZATION

The nodalization has been qualified by means of the blind simulations of two experiments: 1) a loss of FW flow postulated accident and, 2) a natural circulation test. The results of the simulations are briefly outlined hereafter. The complete set of imposed sequence of main events, boundary and initial conditions and results have been issued in the framework of the IAEA ICSP, see Refs. [12] and [14].

5.1 SP-2: Loss of Feedwater Transient with Subsequent ADS Operation and Long Term Cooling

5.1.1 Steady state results

The experimental and calculated initial conditions of the test SP-2 are reported in Tab. 5.1. The initial conditions of the simulation are achieved running the code for 5000s with the 'TRANSNT' (transient) option. The last 100s (from -100s up to 0s) have been considered to verify the stability of the parameter trends.

The lower parts of the HPC and of the CPV are initialized with liquid water at 0.101 MPa and 298 K. Therefore, the pressure in the bottom of these tanks is the atmospheric pressure plus the static head of the column of water. The upper volumes, above the liquid level free surface (Tab. 5.1), are initialized with nitrogen. The HPC is kept closed. Nevertheless a trip, which activates the SV-800 valve, is implemented on high pressure signal in HPC. The CPV system is kept open during the overall transient: the top of the tank is connected with the environment.

Steady state and initial conditions are achieved accordingly with the specifications. Few minor deviations are observed with the experimental results. The main difference is the core inlet temperature, which results underestimated (i.e. 5 K with respect to the specifications). It is observed a drift of the primary pressure of about 0.0015bar/s, during the last 100s. The temperatures of the coolant in primary system are stable.

5.1.2 Blind pretest results and preliminary analysis

The resulting sequence of main events is reported in Tab. 5.2. The times of the ADS valve 1 openings and closures are compared in Ref. [12]. Four phases and related phenomena are identified in the transient as hereafter reported (Tab. 5.2). The timing reported in parenthesis are referred to the code results.

1. **Phase 1** – *increase of energy in primary system (0-54s)*: from loss of FW up to the ADS vent valve 1 opening;
2. **Phase 2** – *primary system depressurization (54-168s)*: from the ADS vent valve 1 opening up to the high pressure signal in HPC;
3. **Phase 3** – *ADS vent valve 1 cycling (168-3882s)*: from the first high pressure signal in HPC up to the low pressure difference between primary system and HPC;

4. **Phase 4** – *long term cooling (3882-21812s)*: from the low pressure difference between primary system and HPC up to the end of transient.

The main parameter trends of the tests are reported from Fig. 5.1 to Fig. 5.6. The full set of comparisons is available in Refs. [12] and [14]. They are the parameter trends required in the output specifications of the IAEA ICSP benchmark.

The test starts (**phase 1**) with the primary system in single phase natural circulation. It implies no saturated void occurrence in the upper plenum of the system. The mass flow is driven from the balance between driving and resistant forces. Driving forces are the result of fluid density differences occurring between ascending (core side, inner zone) and descending sides (SG side, annular zone) of the main vessel. Resistant forces are due to irreversible friction pressure drops along the entire loop. Resulting fluid velocities are sufficient for removing core power in sub-cooled nucleate boiling or forced convection heat transfer regimes. The correct prediction of this phase is mainly connected with the calculation of the pressure drop in the system, thus the set up of the energy loss coefficients, and the calculation of the heat exchange across the core and the SG. It should be noted that, the heat transfer in covered core is correctly calculated by the code. On the contrary, model deficiencies (convective heat transfer in the inner SG tubes) and user effect are critical issues for the heat transfer across the SG and for the pressure drop evaluations. At time 0s, the FW pump is switched off according with the test specifications and the mass flow rate feeding the steam generator secondary side is 0 kg/s in 1 s. From this time on, the loss of heat sink causes the unbalance of energy in the primary system, and the primary pressure (Fig. 5.1) starts to rise. The rate of pressure increase is driven by the difference between the core power (plus the heaters power) and the heat losses with the environment (Fig. 5.6), assuming that the total mass inventory is correct (no experimental data is available). Once the first high pressure signal is met (Tab. 5.2), the electrical power is switched off (SCRAM), and it is imposed according with the specifications[13].

The coolant temperature difference across the core decreases rapidly (Fig. 5.3), nevertheless primary pressure continues to increase until the second high pressure signal in primary system is achieved. This is the set point of the ADS vent valve 1 opening and of PRZ heaters off (beginning of phase 2). The mass flow of steam discharged through the ADS vent valve 1 is calculated in the code by the chocked flow model at the valve. The model used in the simulation is Henry Fauske, which is expected to overestimate the single steam phase critical flow [15]. The opening of the valve at the top of the PRZ causes a large discharge of energy and a small discharge of mass from the primary system to the HPC as demonstrated by the pressure (Fig. 5.1) and the levels trends (Fig. 5.2). It should be noted that during the first discharge liquid water is transported through the break (two phase critical flow). Several phenomena occur during this phase: the critical flow across the ADS vent valve, the natural circulation in primary system, the heat transfer in covered core, the condensation of the vapor phase on the HPC wall and on the liquid free surface, the heat transfer across the HPC-CPV wall, thermal mixing and stratification in HPC and CPV, and the heat losses. Fig. 5.5 highlights the coolant temperature stratification in HPC. The correct prediction of the coolant thermal mixing and stratification phenomena cannot be accurately predicted by RELAP5 code. However, they can be roughly calculated by means of fictitious 3D modeling of the tank, based on parallel stack of pipes. The nodalization (or user) effect is expected to be crucial. Indeed, depending upon the nodalization scheme assumed the mixing can be limited or largely overestimated.

Once the high pressure signal in HPC is met the ADS vent valve 1 is closed (beginning of phase 3) to avoid the over pressurization of the system (Fig. 5.1). This implies that the primary pressure increases again, whereas the HPC pressure decreases because the heat exchanged through the plate with the CPV (besides the heat losses). This can be observed by the temperatures of the coolant and of the metallic structures of the HPC and CPV. When the HPC pressure drops below 1.48MPa the ADS vent valve 1 is opened again. The cycling of the valve across the two set point (1.82MPa closure and 1.48MPa opening) lasts until the pressure difference between the primary side and the HPC pressures is 0.034MPa. This event is calculated after 3882 s from the starting of the transient, thus slightly anticipated if compared with the experimental results. It represents the beginning of phase 4. The main phenomena expected during this phase are those already mentioned for phase 2. The correct prediction of this phase (main parameter trends) is connected with the correct simulation of the valve operation and the overall energy stored in the primary system, besides the reliable simulation of the valve flow rate and behavior of the HPC system (mixing and stratification in the pool and condensation on the liquid free surface and on the wall).

Phase 4 starts with the full opening of the SUMP and ADS vent valves (cooldown procedure). The primary and the HPC systems are connected. The flow circulation between the systems is effective to remove the electrical core power through the HPC-CPV wall. According with the code results, at the beginning of this phase, oscillatory voiding is observed at the top of the primary system, upstream the SG inlet and below the PRZ plate (Fig. 5.7). No CHF conditions are observed during the overall transient (Fig. 5.4). Main phenomena/processes expected during this phase are summarized in Tab. 5.2. The experiment is stopped at 15821s, with the primary system pressure equal to 0.51 MPa and the coolant temperature at core outlet equal to 160°C. After the same span of time the code simulation predicts a primary pressure equal to 0.35MPa and a coolant temperature of 135°C.

5.1.3 Summary of the results

The following conclusions apply.

- During the steady state calculation, the heat exchange across the helical-coil SG is correctly simulated. It should be noted that the heat exchange is calculated using a value of the fouling factor, in the inner tube side, different form the default.
- The main phenomena and parameters trends are well predicted and consistent with the expectations.
- Challenging for the code have been detected as following:
    - the SG heat exchange model, in particular when annular mist flow regime occurs in the SG tubes (specific model for helical-coil SG should be implemented);
    - mixing and thermal stratification in a pool system (only bounding analysis possible);
    - the condensation on the free surface and on the wall in presence of noncodensable (specific separate effect tests should be used for a quantitative evaluation);
    - the chocked flow;

- the coupling primary system containment and the presence of noncondensable in the HPC.

Tab. 5.1 – OSU-MASLWR Test SP-2: steady-state results

Parameter	OSU-MASLWR gage	Unit	Experiment	RELAP5
Pressurizer pressure	PT-301	MPa(a)	8.619 (gauge)	8.64 (abs)
Pressurizer level	LDP-301	m	0.3607	0.33
Power to core heater rods	KW-101/102	kW	--	297.3
Feedwater temperature	TF-501	ºC	21.4	20
Steam temperature	FVM-602-T	ºC	205.4	202
Steam pressure	FVM-602-P	MPa(a)	1.411	1.45 (abs)
Ambient air temperature	[redacted]	ºC	[redacted]	24
HPC pressure	PT-801	MPa(a)	0.0255 (gauge)	1.35 (abs)
HPC water temperature	TF-811	ºC	26.7	23.1
HPC water level	LDP-801	m	2.820	2.88
CPV water temperature	TF-815	ºC	27	23
Primary flow at core outlet	FDP-131	kg/s	--	1.48
Primary coolant temperature at core inlet	TF- 121/122/ 123/124	ºC	215.0	210
Primary coolant temperature at core outlet	TF-106	ºC	251.5	250
Feedwater flow	FMM-501	kg/s	--	0.1256
Steam flow	FVM-602-M	kg/s	--	0.1256
Primary coolant subcooling at core outlet	[redacted]	ºC	[redacted]	50
Total heat loss through primary system	[redacted]	kW	[redacted]	--
Heat transfer through SG	[redacted]	kW	[redacted]	278
Max. surface temp.of core heater rods	[redacted]	ºC	[redacted]	303
Location from the SG secondary inlet to reach - saturation - superheat	[redacted]	m	[redacted]	Heated length • (0-6.15) • 1.7 • 5.2

Tab. 5.2 –OSU-MASLWR Test SP-2: resulting sequence of main events

#	Ph.W.	Phenomena/Processes	Event	Time (s)	
				EXP	R5
1.1	**Phase I (0-54s)**	Pressure drop at discontinuities Wall to fluid friction Condensation in stratified conditions Global multidimensional coolant temperature and flow distribution Heat transfer in covered core Heat transfer in SG Heat transfer in passive structures and heat losses Parallel channel instability in SG tubes Single phase natural circulation in primary system	Start of simulation – steady state (start of data collection)	0	0
1.2			Stop MFP Close HPC vent valve SV-800	0	0
1.3			PT-301 (P_{PRZ}) = 9.064 MPa (a) (1300 psig) Enter decay power mode	36.2	37.4
2.4	**Phase II (54-168s)**	Pressure drop at discontinuities Wall to fluid friction Critical flow in valve (two phase and vapor phase) Single / two phase natural circulation in primary system Global multidimensional coolant temperature, void and flow distribution Pool TH in HPC and CPV Heat transfer in covered core Heat transfer across the HPC-CPV wall Heat transfer in passive structures and heat losses Thermal mixing and stratification in HPC and CPV Condensation in stratified conditions on the HPC wall and on the liquid free surface Non-condensable effect.	PT-301 (P_{PRZ}) = 9.409 MPa (a) (1350 psig) De-energize PZR heaters Open ADS vent valve (PCS-106A)	51	54
3.5	**Phase III (168-3882s)**	Pressure drop at discontinuities Wall to fluid friction Critical flow in valve (vapor phase) Single / two phase natural circulation in primary system Global multidimensional coolant temperature, void and flow distribution Pool TH in HPC and CPV Heat transfer in covered core Heat transfer across the HPC-CPV wall Heat transfer in passive structures and heat losses Thermal mixing and stratification in HPC and CPV Condensation in stratified conditions on the HPC wall and on the liquid free surface Non-condensable effect	1ST closure of ADS vent valve (PCS-106A)	131	168
3.6			Record opening and closing times for PCS-106A	Ref. [12]	
3.7			Record opening and closing times for SV-800	--	-- (always closed)
4.8	**Phase IV (3882-21812s)**	Pressure drop at discontinuities Wall to fluid friction Flow in valves (ADS - vapor and SUMP – liquid phases) Single / two phase natural circulation in primary system Boiler condenser mode in primary and HPC systems Global multidimensional coolant temperature, void and flow distribution Heat transfer in covered core Heat transfer across the HPC-CPV wall Heat transfer in passive structures and heat losses Thermal mixing and stratification in HPC and CPV Condensation in stratified conditions on the HPC wall and on the liquid free surface Non-condensable effect	Long-term cooling → PT-301 (P_{PRZ}) - PT-801 (P_{HPC}) < 0.034 MPa (5 psi) PCS-106A and PCS-106B opened PCS-108A and PCS-108B opened	4024	3882
4.9			End of test if (or): - PZR pressure ≤ 0.135 MPa(a) (5 psig) - Primary coolant temperature (TF-132) ≤ 35 ºC (95 ºF) - 5 hours have elapsed	15821 [P_{PZR}= 0.51MPa T_{PS}. = 160 °C]	15821 [P_{PZR} = 0.33MPa T_{PS}. = 145 °C]

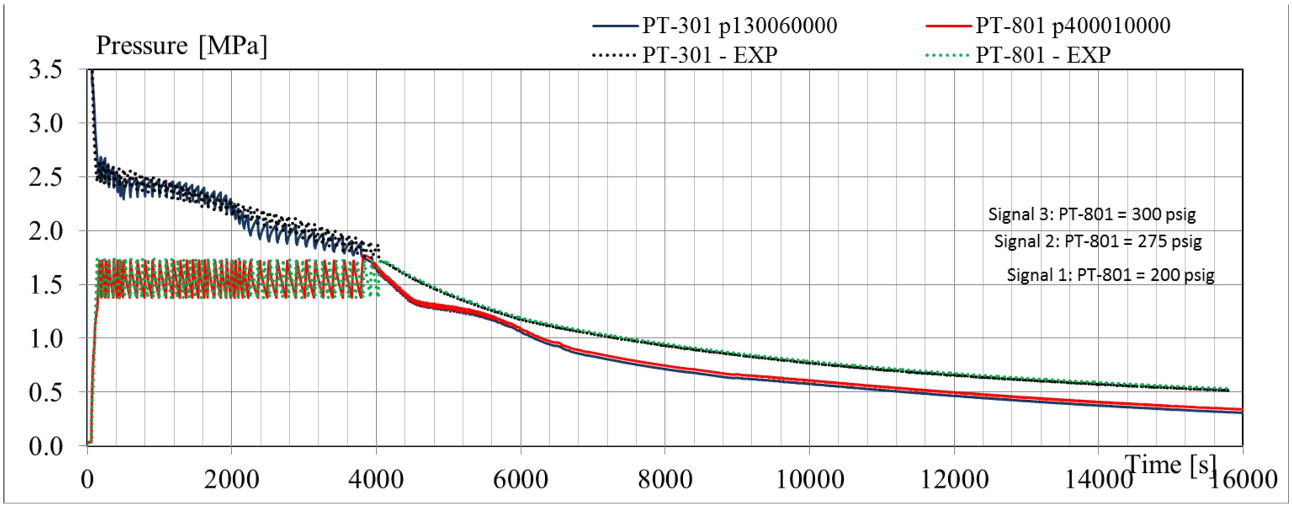

(a) Overall transient

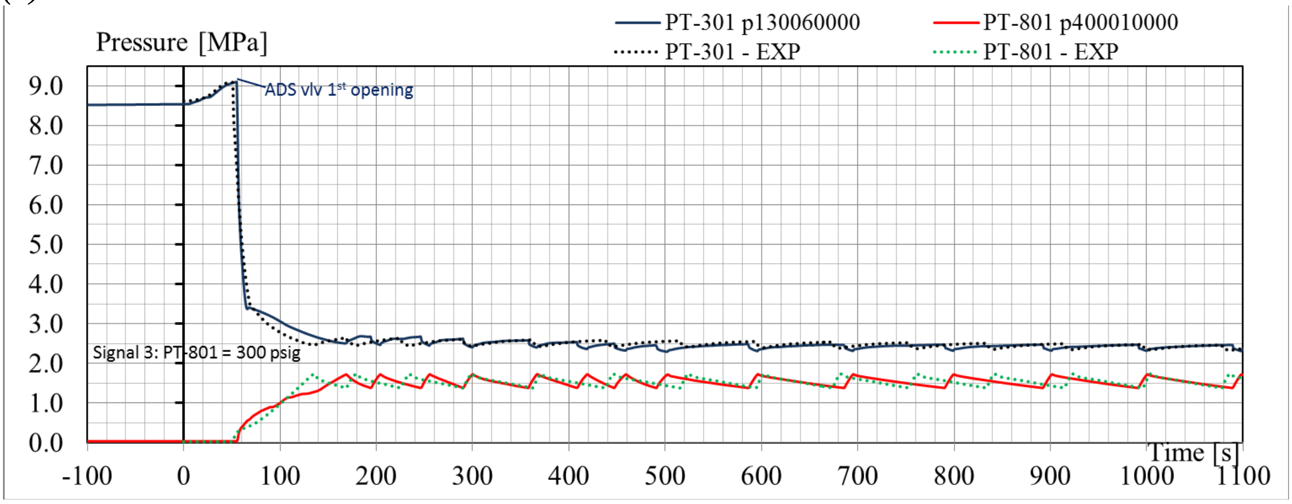

(b) From -100s to 1100s

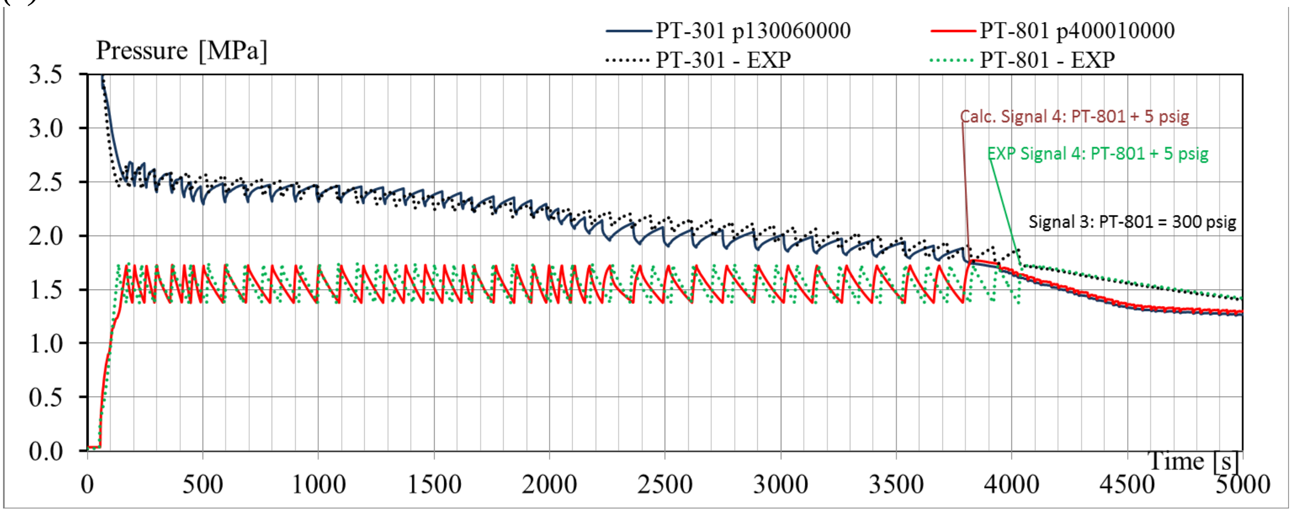

(c) From 000s to 5000s

Fig. 5.1 – Test SP2, blind pretest vs. experimental results: PS and HPC pressures

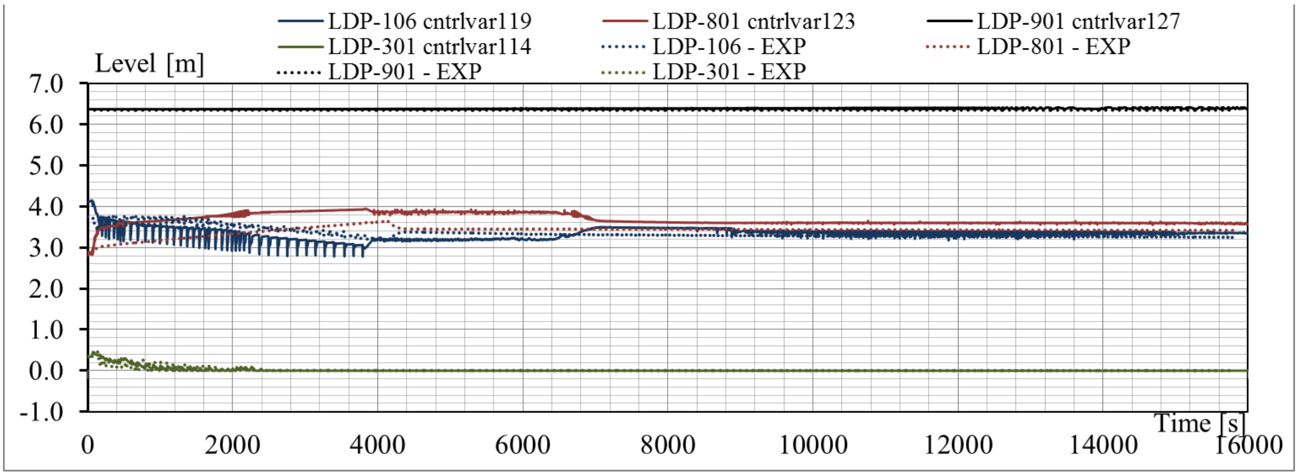

(a) Overall transient

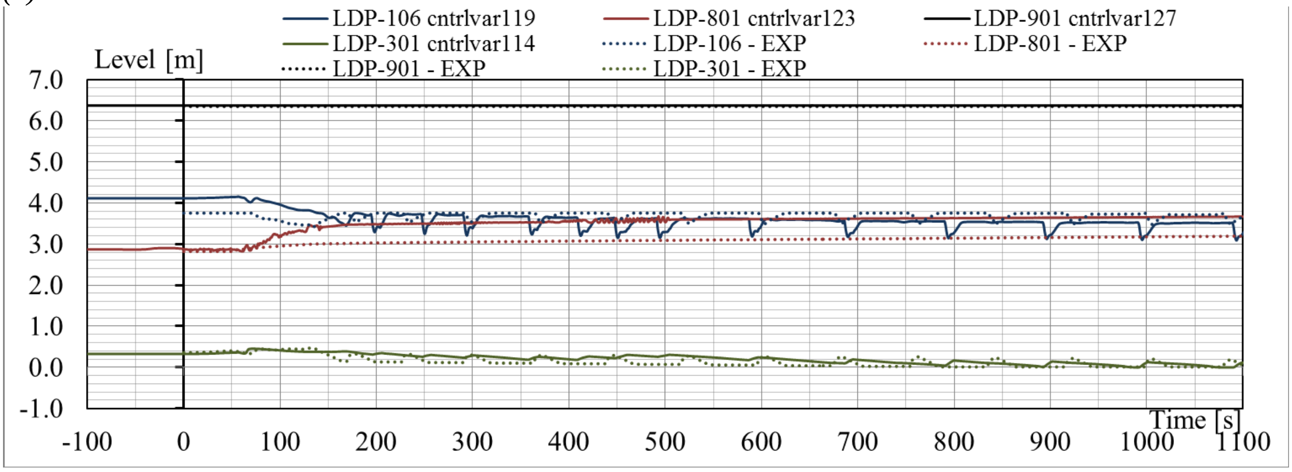

(b) From -100s to 1100s

Fig. 5.2 – Test SP2, blind pretest vs. experimental results: PS (blue), HPC (red), CPV (black) and PRZ (green) levels

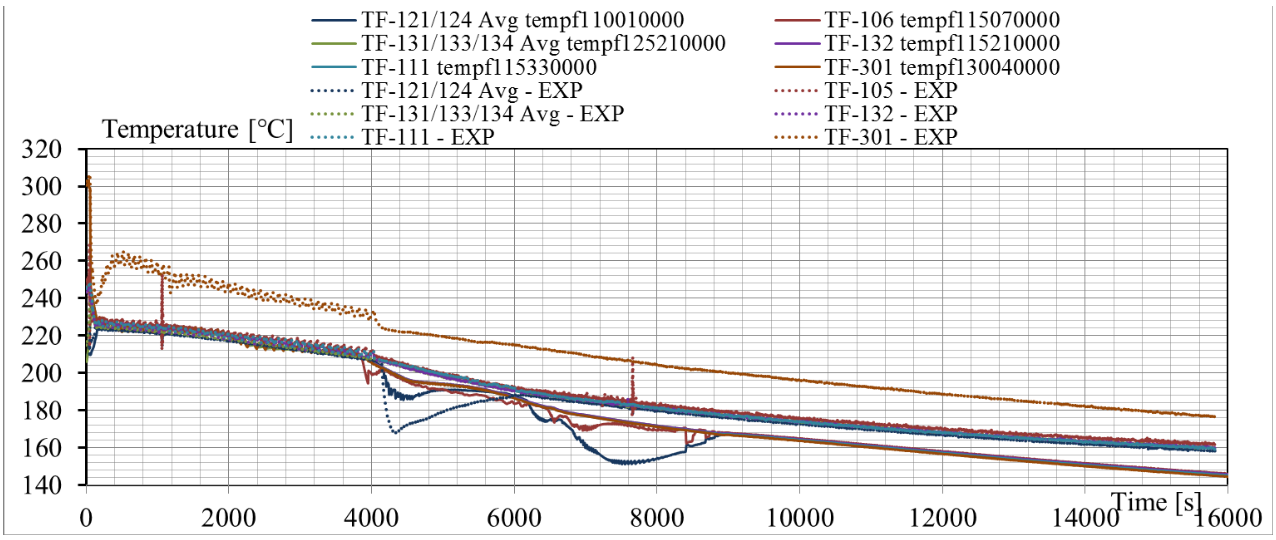

Fig. 5.3 – Test SP2, blind pretest vs. experimental results: primary system coolant temperatures, liquid phase (lower plenum, core outlet, SG outlet, riser, riser outlet and PRZ)

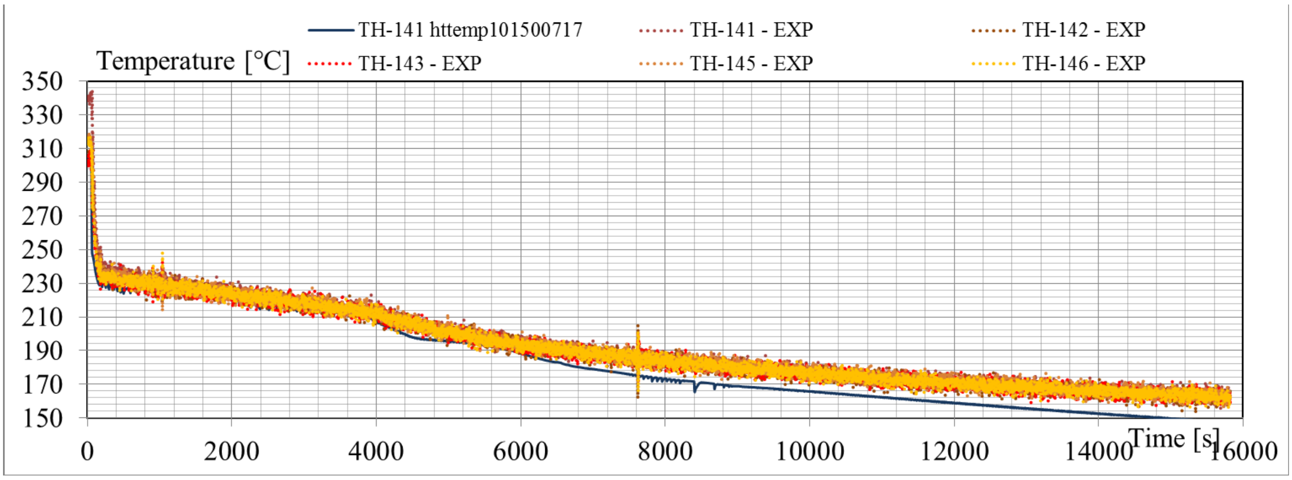

Fig. 5.4 – Test SP2, blind pretest vs. experimental results: cladding temperatures

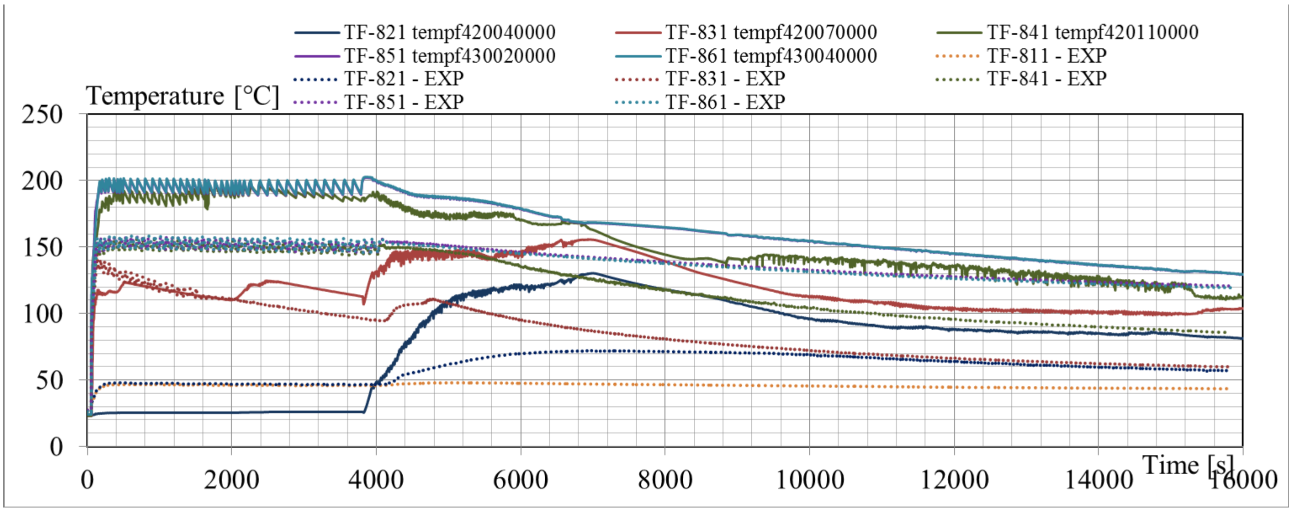

Fig. 5.5 – Test SP2, blind pretest vs. experimental results: HPC coolant temperatures

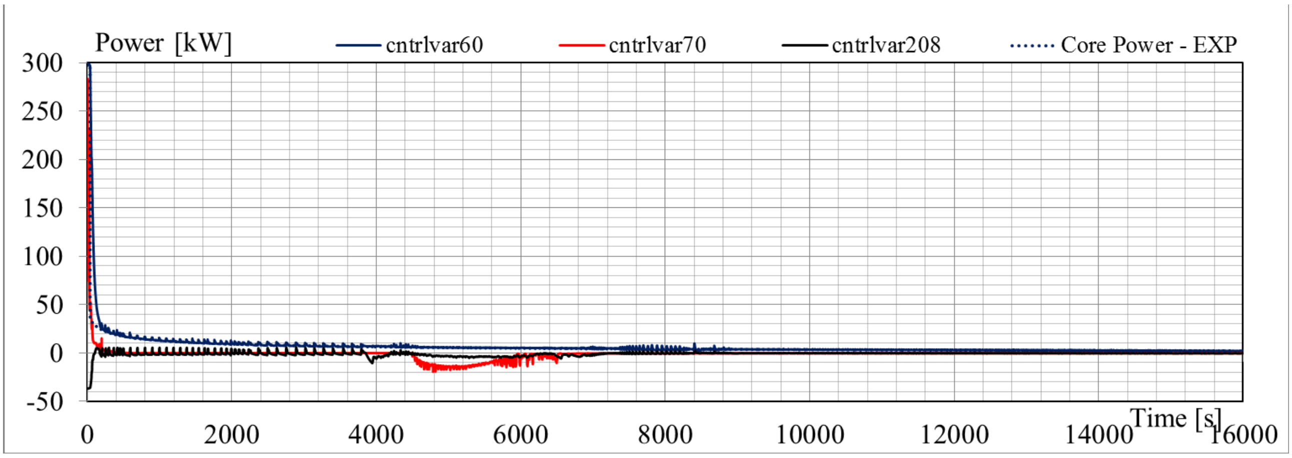

Fig. 5.6 – Test SP2, blind pretest vs. experimental results: core power (transfer to fluid for the code result and electrical power for the experimental trend) – cntrlvar60, SG power – cntrlvar70, power exchanged across the chimney – cntrlvar208.

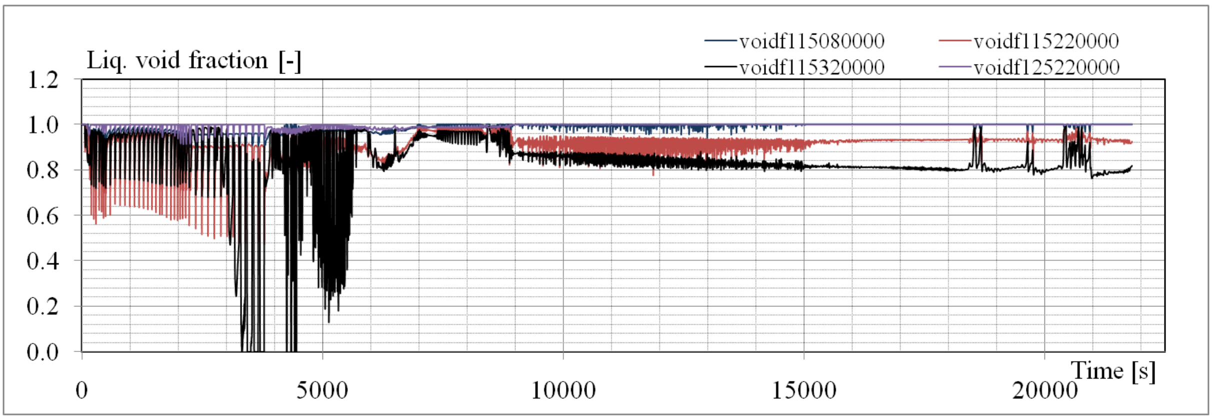

Fig. 5.7 – Test SP2, blind pretest: liquid void fraction core outlet, riser bottom, riser top, SG outlet

5.2 SP-3: Normal Operating Conditions at Different Power Levels

The experiment is a natural circulation test at different core power levels (from 40kW to 300kW). Only the primary and the secondary systems are involved in the analysis. Single phase natural circulation is expected in primary system.

The input deck of the test SP2 (section 5.1) has been used **without modifications** except for and improved implementation of the PI control for the PRZ heaters. This system is needed in the test to keep the pressure constant.

5.2.1 Steady state results

The initial conditions of the pretest SP-3 are reported in Tab. 5.3. They are achieved running the code for 3000s with the 'TRANSNT' (transient) option. The last 100s (from -100s up to 0s) of the calculation are used to verify the stability of the parameter trends.

Steady state and initial conditions are achieved accordingly with the specifications of Ref. [13]. Few minor deviations are observed. The main difference is the temperature of the vapor at SG outlet. The calculated temperature is 260°C, which corresponds to the most frequently measured temperatures at the outlet of the SG tubes. Nevertheless, it largely differs from the main steam line temperature transducers, which measures a temperature about 55 °C lower. Indeed, according with the explanations given by OSU[16], the experimental facility has two steam line (i.e. small and large steam lines). One is used during the start-up phase and the second during the experiment. The steam line temperature (transducer FVM-602-T) records the temperature of the large steam line, which was opened few minutes before the starting of the experiment and therefore of recording. It means that the metallic structures were not in thermal equilibrium with the steam phase flowing from the SG tubes. This implies that due to the inertia of the cold metallic structures, the experimental value of the temperature measured by the transducer FVM-602-T was not reliable during the first part of the test.

Stationary conditions are considered achieved in the code simulation. Nevertheless, the coolant temperature calculated in the primary system at core inlet rises with a rate of about 0.004°C/s. This can be explained with a not correct calculation of the heat exchange from primary to secondary systems.

Nevertheless, it should be noted that the thermal balance with the data provided in the specifications (before the experimental data were issued) implies a “quasi” steady state condition achievable only if the heat losses are larger than 11kW (about double than in the RELAP5 model, in which the heat losses are consistent with Ref. [16]). Indeed, the power removed by the SG in the experiment is less than 29kW. It is calculated assuming that the superheated steam at the outlet of all tubes is 262°C (which is an assumption that provides an upper bound of the heat exchange). Assuming (conservatively) that the pressurizer heaters are switched off (power equal to 0 kW), and considering that the core power is 40kW, the balance of power in the system is achieved with 11kW of heat losses. According with Ref. [16], the heat losses of OSU-MASLWR facility are estimated in these conditions about 5 – 6 kW. Therefore, it is reasonable the unbalance calculated by the code.

5.2.2 Blind pretest results and preliminary analysis

The simulation is set up imposing the core power, the FW flow and temperature versus time (as they were provided in Ref. [13]).

The main parameter trends are reported from Fig. 5.8 to Fig. 5.15. The full set of comparisons is available in Refs. [12] and [14]. They are the parameter trends required in the output specifications of the IAEA ICSP benchmark.

The expected phenomena and processes are the same during the overall test, as following summarized:

- Pressure drop at discontinuities
- Wall to fluid friction
- Condensation in stratified conditions (in PRZ)
- Global multidimensional coolant temperature and flow distribution
- Heat transfer in covered core
- Heat transfer in SG
- Heat transfer in passive structures and heat losses
- Parallel channel instability in SG tubes
- Single phase natural circulation in primary system

The test starts with the system in single phase natural circulation. Imposed core power is available in Fig. 5.15. The mass flow (Fig. 5.14) is driven from the balance between driving and resistant forces (see also the description in sect. 5.1.2). Driving forces are the result of fluid density differences. Resistant forces are due to irreversible friction pressure drops along the entire loop. Resulting fluid velocities are sufficient for removing core power. The correct prediction of this phase is mainly connected with the calculation of the pressure drop in the system (calculated using the same input parameters as in test SP2), and the calculation of the heat exchange across the core and the SG. Same considerations as for test SP2 applies.

No steady state conditions are achieved from about 1000s up to about 3000s (power range 120kW - 200kW). Pseudo stationary conditions are roughly achieved for the others power levels. The duration of each plateau would be longer to ensure the parameter trends are stabilized, with particular regards to the SG steam temperatures at tubes outlet (Fig. 5.12) and in the steam line (Fig. 5.11). The sub-cooling at core outlet limits (20 and 15°C) defined in the specifications are always respected (see Fig. 5.13). However, the unbalance of power is confirmed, as stated above. This highlights that the convective heat transfer model of RELAP5 code is affected by an evident underprediction of the heat exchange (Fig. 5.12).

The experimental FW flow (Fig. 5.9 and Fig. 5.10) between 2700s and 3700s is inconsistent with the overall power to be removed. As consequences, during this time the primary pressure (Fig. 5.8) is kept constant by PRZ heaters in the test and in the simulation, Ref. [13].

The PRZ level trend follows the energy of the primary pressure. The FW temperature is imposed according with the specification and the SL temperature corresponds with the saturation see Refs. [12] and [14].

No CHF conditions are met in the pretest simulations as well as in the experimental results.

5.2.3 Summary of the results

The following observations apply comparing the code results with the experimental data.

- Pseudo stationary conditions are achieved during steady state: indeed the coolant temperature in primary system increase with a rate of about 0.004°C/s. The coolant temperature at SG outlet calculated by the code is 262°C seems reasonable, as recorded by the gauges at SG tubes outlet.
- The main phenomena and parameters trends are well predicted and consistent with the expectations.
- Reasonable behavior of the heat exchange primary to secondary is observed at the lower and higher powers (i.e. <80kW and 280 – 320kW). Larger errors are detected for the other power values. It should be reminded that the RELAP5 model is not optimized to simulate the convective heat transfer in the helical coil steam generator tubes inner side. New correlation would be needed to improve the results.

Tab. 5.3 – OSU-MASLWR Test SP-3: steady-state results

Parameter	OSU-MASLWR gage	Unit	Experiment	RELAP5
Pressurizer pressure	PT-301	MPa	8.618 (gage)	8.70
Pressurizer level	LDP-301	m	0.3574	0.347
Power to core heater rods	KW-101/102	kW	40	40
Feedwater temperature	TF-501	ºC	31.49	31
Steam temperature	FVM-602-T	ºC	205.44 (from 242 to 260°C in tubes)	262
Steam pressure	FVM-602-P	MPa	1.446	1.45
Ambient air temperature	[redacted]	ºC	[redacted]	24
Primary flow at core outlet	FDP-131	kg/s		0.677
Primary coolant temperature at core inlet	TF-121/122/123/124	ºC	250	253.0
Primary coolant temperature at core outlet	TF-106	ºC	262.76	264.8
Feedwater flow	FMM-501	kg/s	0.010213	0.0102
Steam flow	FVM-602-M	kg/s	--	0.0102
Primary coolant subcooling at core outlet	[redacted]	ºC	[redacted]	36.5
Total heat loss through primary system	[redacted]	kW	[redacted]	6.7
Heat transfer through SG	[redacted]	kW	[redacted]	29
Maximum surface temperature of core heater rods	[redacted]	ºC	[redacted]	264.9
Location from the SG secondary inlet to reach - saturation - superheat	[redacted]	m	[redacted]	Heated length (0-6.15) 0.38 0.96

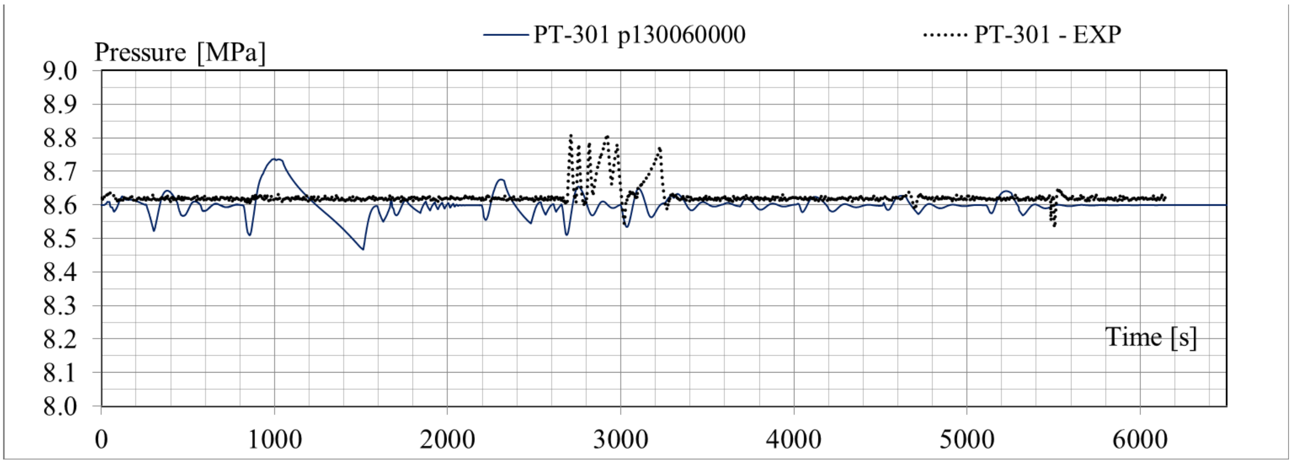

Fig. 5.8 – Test SP3, blind pretest vs. experimental results: PS pressure

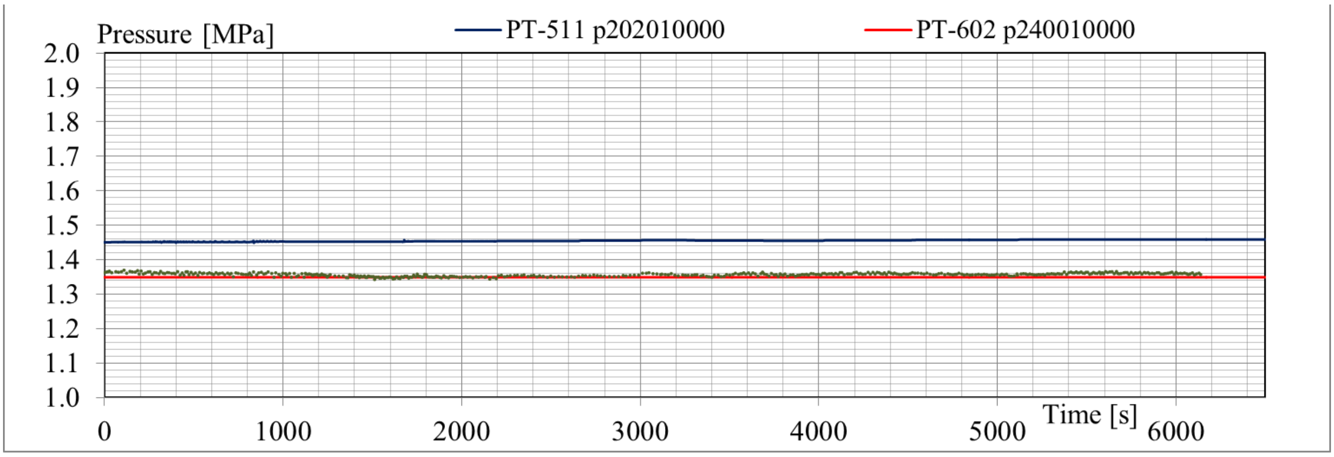

Fig. 5.9 – Test SP3, blind pretest vs. experimental results: steam generator inlet (only experimental) and outlet pressures

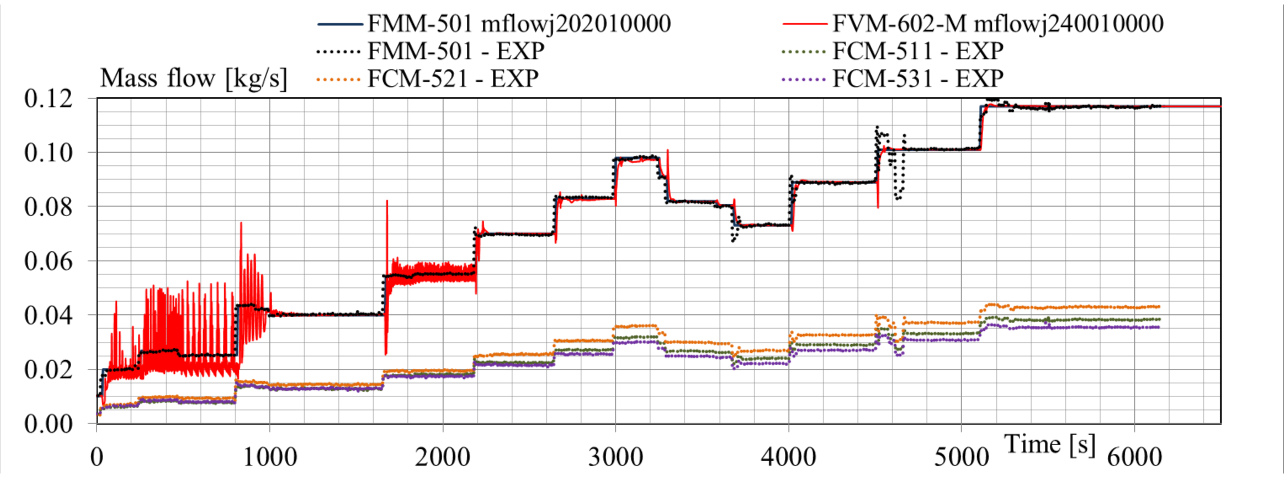

Fig. 5.10 – Test SP3, blind pretest vs. experimental results: FW total mass flow rate, FW inner/central and outer tubes (experimental trends) mass flow rate and SG outlet (calculated value) mass flow rate

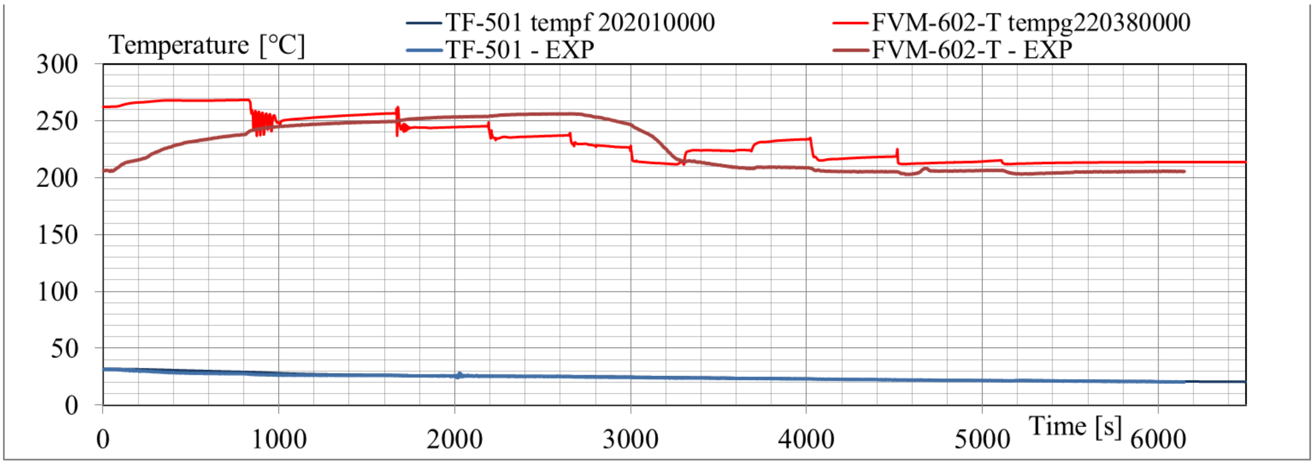

Fig. 5.11 – Test SP3, blind pretest vs. experimental results: FW and steam line temperatures

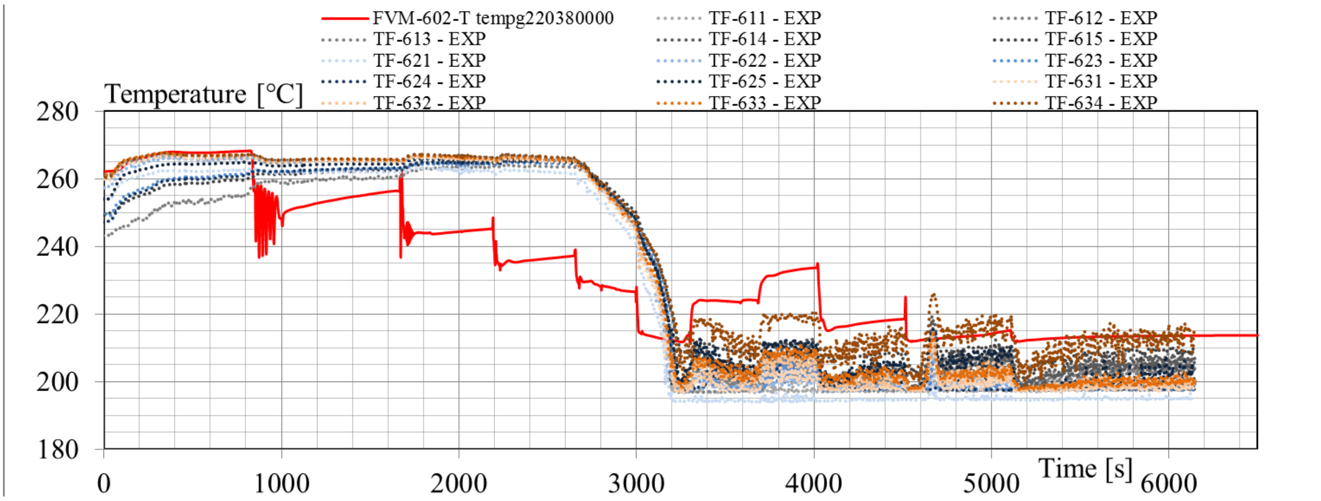

Fig. 5.12 – Test SP3, blind pretest vs. experimental results: calculated steam temperature at SG outlet and SG tubes outlet fluid temperatures

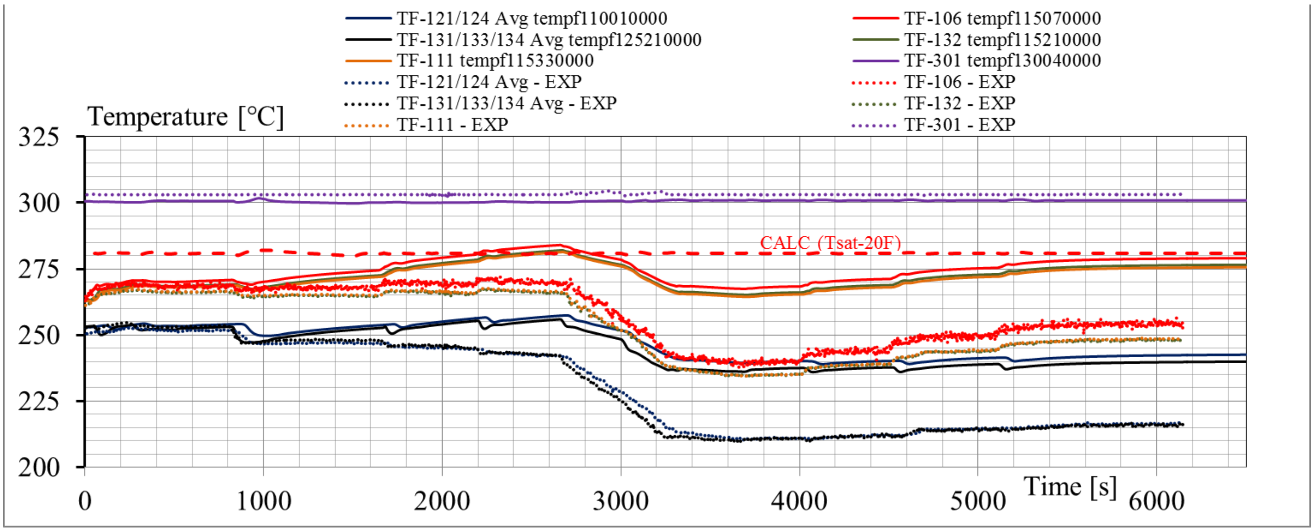

Fig. 5.13 – Test SP3, blind pretest vs. experimental results: primary system coolant temperature, liquid phase (lower plenum, core outlet, SG outlet, riser, riser outlet and PRZ)

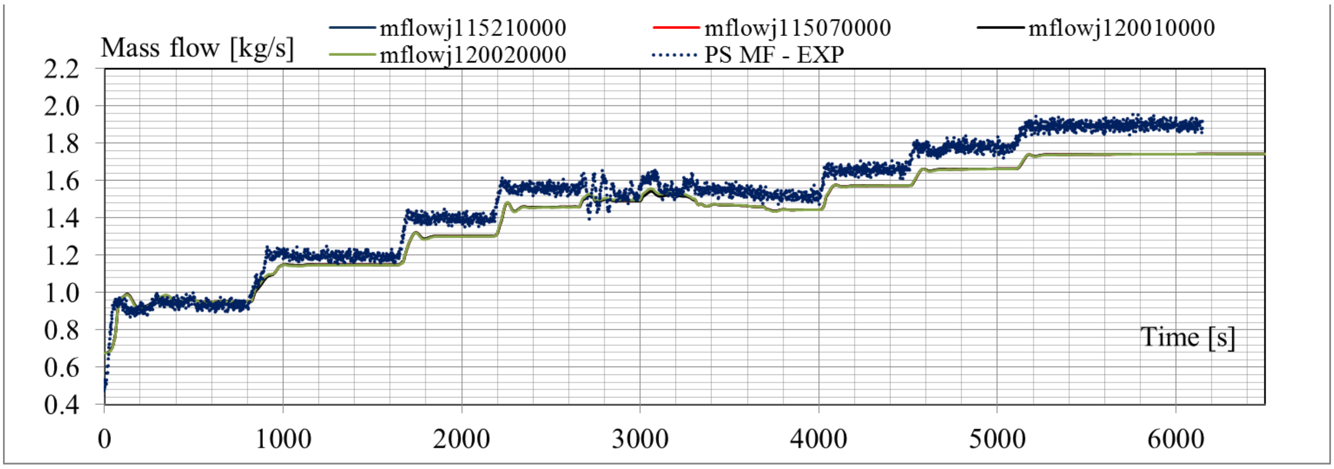

Fig. 5.14 – Test SP3, blind pretest vs. experimental results: primary system mass flow rate (core inlet, outlet chimney outlet SG inlet)

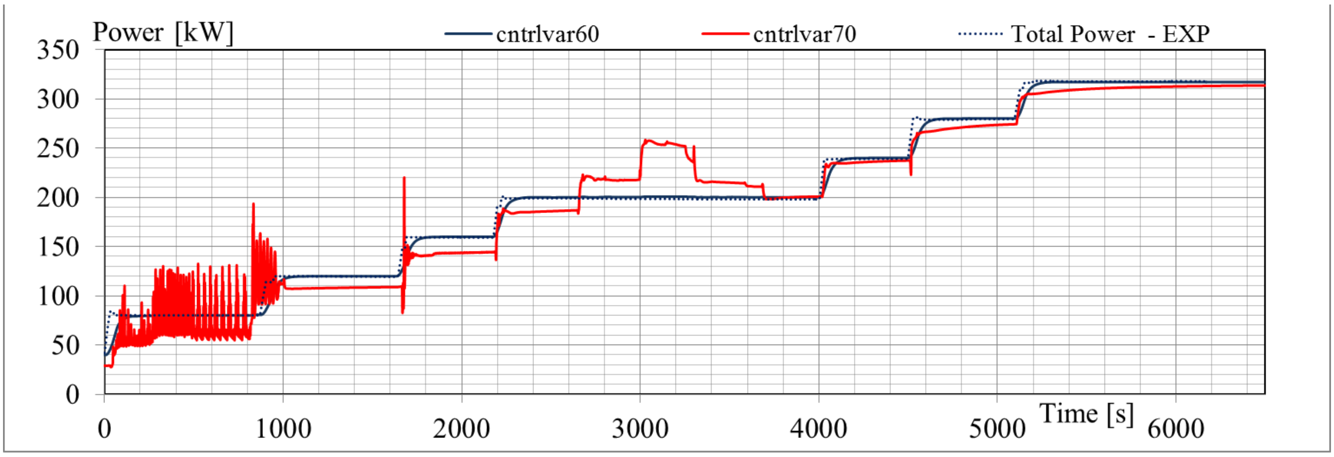

Fig. 5.15 – Test SP3, blind pretest vs. experimental results: calculated core power - cntrlvar60 (transfer to fluid), calculated SG power cntrlvar70, experimental electrical power

6 ANALYSIS OF A STATION BLACKOUT ACCIDENT SCENARIO

This application does not have any objective to provide judgments on the performance of the MASLWR NPP design as well as to any other SMR design. Indeed, the logics of the safety systems (i.e. set point and operation) involved are based on the specifications applied in the framework of the double blind and of the blind calculations of the ICSP and they are not representative of any SMR.

The RELAP5 nodalization has been applied to investigate the behavior of an integral passive reactor design in case of complete station blackout and the main phenomena occurring during this sequence. The analyses of the results is aimed at improving the level of understanding of the complex interaction between primary system and containment. The OSU-MASLWR nodalization was modified according with the following assumptions: 1) the heat losses were completely neglected; 2) the reference power for the decay heat is based on the nominal power (i.e. 150MWth); 3) the decay heat curve is imposed for the analyses using the ANS 1979 + 2σ standard for infinite operating time; 4) the decay heat curve is increased preserving the integral energy to account for the lower steady state power (i.e. 300kWth instead of 600kWth).

The analyses were performed with the objective to demonstrate that the system is able to cope with the postulated accident scenario for 7 days without the intervention of any active system (i.e. in this case the activation of the sump pumps for the use of SG in decay heat power mode was disregard).

The following parameters were of major interest for the analysis: 1) CHF conditions in the core; 2) the HPC pressure below the high pressure signal for the SV-800 valve opening, set point at 2MPa; 3) the total amount of water evaporated from the CPV.

The steady state is achieved after 1000s seconds of null transient. Tab. 6.1 reports the initial conditions, when the initiating event occurs. Tab. 6.2 provides the imposed sequence of main events of the simulation.

6.1 Transient results

The postulated accident, SBO, occurs at time 0s. As consequence, the core power is switched in decay mode, the FW pump is stopped (see Fig. 6.1 and Fig. 6.2), and the pressurizer heaters are not anymore available. The systems considered in the simulation are: the ASD vent valve 1 and 2, the sump valves 1 and 2 and the HPC relief valve SV-800. The coolant temperature difference across the core constantly decrease (Fig. 6.6b), because the power is off (Fig. 6.11), until about 100s, when they are almost equalized. The complete loss of heat sink causes a constant increase of primary pressure (Fig. 6.4b) up to 1080s, when the set point of high pressure in primary system is met. The complete opening of the ADS vent valve 1 (see Fig. 6.8b) causes a sharp decrease of the primary system pressure and the simultaneous increase of the HPC pressure and temperature (Fig. 6.9). Liquid phase flows across the valve, as highlighted by Fig. 6.5b and Fig. 6.8b. According with the reference procedure, reported in

Tab. 6.2, the valve ADS vent valve 1 is closed about 100s after its opening, on high pressure signal in HPC (1.8MPa), to avoid the overpressure. Indeed, the HPC is designed for a maximum allowed pressure of 2MPa and a safety valve (SV-800) placed on the top of system is open to ensure its structural integrity.

Following the isolation, the primary system pressure starts to rise until the ADS vent valve 1 is opened again. Indeed this valve, which is in charge to depressurize the primary system during this phase, is controlled on two set point based on the HPC containment pressure. The cycling of the valve lasts about 18000s (5 hours). During this time, the HPC pressure remains always below 2MPa and the average primary system pressure decreases constantly up to about 1.8MPa, thanks to the heat exchanged across the wall between the HPC and CPV (see Fig. 6.9 and Fig. 6.10). When the primary system and the HPC pressures are equalized (Fig. 6.4c), the long term cooling procedure is activated. During this phase the primary system mass flow rate is at rest, with the exception of some spikes corresponding with the cycling of the ADS vent vale (Fig. 6.7c). According with the simulation results, non CHF conditions are experienced in the core during the primary system depressurization phase (Fig. 6.3).

The long term procedure consists of a full opening of the ADS vent and the sump valves (5h19min after the start of transient). The primary and HPC systems level differences are drastically reduced (Fig. 6.5c). The coolant temperature stratification in HPC is reduced because mixing up of the water (Fig. 6.9). The entrance of colder water through the sump valves causes a coolant temperature and pressure decrease of the primary system (Fig. 6.6c). Then, after about 8h primary pressure is roughly stabilized at 0.4MPa. The heat exchanged across the wall between the HPC and CPV is of primarily importance to effectively cooldown the primary system during this phase. The CPV water remains subcooled for a time span larger than 32h (see Fig. 6.10). After that, it starts to evaporate until the end of the transient. The simulation is terminated after 7days of simulation, with the primary and containment pressure and temperature equal to 0.2MPa and about 393K. The total amount of water evaporated in the CPV is 540kg.

The resulting sequence of main events is reported in Tab. 6.2)

6.2 Summary

The following main observations are pointed out on the basis of the simulation.

1. The selected procedure is effective in coping a station blackout postulated event for 7 days. The long term cooling conditions are achieved and maintained starting from the nominal conditions. The coupled primary and containment system remains isolated during the overall transient.
2. It is observed a liquid phase flowing through ADS valve 1 during its first opening. This is might cause the valve stuck open, thus the impossibility to isolate the primary system when the HPC pressure limit is reached. During the other operations, the valve experiences steam phase flow rate.
3. The automatic depressurization procedure of the primary system is able to reach the conditions for the long term cooling procedure without any operator action, any CHF occurrence in the core, and maintaining the HPC system below the maximum design pressure (no opening of the safety valve SV-800).
4. The long term cooldown based on the heat exchanged across the wall between the HPC and CPV causes a total evaporation equal to 540kg. On the basis of the scaling

principle of the system, this would correspond to amount 140tons of water evaporated in an real NPP system.

Tab. 6.1 – Simulation of SBO transient: steady-state results

#	Parameter	Unit	RELAP5
1	Pressurizer pressure	MPa	8.70
2	Pressurizer level	m	0.35
3	Core power	kW	300
4	Primary coolant temperature at core outlet	ºC	10
5	Primary system mass flow rate	kg/s	--
6	Secondary system pressure	MPa	1.45
7	Feedwater flow	kg/s	0.0102
8	Feedwater temperature	ºC	30

Tab. 6.2 – Simulation of SBO transient: imposed and resulting sequence of main events

#	Event description	Trip	RELAP5 simulation (s)	Note
1	Postulated initiating event - SBO	--	0	Imposed
2	Main feed water pump stops	--	0	Imposed
3	Power dacay mode - SCRAM	--	0	Imposed
4	PRZ heaters off	--	0	Imposed
5	ADS vent valve 1 first opening (high pressure signal in primary system)	P_{PRZ} = 9.41 MPa	1080	--
6	HPC opening (high high pressure signal in HPC)	P_{HPC} = 2.00 MPa	--	--
7	ADS vent valve 1 operation (after the first opening - depressurizaion of primary system.) – first closure and second opening closure (pressure signal in HPC) opening (high pressure signal in HPC)	$P_{HPC\_closure}$ = 1.50 MPa $P_{HPC\_opening}$ = 1.80 MPa	1180 1160	Start of ADS vent valve 1cycling
8	ADS vent valve 1 operation – last opening and closure closure (pressure signal in HPC) opening (high pressure signal in HPC)	$P_{HPC\_closure}$ = 1.50 MPa $P_{HPC\_opening}$ = 1.80 MPa	19140 19025	End of ADS vent valve 1 cycling
9	Sump valves 1 and 2 opening – long term cooling procedure	P_{PRZ} - P_{HPC} = 0.034MPa	19160 (5h19min)	Remain open
10	ADS vent valves 1 and 2 fully opening – long term cooling procedure	P_{PRZ} - P_{HPC} = 0.034MPa	19160 (5h19min)	Remain open
11	Occurrence of saturation in CPV	--	117500 (32h38min)	Atmosferic pressure
12	End of calculation	--	650000 (>7day)	Imposed P_{PRZ} = 0.2MPa $T_{coolant\_PS}$ = 395K $T_{coolant\_HPC}$ = 393K Mass lost in CPV 540kg

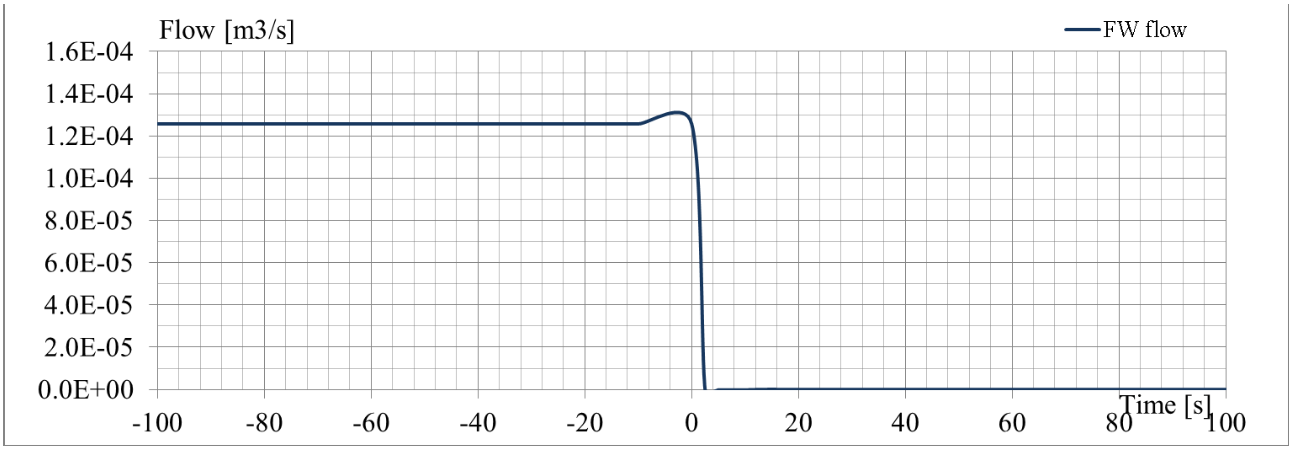

Fig. 6.1 – Simulation of SBO transient: main FW flow

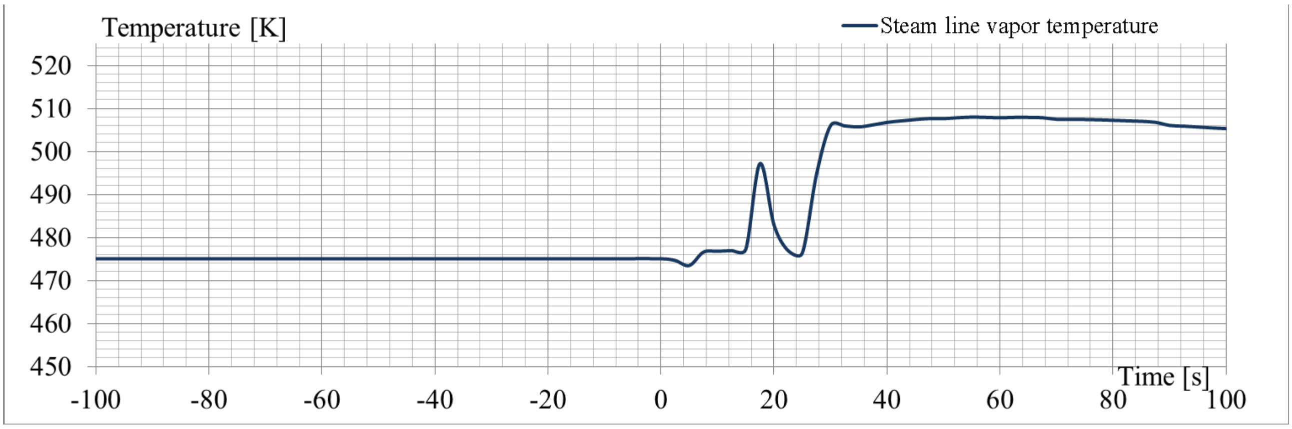

Fig. 6.2 – Simulation of SBO transient: steam line coolant temperature

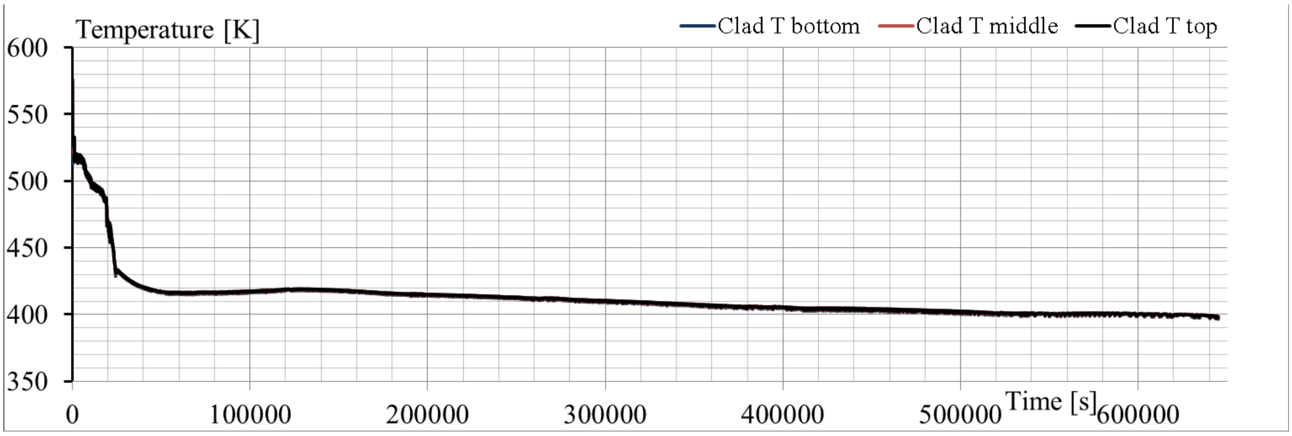

Fig. 6.3 – Simulation of SBO transient: cladding temperature

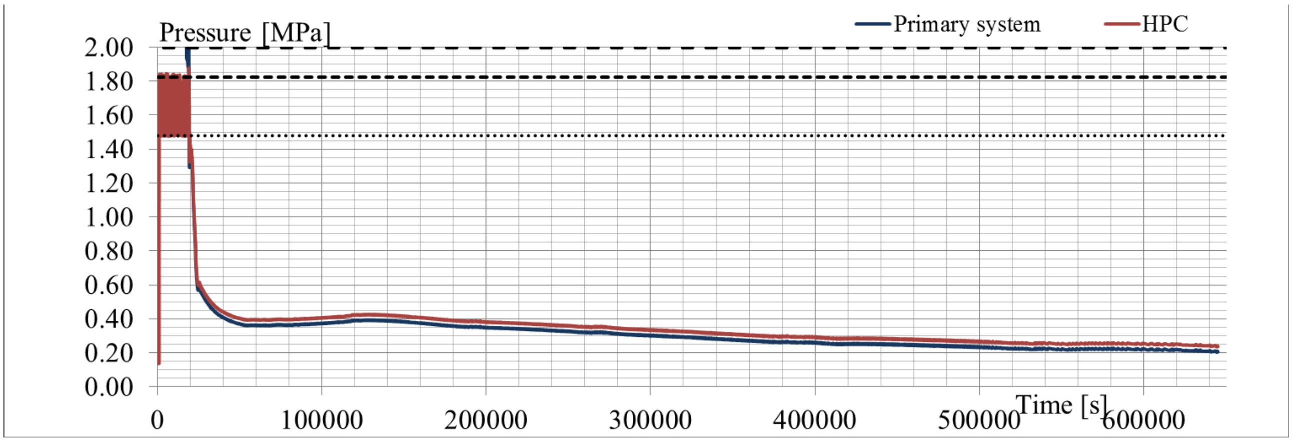

(a) Overall transient, max pressure of y axses 1MP

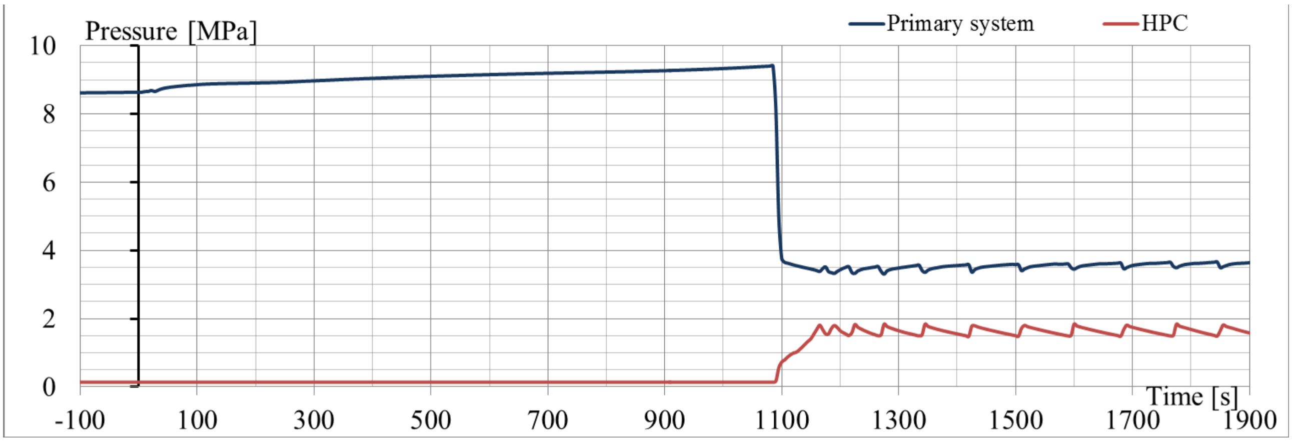

(b) From -100s to 1900s

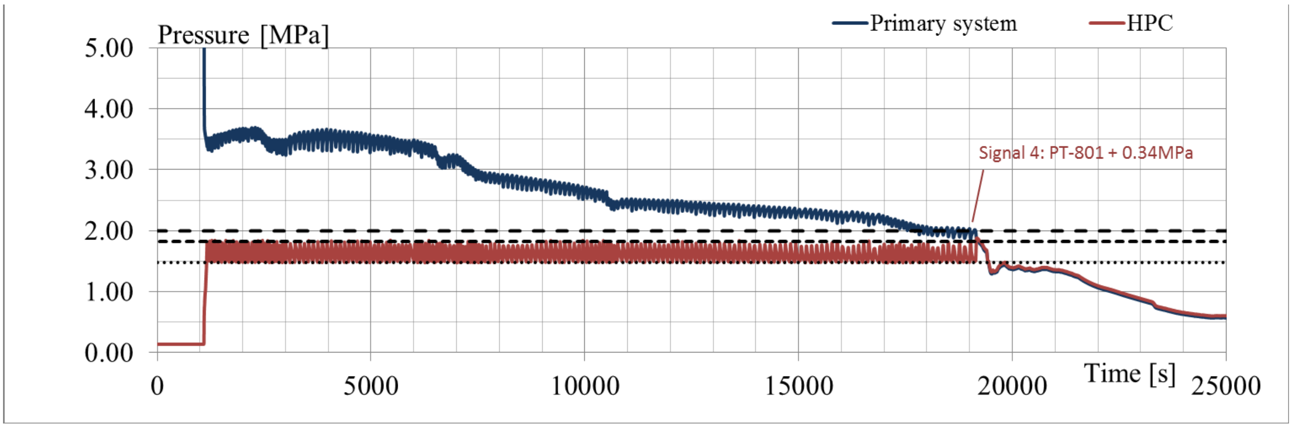

(c) From 0s to 25000s

Fig. 6.4 – Simulation of SBO transient: PS and HPC pressures

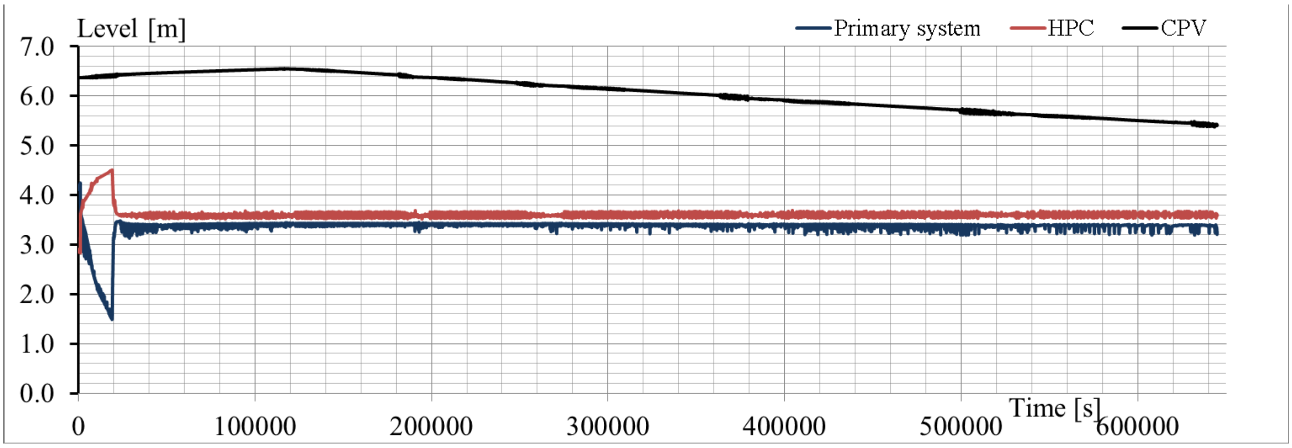

(a) Overall transient

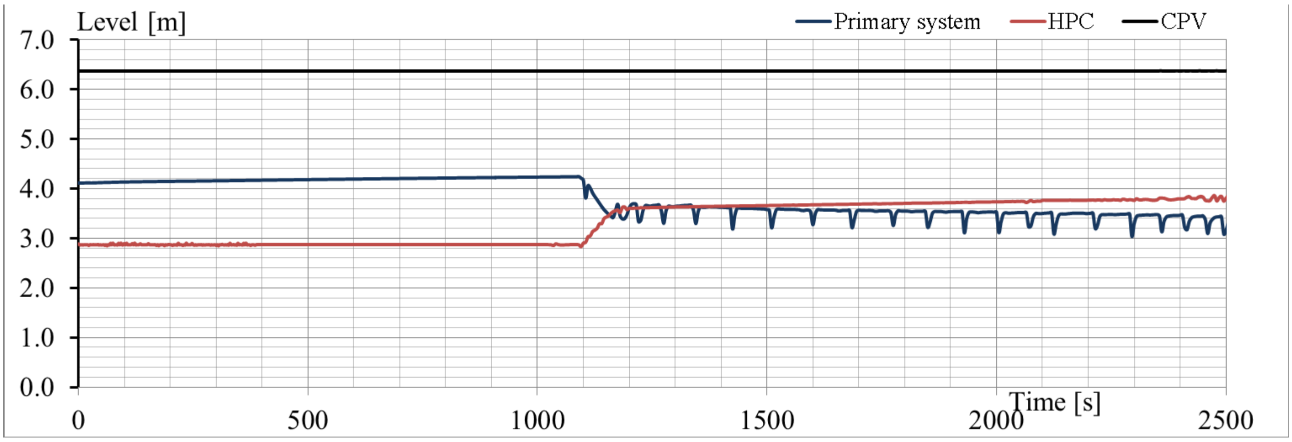

(b) From 0s to 2500s

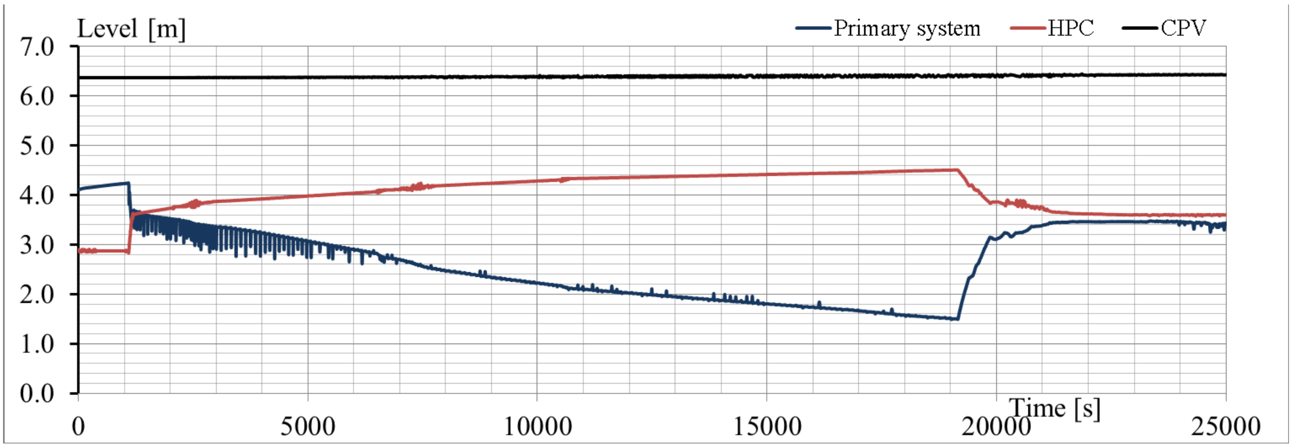

(c) From 0s to 25000s

Fig. 6.5 – Simulation of SBO transient: primary system, HPC and CPV levels

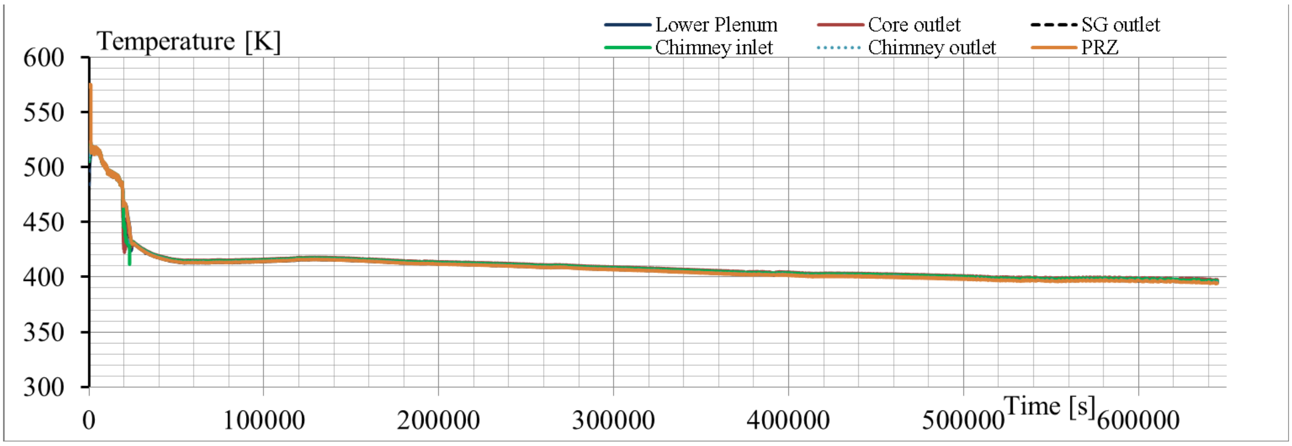

(a) Overall transient

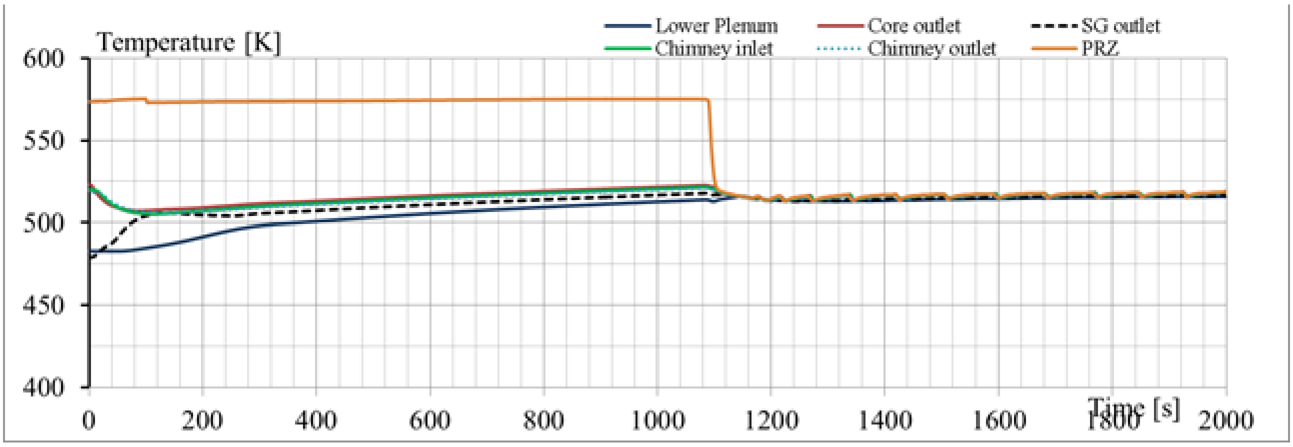

(b) From 0s to 2000s

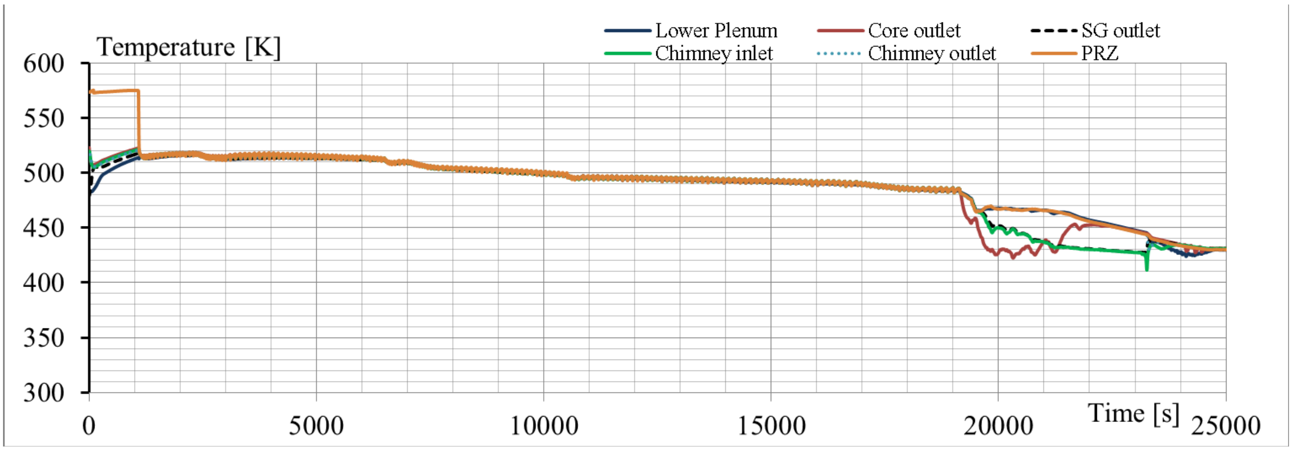

(c) From 0s to 25000s

Fig. 6.6 – Simulation of SBO transient: primary system coolant temperatures

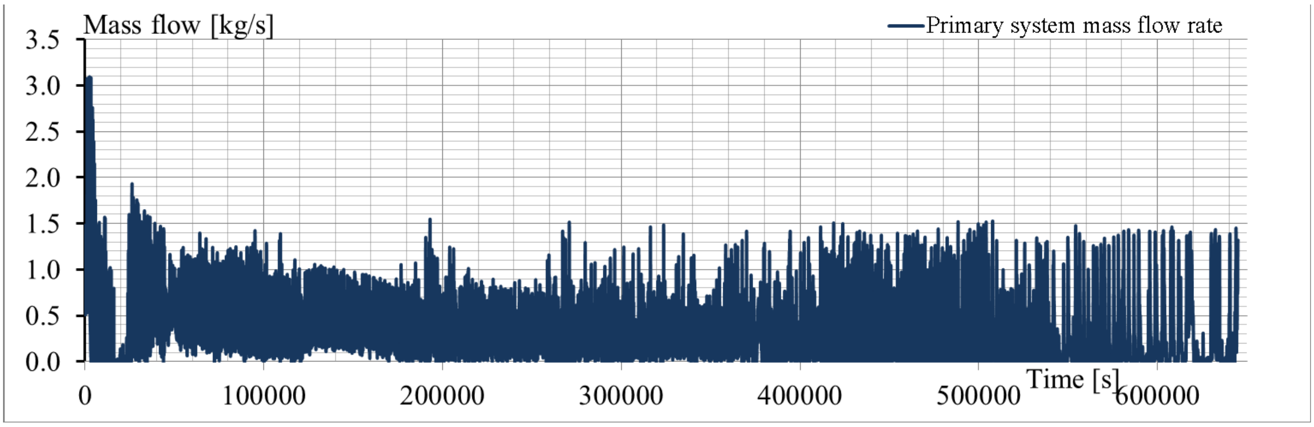

(a) Overall transient

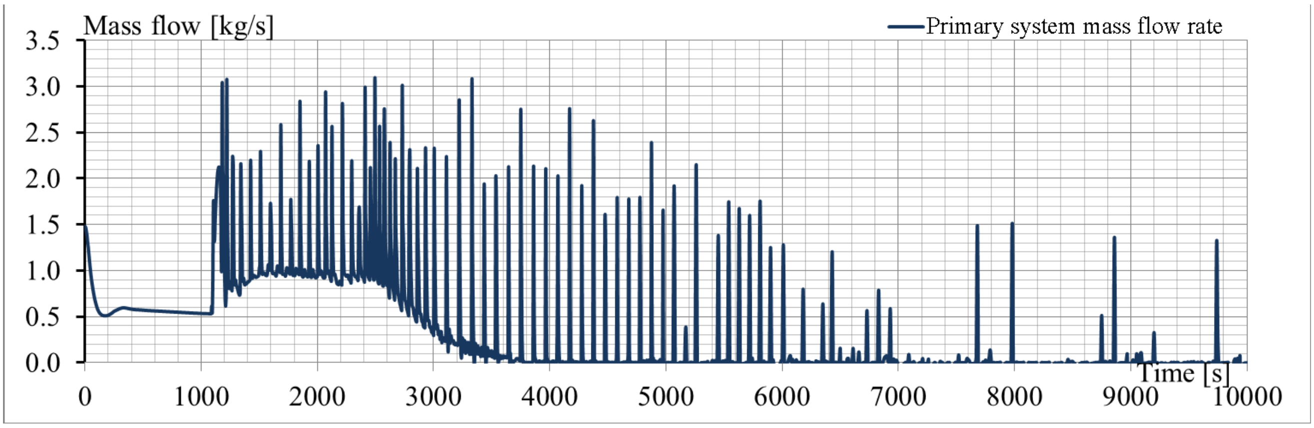

(b) From 0s to 10000s

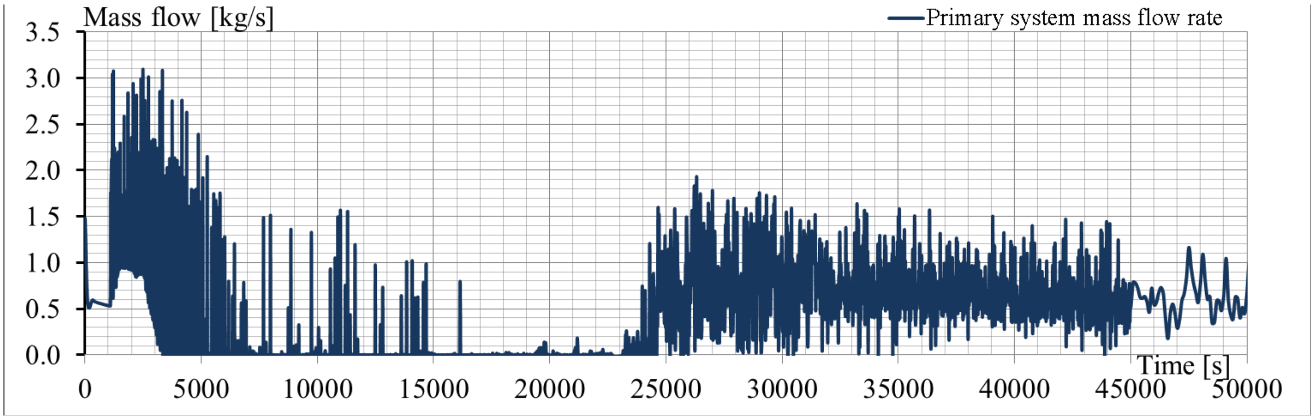

(c) From 0s to 50000s

Fig. 6.7 – Simulation of SBO transient: primary system mass flow rate

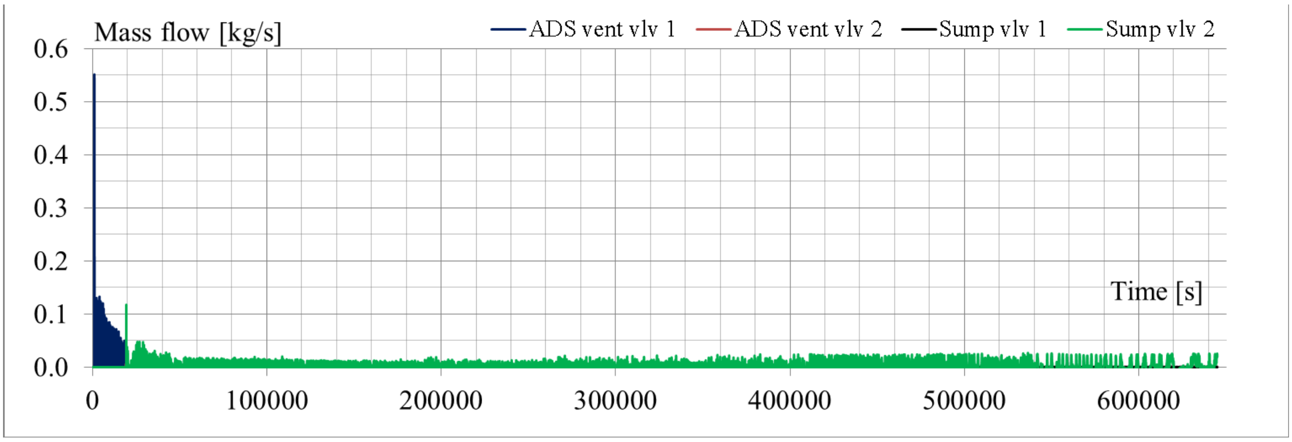

(a) Overall transient

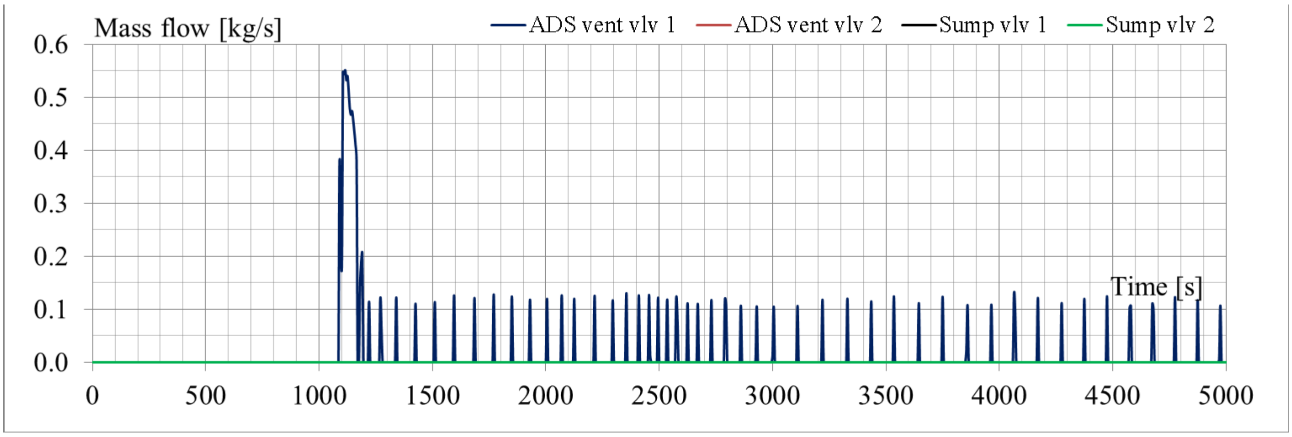

(b) From 0s to 5000s

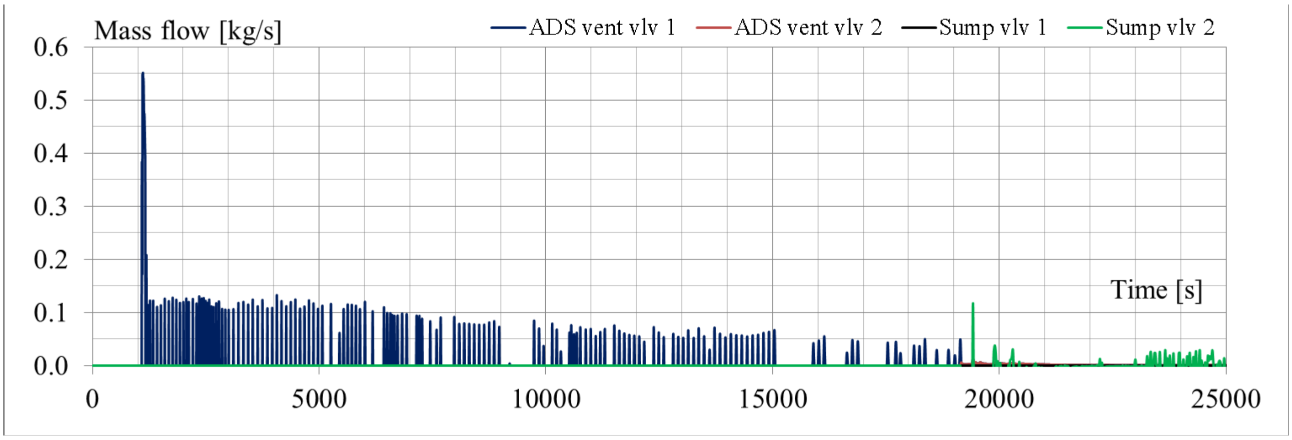

(c) From 0s to 25000s

Fig. 6.8 – Simulation of SBO transient: mass flow rates through ADS vent valves 1 and 2 and sump valves 1 and 2

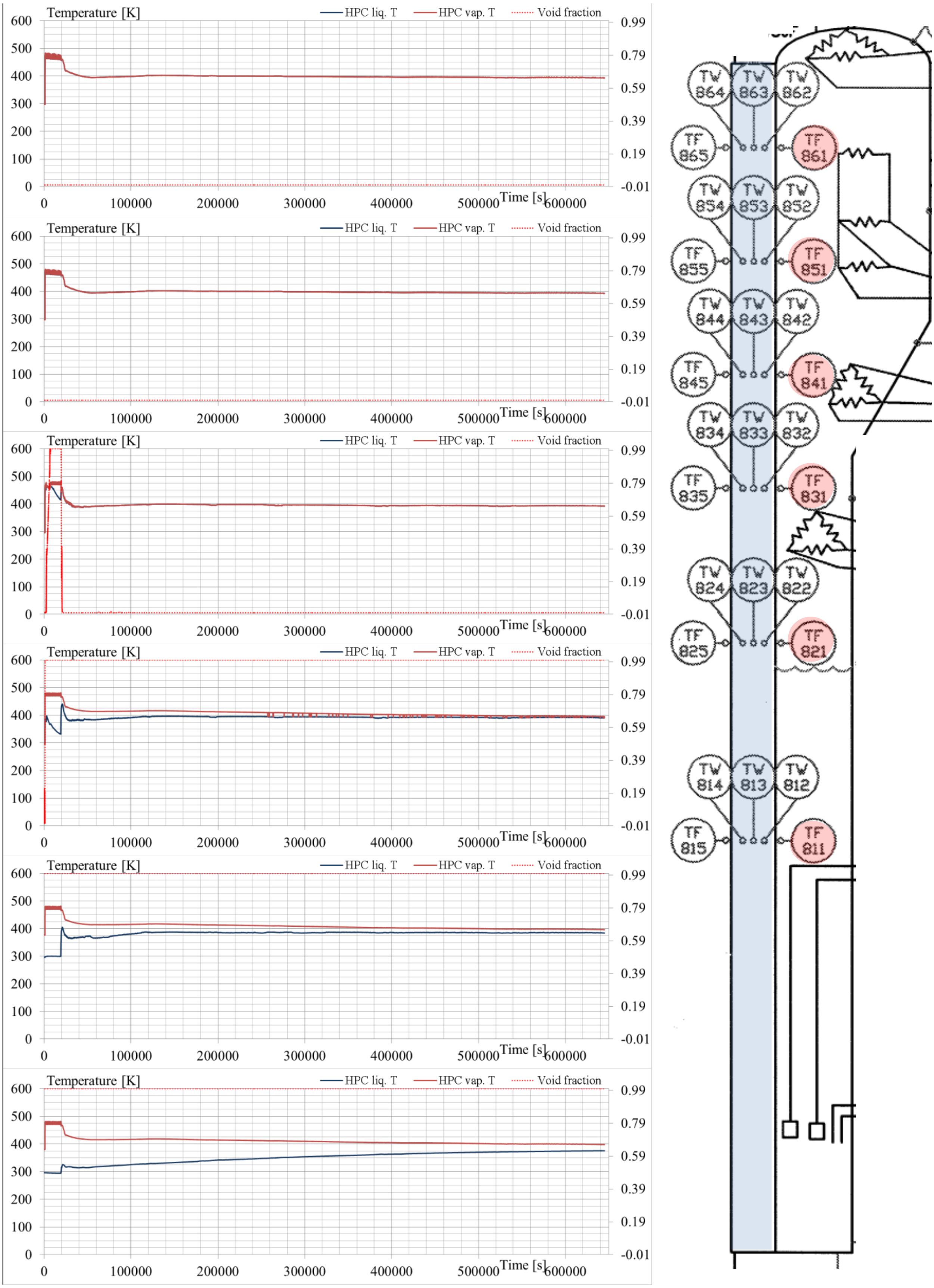

Fig. 6.9 – Simulation of SBO transient: HPC coolant temperatures

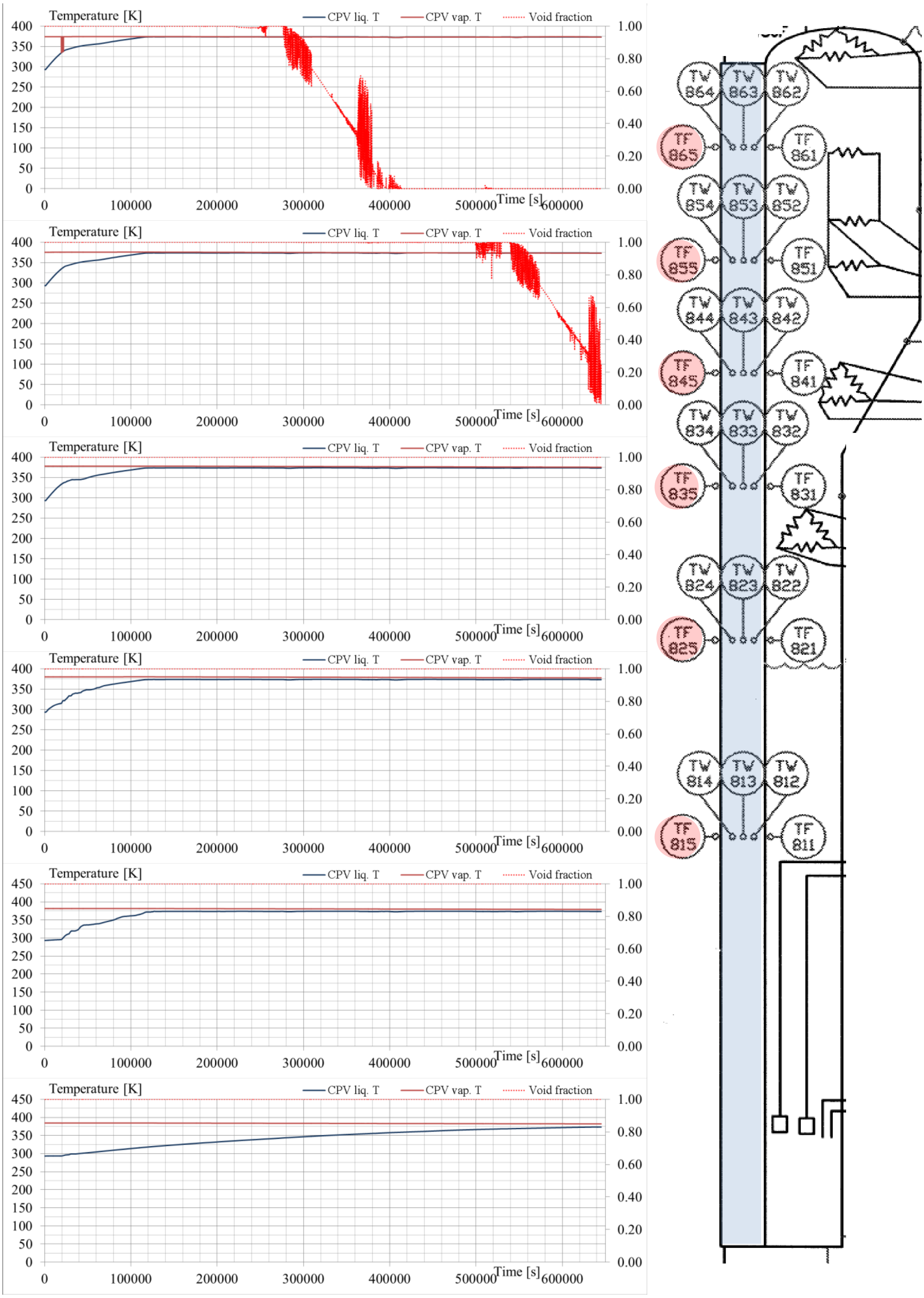

Fig. 6.10 – Simulation of SBO transient: CPV coolant temperatures

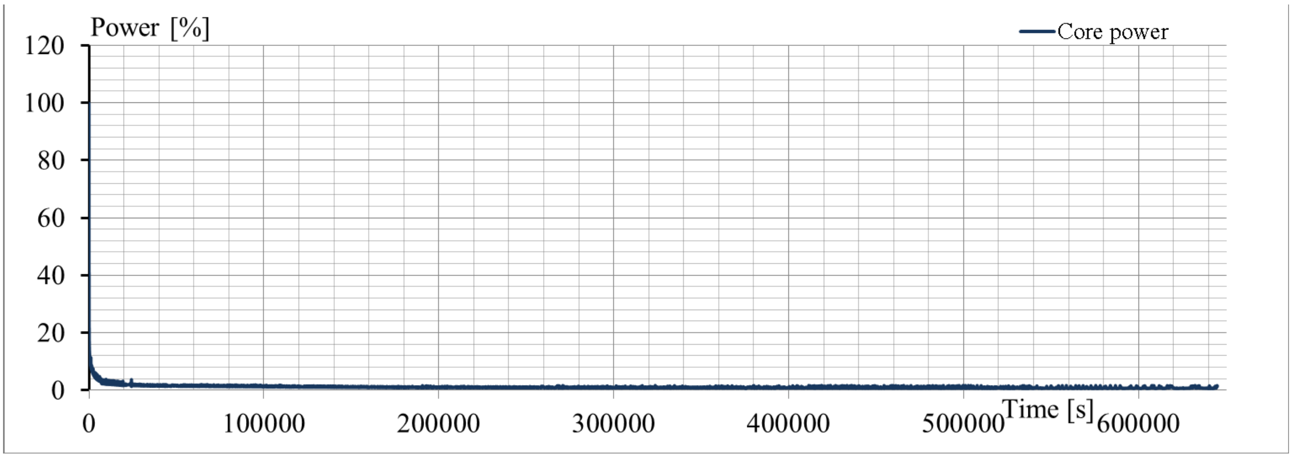

Fig. 6.11 – Simulation of SBO transient: energy exchanged between the primary system heated rods and the coolant

6.3 Sensitivity analyses

Considering the results described in section 6.1 and the consideration in section 6.2, a set of sensitivity analyses has been carried out to investigate: 1) the influence of the ADS vent valves flow area; 2) the consequence of the failure of the ADS vent valve (stuck open); 3) the possibility to achieve the safe cooldown conditions postulating that the valves can be opened only during the first hour and not operated.

Tab. 6.3 reports the list of the sensitivities. The table describes the differences with the reference calculation, the objective; and the main results for each code RUN. Hereafter, the main results of the sensitivities are summarized.

RUN 2 and RUN3
The effect of the ADS vent valve flow area influences the mass flow rate (Fig. 6.12) discharged from primary system to the HPC. The comparison of the results shows that small differences in the evolution of the transient are experienced for rather large changes (factor 2) of the flow area. Therefore, the expected overestimation of the single (steam) phase critical flow [18] should not largely influence the overall transient behavior. On the opposite, a drastic reduction of the ADS vent valve area (i.e. factor 10) causes a large delay of the long term cooling procedure (Fig. 6.13) and consequently a larger mass reduction of the primary system (Fig. 6.14), before its pressure is equalized to the HPC pressure. This causes the CHF (i.e. dryout) occurrence at top of the core, which is triggered by the sump valve opening (Fig. 6.15.).

RUN 4 and RUN5
These sensitivity have been carried out to verify the system behavior in case of SBO and with failure of the ADS vent valve. In case of RUN 4, the SUMP valves are operated on the pressure equalization between primary system and HTC. The availability of the SUMP valve is disregarded in the case of RUN 5, to verify the grace time. The primary pressure drastically drops in all calculations as soon as the ADS vent valve 1 is stuck opened (Fig. 6.16). In the reference case (RUN 1), it is stopped by the closure of the valve on high pressure signal in HPC. The low pressure difference between HTC and primary system triggers the operation of the SUMP valves in RUN 4. This occurs when the HTC pressure is higher than the maximum

allowable in the system, thus the HTC top valve is opened releasing primary coolant outside the containment (Fig. 6.18). The SUMP valves opening cause the fast replenishment of the primary system (Fig. 6.17) and the electrical core does not experiences CHF condition during the transient. RUN 5 during the first part of the transient (up to the SUMP valve opening) evolves as RUN 4, including the opening of the HTC top valve. Nevertheless, because in this sequence the opening of the SUMP valve is disregarded, the continuous bleed of the primary system coolant through the ADS vent valve causes the low level in the core and, therefore, CHF conditions at top of the core after 6 hours. Because no action is postulated in RUN5 after dryout, no chance for recovering the accident is possible.

RUN 6

The main objective is to observe the pressure of the HTC. RUN 6 is similar to RUN 4. The main difference is the set point of the SUMP valve opening, which is on high pressure signal in HPC (1.4MPa) during the first hour. The set point is arbitrary. Moreover the HTC top valve is not operated. The sensitivity shows that the maximum allowed pressure is largely overpassed (Fig. 6.20). Nevertheless, the early opening of the SUMP valves keep the primary system level (Fig. 6.21) relatively high, thus preventing the core heat up.

RUN 7

The sensitivity is performed to check if a different imposed sequence of main events can safely cope a SBO scenario. Only the opening of the valves is taken into account, no operation is considered. The primary system account for the ADS vent, the ADS and the SUMP valves. The ADS valve (instead of ADS vent valve) is opened on the high pressure signal in primary system in order to reduce the HTC pressure trend during the first part of the transient (Fig. 6.24). Then, when the HTC pressure is about 0.6MPa, the ADS vent valve is opened too, in order to achieve a fast equalization of the primary and the HTC systems pressures. The mass flow rates through the ADS valves, as well as for the other valves, are reported in Fig. 6.23. The level in primary system decreases faster (Fig. 6.25) than in the RUN 1, because the ADS valve connects the primary system with the containment below the SG outlet, thus in liquid zone (during the first part of the transient). The maximum pressure in the HTC remains slightly below the maximum allowable (Fig. 6.24) and the HTC top valve is not opened (Fig. 6.23). No CHF (Fig. 6.26) is experienced in the core zone.

Tab. 6.3 – Simulation of SBO transient: sensitivity analyses and main results

RUN	ID	Description of the simulation	Objective	Summary of the results
1	01a	Reference SBO. Trips according with Tab. 6.2	To understand the system behavior during a SBO To verify the capability of the system in coping a SBO for 7 days and in achieving and maintaining the long term cooling conditions.	Procedure effective in keeping the primary system in safe conditions for a time > 7 days
2	01a_vlv05	Reference SBO. ADS vent valves area reduced of a factor 2.	To investigate the influence of the ADS vent valves area (flow rate) on the reference transient	Negligible differences in the transient results. The set point of the long term cooling procedure is achieved and executed with the primary system in safe conditions
3	01a_vlv01	Reference SBO. ADS vent valves area reduced of a factor 10.	To investigate the influence of the ADS vent valves area (flow rate) on the reference transient	Long term cooling procedure is delayed. Lower level in primary system, when the sump valves are opened. CHF experienced in the core.
4	021a	SBO – failure of the ADS vent valves: valve stuck open at the first opening Sump valve operated according with Tab. 6.2	To investigate the consequences of the ADS vent valves stuck open. HTC top valve opened	Primary system coolant released thorugh the HTC top valve outside the containent The set point of the long term cooling procedure is achieved and executed with the primary system in safe conditions
5	022a	SBO – failure of the ADS vent valves: valve stuck open at the first opening Sump valve not operated	To investigate the grace time and the containement pressure peak if the SUMP valves are not operated and the ADS vent valves stuck open. HTC top valve opened	Grace time of about 6 hours before CHF conditions are reached at top of the core. The dryout cannot be quenched Primary system coolant released thorugh the HTC top valve outside the containent
6	03a	SBO – failure of the ADS vent valve 1: valve stuck open at the first opening Sump valve fully opened at 1.4MPa	To investigate the influence of the SUMP valve operation	Primary system coolant released thorugh the HTC top valve outside the containent The set point of the long term cooling procedure is achieved and executed with the primary system in safe conditions
7	082a	SBO. Opening of the ADS valves on high pressure signal (P_{PRZ}=9.4MPa). Opening of ADS vent valves on high pressure signal in containment (P_{HPC}=0.6MPa). Opening of SUMP valves on low pressure difference between PRZ and HPC (P_{PRZ} - P_{HPC} = 0.034MPa)	To study an alternative procedure for achieving the long safe cooldown conditions	Procedure effective in keeping the primary system in safe conditions for a time > 7 days No CHF in primary system. No overpressure in HTC

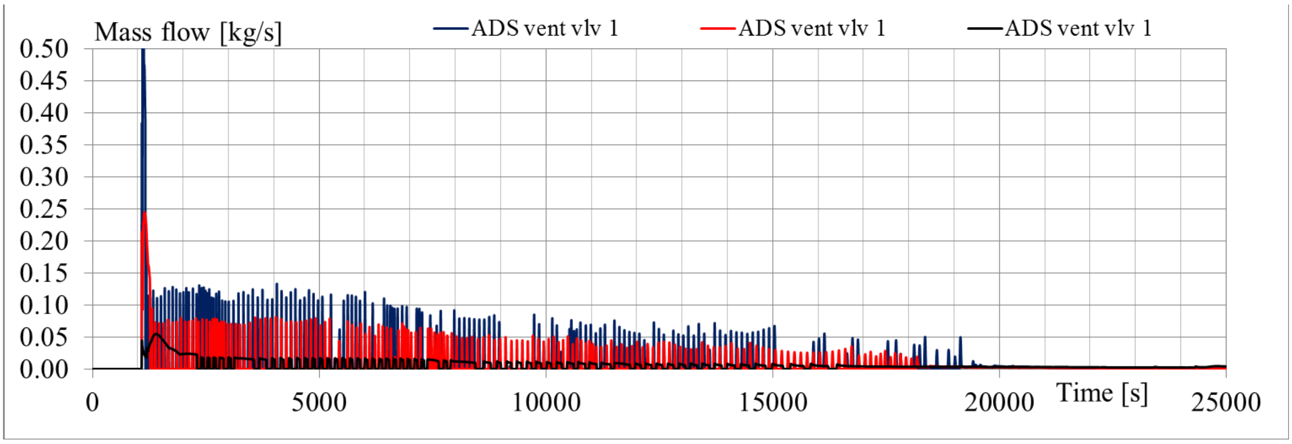

Fig. 6.12 – Sensitivity analysis RUN 1 vs. RUN 2 vs. RUN3: ADS vent valve 1 mass flow rate (blue "01a"; red "01a_vlv05", black "01a_vlv01")

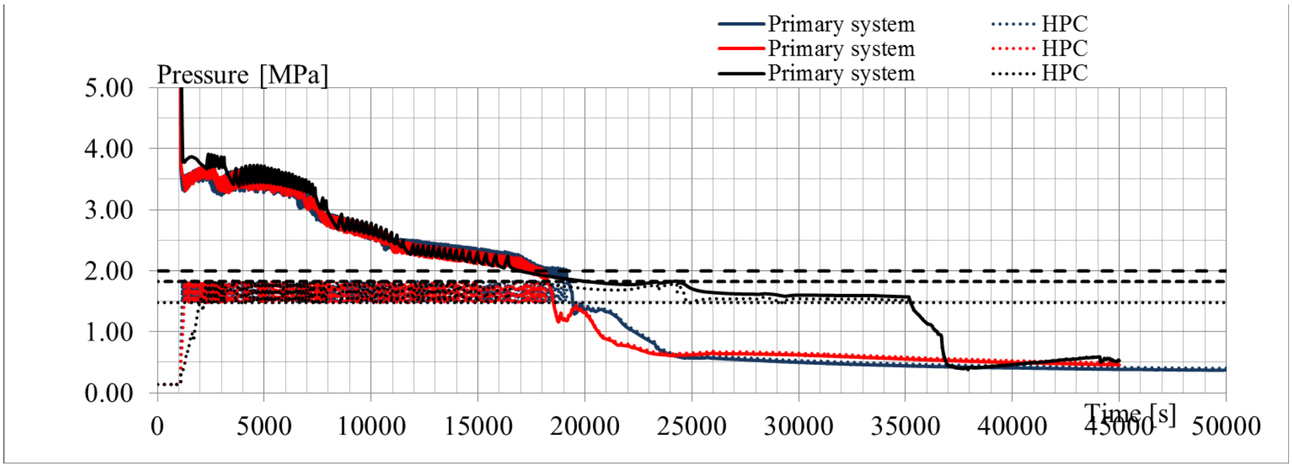

Fig. 6.13 – Sensitivity analysis RUN 1 vs. RUN 2 vs. RUN3: primary system and HPC pressures (blue "01a"; red "01a_vlv05", black "01a_vlv01")

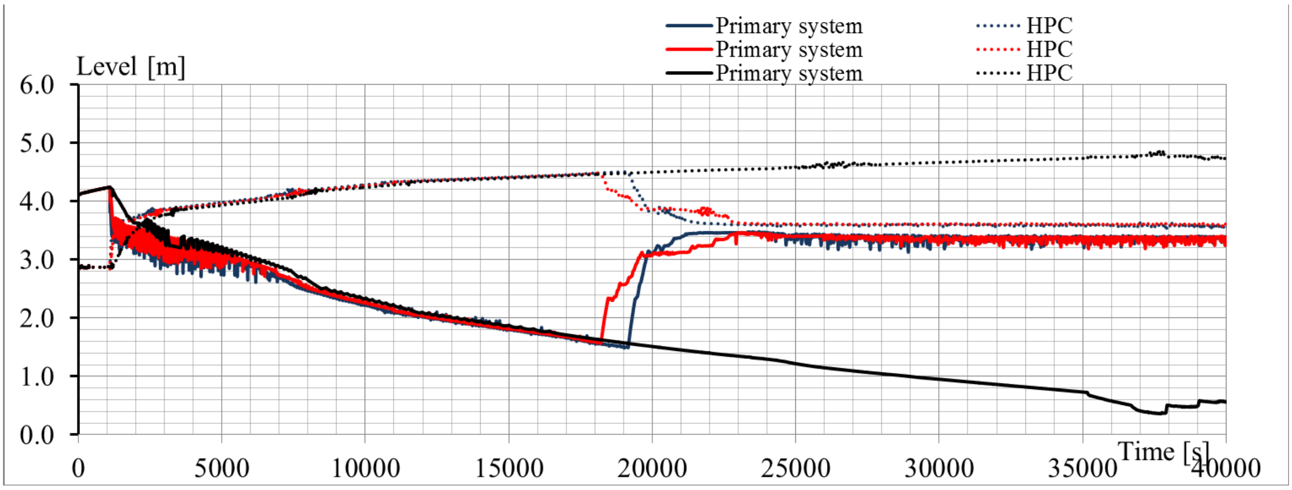

Fig. 6.14 – Sensitivity analysis RUN 1 vs. RUN 2 vs. RUN3: primary system and HPC levels (blue "01a"; red "01a_vlv05", black "01a_vlv01")

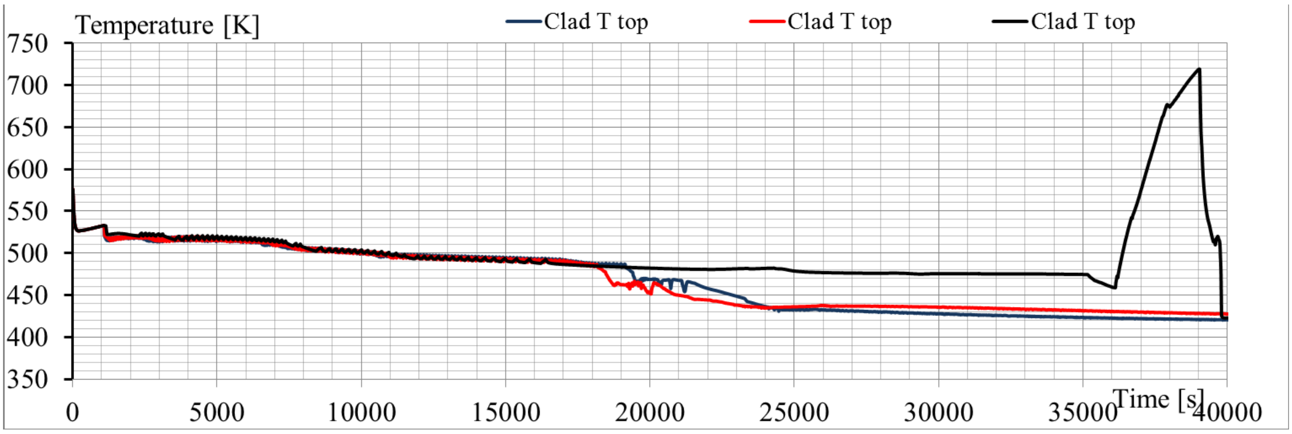

Fig. 6.15 – Sensitivity analysis RUN 1 vs. RUN 2 vs. RUN3: cladding temperature at top of the electrical core (blue "01a"; red "01a_vlv05", black "01a_vlv01")

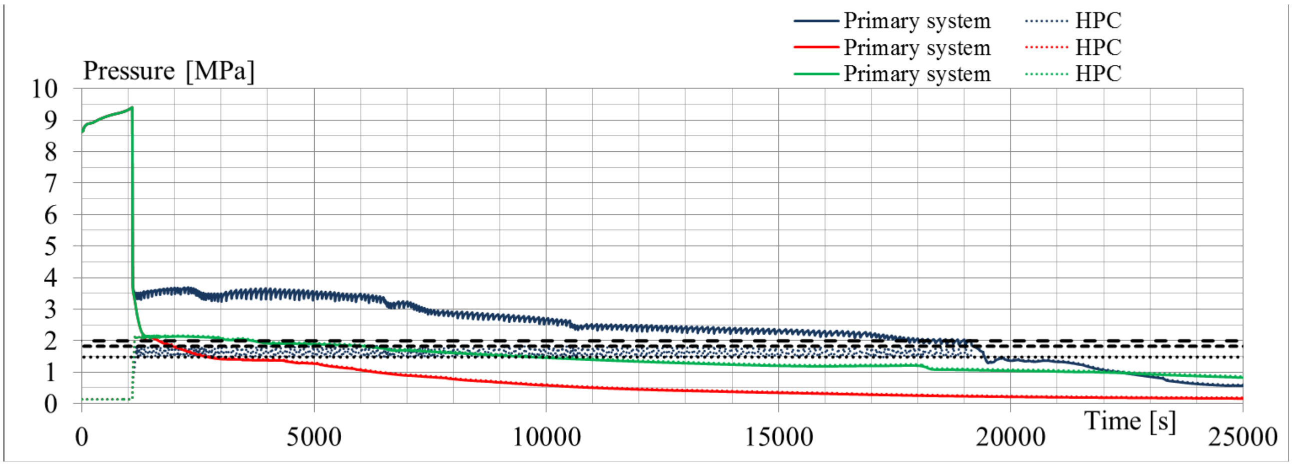

(a) from 0s to 25000s

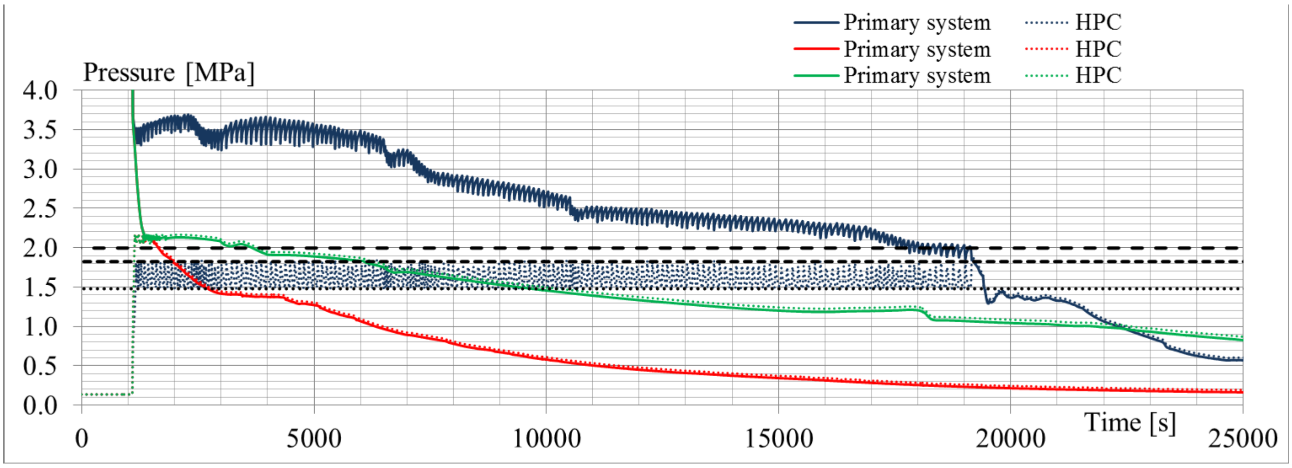

(a) from 0s to 25000s – zoom

Fig. 6.16 – Sensitivity analysis RUN 1 vs. RUN 4 vs. RUN5: primary and HPC pressures (blue "01a"; red "021a", green "022a")

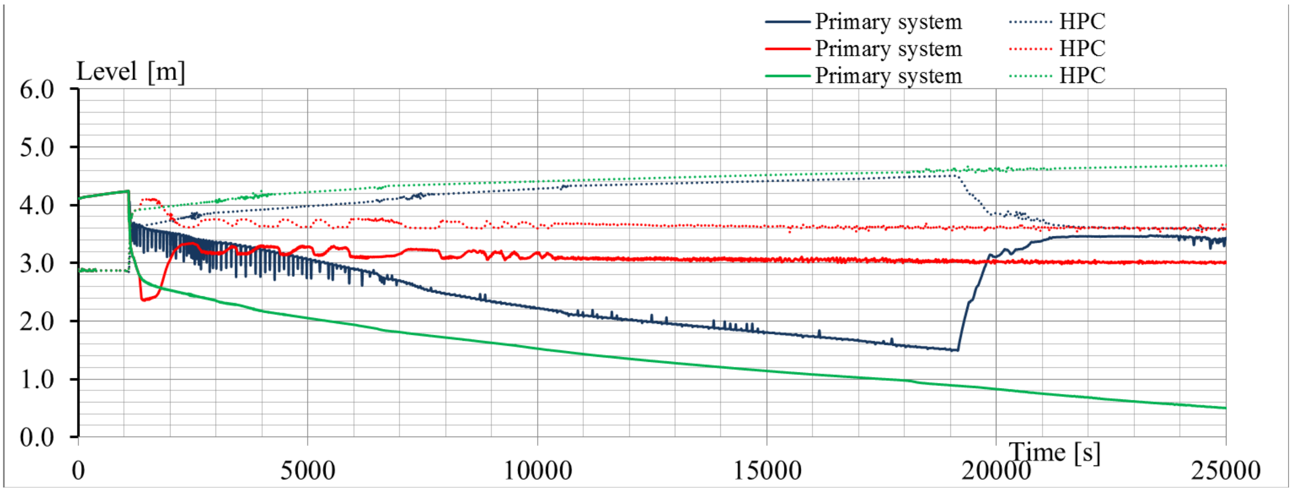

Fig. 6.17 – Sensitivity analysis RUN 1 vs. RUN 4 vs. RUN5: primary and HPC levels (blue "01a"; red "021a", green "022a")

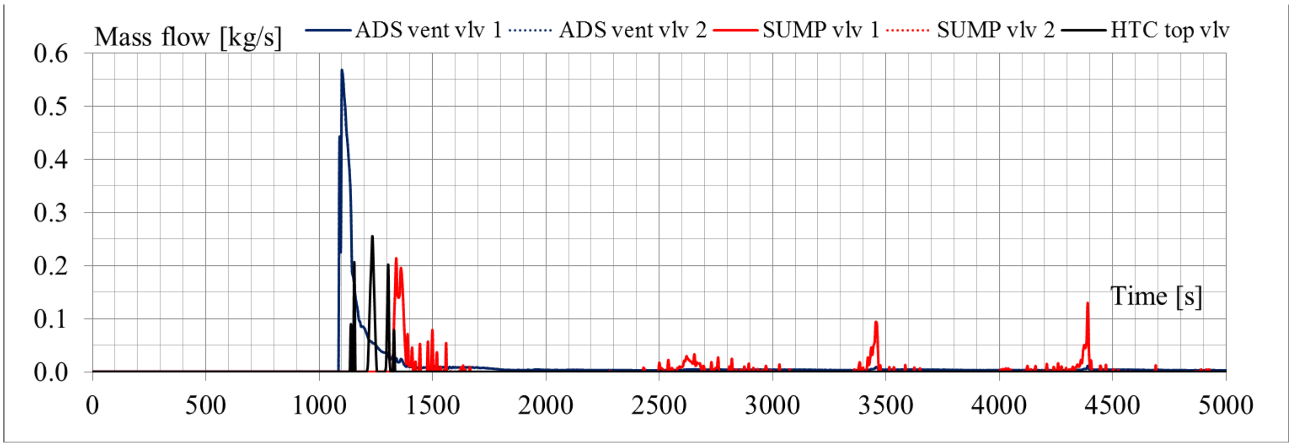

(a) RUN 4 – ID: "021a"

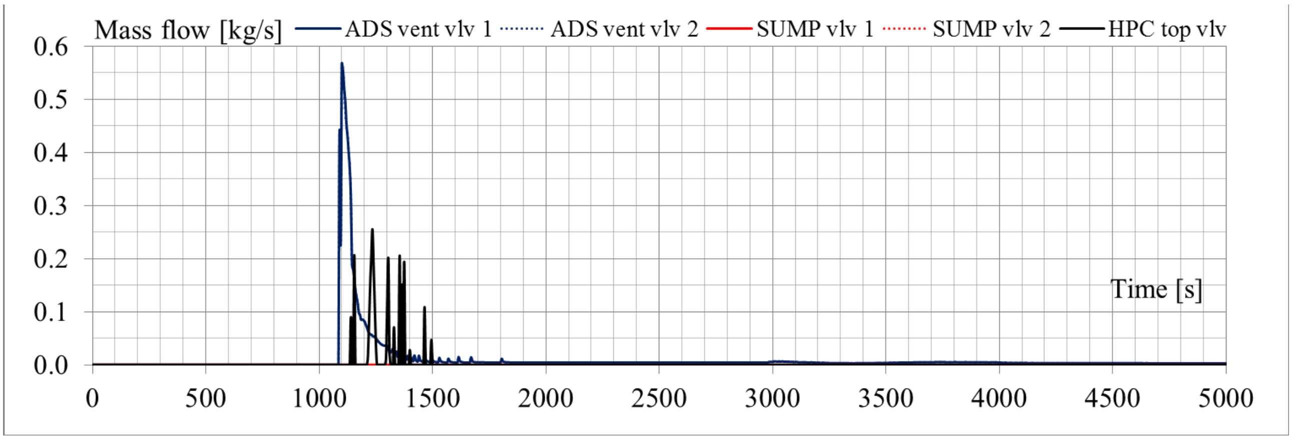

(b) RUN 5 – ID: "025a"

Fig. 6.18 – Sensitivity analysis RUN 4 vs. RUN5: ADS vent valves, SUMP valves and HTC top valve mass flow rates

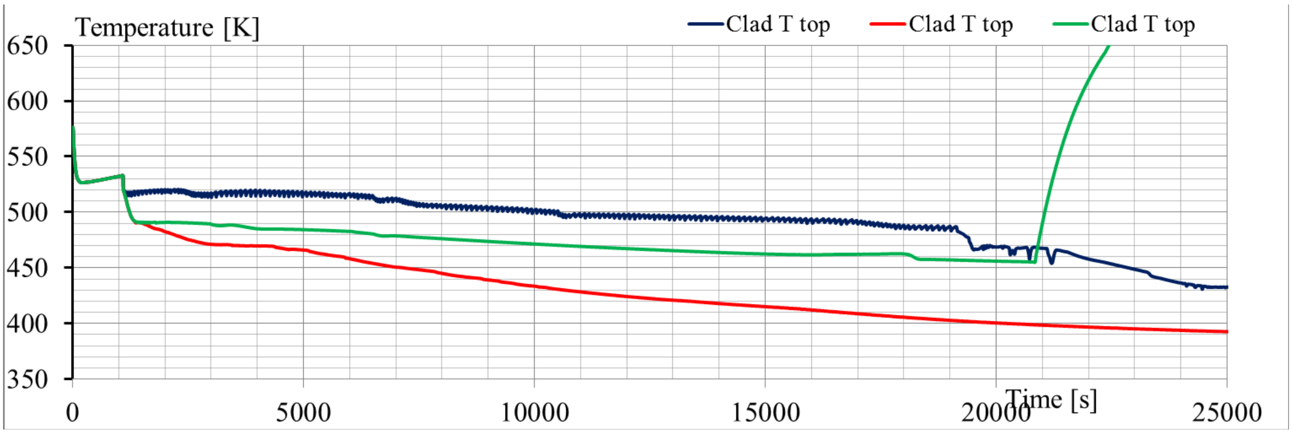

Fig. 6.19 – Sensitivity analysis RUN 1 vs. RUN 4 vs. RUN5: cladding temperature at top of the electrical core (blue "01a"; red "021a", green "022a")

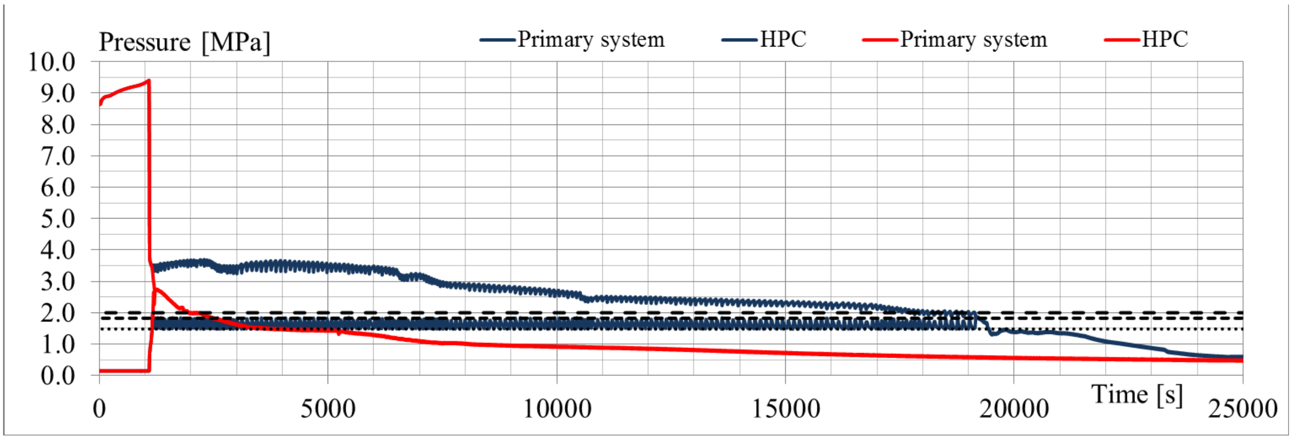

(a) from 0s to 25000s

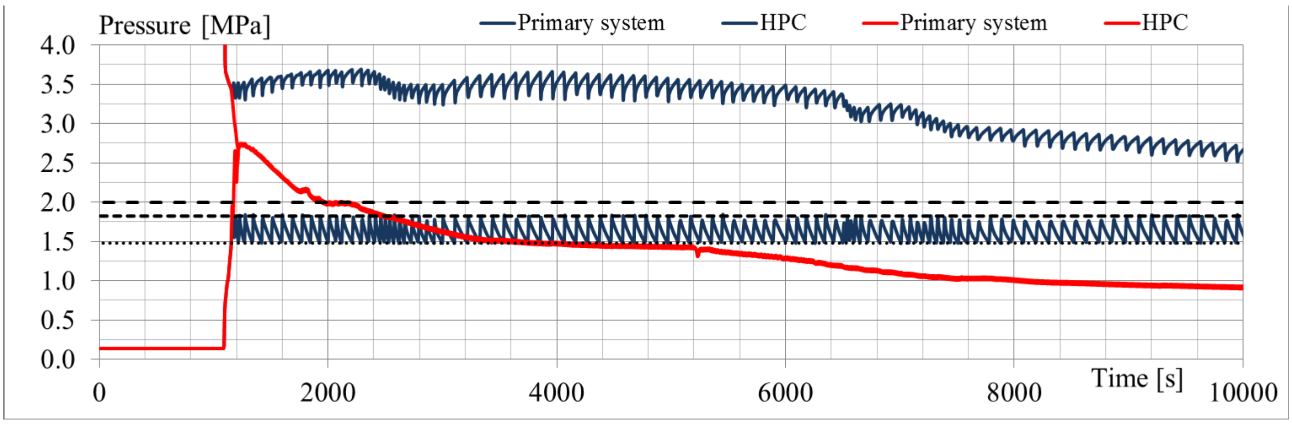

(a) from 0s to 10000s – zoom

Fig. 6.20 – Sensitivity analysis RUN 1 vs. RUN 6: primary and HPC pressures (blue "01a"; red "03a")

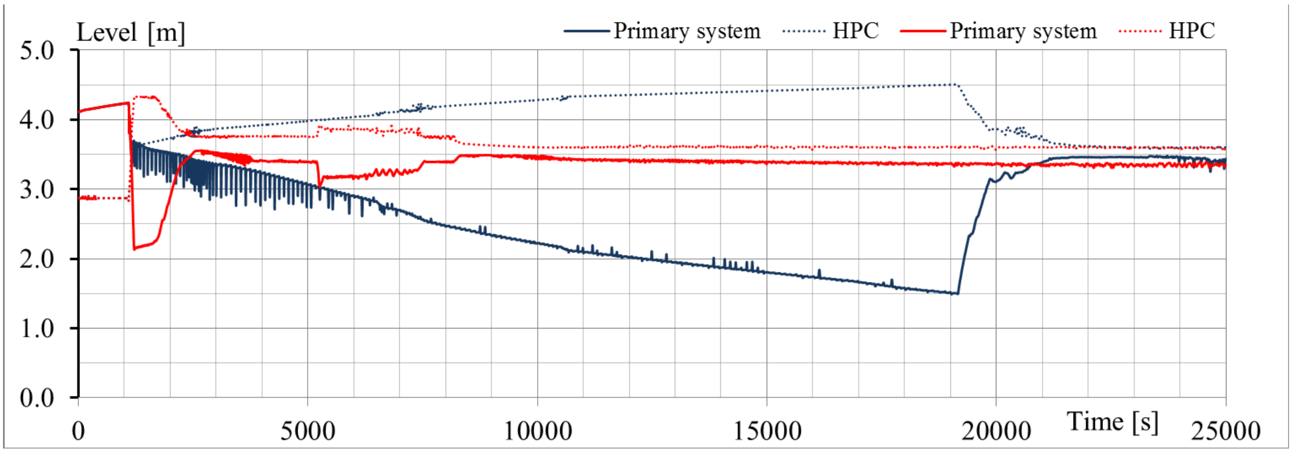

Fig. 6.21 – Sensitivity analysis RUN 1 vs. RUN 6: primary and HPC levels (blue "01a"; red "03a")

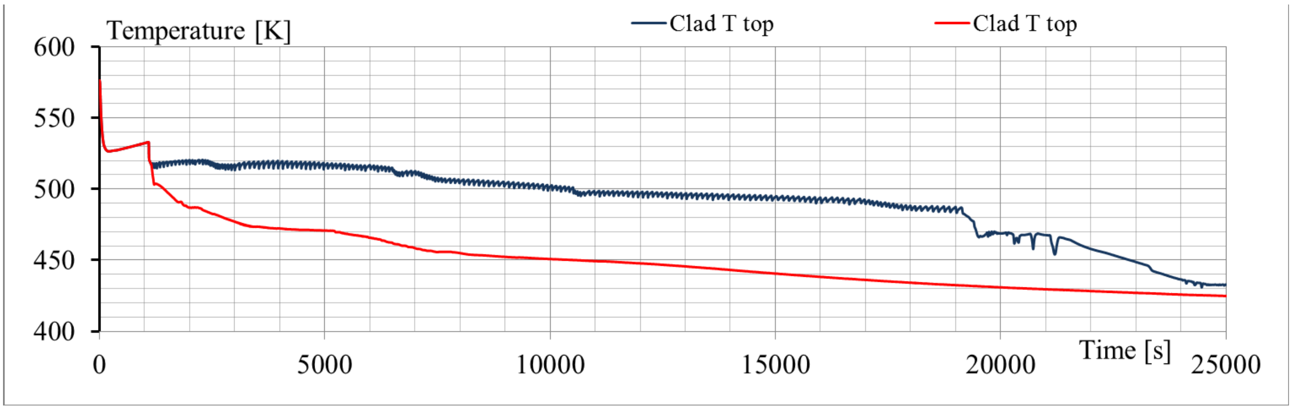

Fig. 6.22 – Sensitivity analysis RUN 1 vs. RUN 6: cladding temperature at top of the electrical core (blue "01a"; red "03a")

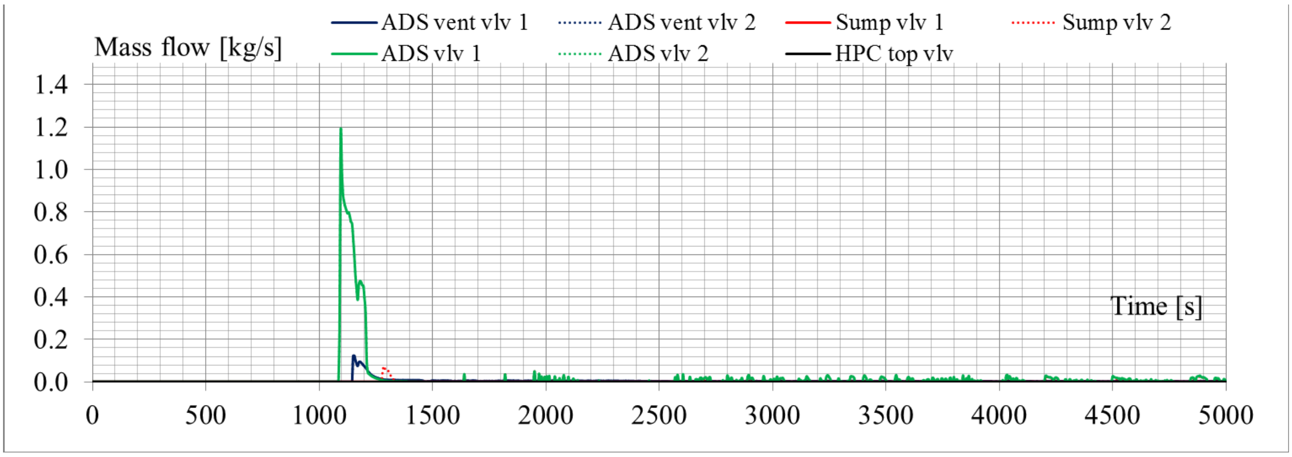

Fig. 6.23 – Sensitivity analysis RUN 7 (ID "082a"): ADS VENT valves, ADS valves, SUMP valves and HTC top valve mass flow rates

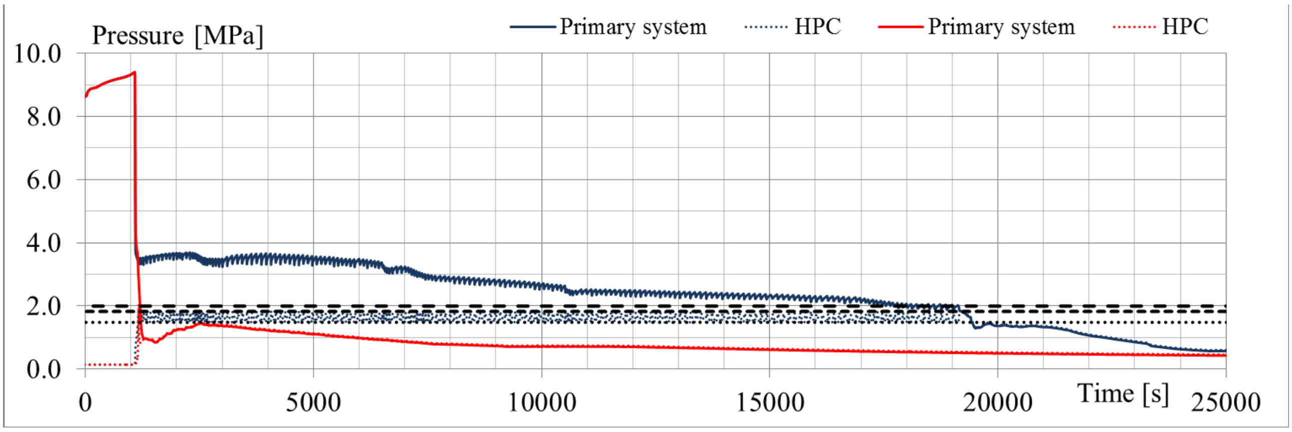

(a) from 0s to 25000s

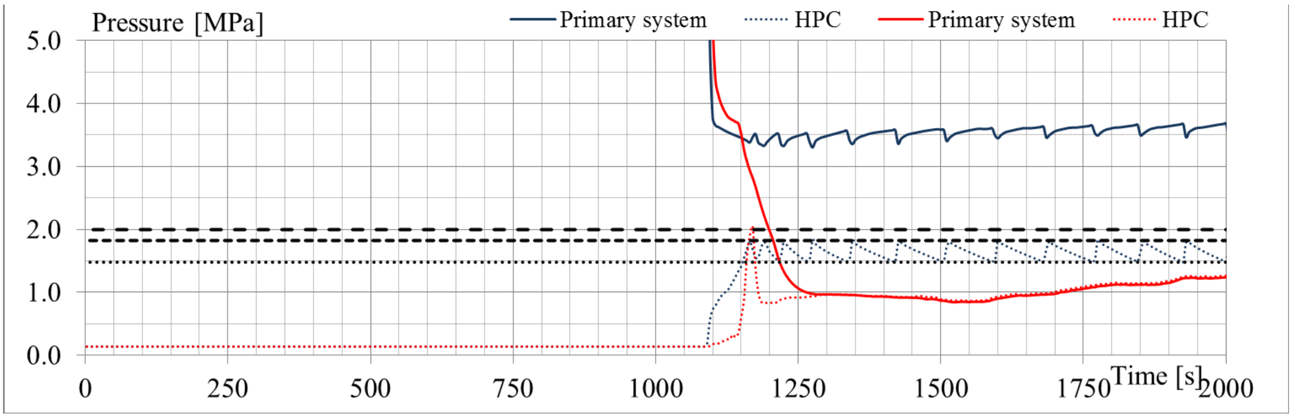

(a) from 0s to 2000s – zoom

Fig. 6.24 – Sensitivity analysis RUN 1 vs. RUN 7: primary and HPC pressures (blue "01a"; red "082a")

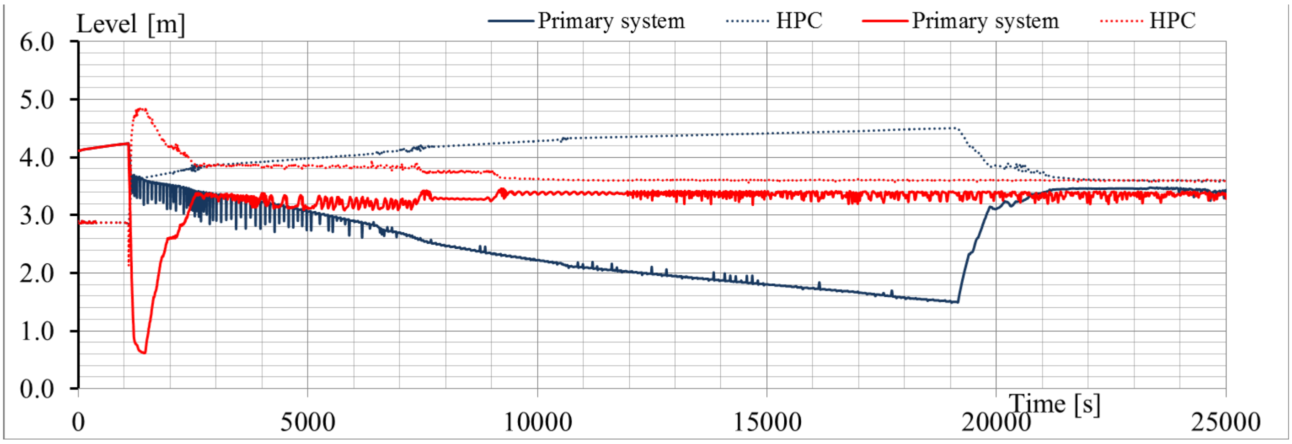

Fig. 6.25 – Sensitivity analysis RUN 1 vs. RUN 7: primary and HPC levels (blue "01a"; red "082a")

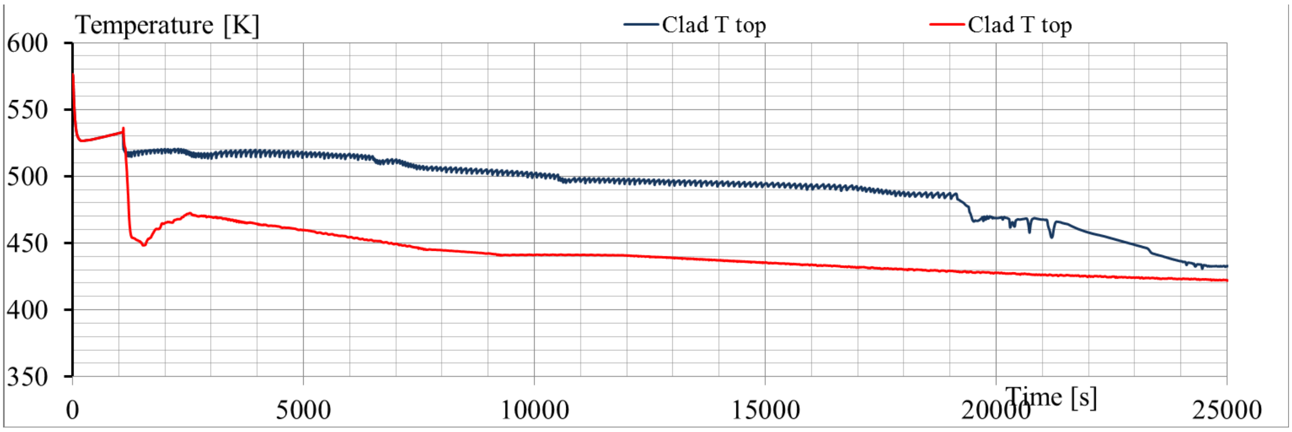

Fig. 6.26 – Sensitivity analysis RUN 1 vs. RUN 7: cladding temperature at top of the electrical core (blue "01a"; red "082a")

7 CONCLUSIVE REMARKS

The aim of the activity is the investigation of a SBO transient in a small modular reactor (SMR) design, cooled and moderated with light water and having an integral primary system layout. The activity activity is based on the OSU-MASLWR integral test facility, which is the scaled down model (1:254 in volume) of the SMR design, MASLWR. It relies on natural circulation and on passive safety features. Two main objectives have been pursued: 1) the set up and qualification of a RELAP5/Mod3.3 nodalization used for the numerical simulation of the system and 2) deterministic investigations related to the capability of this small modular reactor design to cope with a station blackout postulated accident scenario.

A RELAP5 code nodalization of the experimental facility has been set up and applied to simulate two experimental tests on the basis of their specifications (blind calculations). They are a natural circulation experiment aimed at characterizing the system performances at different power levels and a total loss of feedwater flow accident scenario. Once the experiments have been executed, the code results have been compared with the experimental parameters trends to assess the RELAP5 capabilities in predicting the relevant phenomena and processes. The analysis of the results brings to the following conclusions.

- The main phenomena and parameters trends of tests SP-2 and SP3 are predicted by the code and consistent with the expectations.
- The trends of the primary system and HPC pressures are well predicted in test SP2. These are influenced by the chocked flow at ADS valve during the first part of the transient, by the flows at the ADS and SUMP valves during the long term cooling phase, by condensation on the free surface in presence of noncodensable; by mixing and thermal stratification in HPC system; the convection and conduction across the heat transfer plate connecting the CPV and HPC; and the heat losses. Compensation of errors are plausible but not identifiable on the basis of the experimental results.
- The mixing and thermal stratification in CPV system is reasonably simulated. However, considering the RELAP5 capabilities, only bounding analyses are possible.
- The coupling primary system containment and the presence of noncondensable in the HPC is challenging for the code.
- The limits of RELAP5 heat exchange model in simulating the helical-coil SG are detected, in particular in test SP-3. This is mainly connected to the convective heat transfer correlation used for the inner side of the tubes (secondary side). The correction, set-up modifying the fouling factor, reasonably works at the lower and higher powers (i.e. <80kW and 280 – 320kW). Larger errors are detected for the other power values. New correlation would be needed to improve the results.

Then, the nodalization has been employed to carry out deterministic investigations of station blackout scenario. Reference results and sensitivity analyses are performed to understand the behavior of the system. The preliminary results highlight the potential capability of this design to cope with a station blackout without any external intervention for at least 72 hours, thanks to the low power density and the large water inventory.

LIST OF REFERENCES

[1] American Nuclear Society, Small Nuclear Power Reactors, http://www.world-nuclear.org/info/inf33.html, updated July 2012.

[2] S. M. Modro, et al., Generation-IV Multi-Application Small Light Water Reactor (MASLWR), Proc. of ICONE 10, April 14-18, 2002 Arlington, Virginia, USA.

[3] S. M. Modro, et al., Multi-Application Small Light Water Reactor Final Report, INEEL/EXT-04-01626, Dec. 2003.

[4] J. N. Reyes Jr., Innovative Water-Cooled Reactor Concepts – SMR, Conf. on Opportunities and Challenges for Water- Cooled Reactors in the 21st Century, Vienna, Austria, Oct. 27- 30, 2009.

[5] IAEA, Natural circulation in water cooled nuclear power plants, IAEA-TECDOC-1474, November 2005.

[6] N. T. Demick, et al., OSU MASLWR Test Facility Description Report, OSU-MASLWR-07001 (Revision NC), August 2, 2007.

[7] Mark R. Galvin, et al., OSU MASLWR Test Facility Modification Description Report IAEA Contract Number USA-13386, OSU-MASLWR-07002 (Revision 2), August 16, 2010.

[8] Information Systems Laboratories, Relap5/MOD3.3 Beta Code Manual, NUREG/CR-5535/Rev.1 – May 2001.

[9] Information Systems Laboratories, Relap5/MOD3 Code Manual, Volume IV: Models and Correlations, NUREG/CR-5535-Vol. 4 Idaho, 1995.

[10] Information Systems Laboratories, Relap5/MOD3 Code Manual, Volumes I and II, NUREG/CR-5536, INEL-95/0174, Idaho, 1995.

[11] A. Del Nevo, Session 2: Presentation and discussion on plan and approach OSU MASLWR ITF by RELAP5-3D code, 1st Workshop for IAEA ICSP on “Integral PWR Design NC Flow Stability and TH Coupling of Containment and Primary System during Accidents”, 16-19 March, 2010, OSU, Corvallis, Oregon, USA.

[12] A. Del Nevo, IAEA ICSP on Integral PWR Design Natural Circulation Flow Stability and TH Coupling of Containment and Primary System during Accident, Blind Calculation Results, May 2012.

[13] B. G. Woods, et al., Problem Specification for the IAEA International Collaborative Standard Problem on Integral PWR Design Natural Circulation Flow Stability and

Thermo-hydraulic Coupling of Containment and Primary System during Accidents, OSU-MASLWR-10005-R1, August 2011.

[14] A. Del Nevo, IAEA ICSP on Integral PWR Design Natural Circulation Flow Stability and TH Coupling of Containment and Primary System during Accident, Final ICSP results, October 2012 (to be issued).

[15] A. Del Nevo, et al., Analytical Exercise on OECD/NEA/CSNI PKL-2 Project Test G3.1: Main Steam Line Break Transient in PKL-III Facility Phase 2: Post-Test Calculations, OECD/NEA/CSNI PKL-2 Project, TH/PKL-2/02(10) Rev. 1, Pisa, March 2011.

[16] J.H. Choi, Summary of 3rd Workshop IAEA ICSP on Natural Circulation during Power Maneuvering and Loss of Feedwater Transient in Integral PWR Design MASLWR, 27-30 March 2012, Daejeon, Rep. of Korea.

[17] A. Del Nevo, A. Manfredini, L. Oriani, F. Oriolo, S. Paci, Integrated Analysis for a Small Break LOCA in the IRIS Reactor Using MELCOR and RELAP5 Codes, Nuclear Option in Countries with Small and Medium Electricity Grids, vol. CD, pp. 1-17, Dubrovnik (HR) 2004.

[18] A. Del Nevo, et al., Analytical Exercise on OECD/NEA/CSNI PKL-2 Project Test G3.1: Main Steam Line Break Transient in PKL-III Facility Phase 2: Post-Test Calculations, OECD/NEA/CSNI PKL-2 Project, TH/PKL-2/02(10) Rev. 1, Pisa, March 2011.